Publication No. 01-119-133

ENHANCED FILTRATION OF PHOSPHOGYPSUM

Prepared by
University of Florida

under a grant sponsored by

December 1995

The Florida Institute of Phosphate Research was created in 1978 by the Florida Legislature (Chapter 378.101, Florida Statutes) and empowered to conduct research supportive to the responsible development of the state's phosphate resources. The Institute has targeted areas of research responsibility. These are: reclamation alternatives in mining and processing, including wetlands' reclamation, phosphogypsum storage areas and phosphatic clay containment areas; methods for more efficient, economical and environmentally balanced phosphate recovery and processing; disposal and utilization of phosphatic clay; and environmental effects involving the health and welfare of the people, including those effects related to radiation and water consumption.

FIPR is located in Polk County, in the heart of the central Florida phosphate district. The Institute seeks to serve as an information center on phosphate-related topics and welcomes information requests made in person, by mail, or by telephone.

Research Staff

Executive Director
Paul R. Clifford

Research Directors

G. Michael Lloyd Jr.	**-Chemical Processing**
Jinrong P. Zhang	**-Mining & Beneficiation**
Steven G. Richardson	**-Reclamation**
Gordon D. Nifong	**-Environmental Services**

Florida Institute of Phosphate Research
1855 West Main Street
Bartow, Florida 33830
(863) 534-7160
Fax:(863) 534-7165
http://www.fipr.state.fl.us

Final Report

Enhanced Filtration of Phosphogypsum

(FIPR Grant No. 91-01-094R)
and
(FIPR Grant No. 94-01-119)

Submitted to:

Florida Institute of Phosphate Research

Bartow, Florida

Submitted by:

Brij M. Moudgil
Mineral Resources Research Center
Department of Materials Science and Engineering
University of Florida
Gainesville, Florida 32611

December 1995

DISCLAIMER

The contents of this report are reproduced herein as received from the contractor.

The opinions, findings and conclusions expressed herein are not necessarily those of the Florida Institute of Phosphate Research, nor does mention of company names or products constitute endorsement by the Florida Institute of Phosphate Research.

PERSPECTIVE

The manufacture of wet process phosphoric acid has often been described as the art of producing an acceptable by-product, phosphogypsum. Both the size and the shape of the phosphogypsum crystals are critical to achieving optimum filtration rates and filtration rates dictate both production rates and yields.

It has long been recognized that the size and/or shape of the phosphogypsum crystals can be modified by the addition of trace quantities of certain chemicals and much time and effort has been expended to find an economical crystal modifier that would that would guarantee optimum filtration rates under any and all operating conditions. Improved production rates and yields would offer financial benefits to the industry and the improved yields would help reduce the potential for ground water contamination by lowering the acid content of the pond water.

This project looked at two methods of modifying the phosphogypsum crystals. The first procedure is perhaps the most traditional where a chemical agent is added after the crystals are formed to flocculate the smaller sized crystals that impede the filtration separation of the phosphoric acid from the phosphogypsum.

The second crystal modification method is perhaps more interesting in that a chemical agent is added to the phosphoric acid reactor to modify the phosphogypsum crystals as they are formed from the reaction of phosphate rock and sulfuric acid. Modifying the crystals during the formation stage has the potential to produce decidedly superior crystals that can be readily separated from the phosphoric acid at high production rates with superior yields.

While the flocculation method improved the crystals the second method -- changing the way the crystals grow -- was decided superior. If this second technique can be demonstrated successfully enough on a plant scale that it is widely adopted, it could make a significant environmental and financial contribution to the phosphate industry.

ACKNOWLEDGMENTS

The Florida Institute of Phosphate Research is acknowledged for sponsoring this study (FIPR Grant # 91-01-094R and Grant # 94-01-119). The opinions, findings and conclusions expressed herein are not necessarily those of the Florida Institute of Phosphate Research, nor does the mention of company names or products constitute endorsement by the Florida Institute of Phosphate Research.

The FIPR Chemical Processing Technical Advisory Committee (TAC) members, Frank P. Achorn, Art Baumann, Ming Lei Chen, Samuel A Gardner, George M. Hebbard Jr., John J. O'Connor, Jr., Ken Parks, Mike Puerner, Regis Stana, and John Surber are greatly acknowledged for their support, guidance and suggestions. Mike Caeser and Eugene Mays are acknowledged for the experimental help.

The authors wish to thank IMC-Agrico for providing most of the phosphate feed rock used in this study. Also, the samples provided by Union Carbide, Arr-Maz, Allied Colloids, and Witco Chemical companies are gratefully acknowledged.

PROJECT PERSONNEL

Principal Investigator:

Dr. Brij M. Moudgil

Co-Investigators:

Dr. Stanley Bates
Dr. Wallace Brey
Dr. Cliff Johnston

Post-Doctoral Associates:

Dr. Bethany Bechtel
Dr. Michael L. Free

Graduate Students:

Shaobin Du
Joseph Kudla
Vikram Shishodia
Shoulian Zhu

Part-Time Student Technicians:

William Ahlmark
Adam Bogan
Andrew Garstkiewicz
Andrew Kulchin

TABLE OF CONTENTS

LIST OF TABLES

LIST OF FIGURES

SUMMARY

This study has focussed on improving phosphogypsum filtration through the addition of additives, as well as gaining a more clear understanding of the role of additives in enhanced filtration. The results from this study show that several additives are effective in enhancing filtration. The most effective additives are polyethyleneoxide, alkylated sulfonates, and polyacrylamides. The addition of the additives has been shown to increase the hydrodynamic size of the phosphogypsum particles when added during the digestion stage of phosphoric acid production. Experimental results indicate that the phosphogypsum particle size is altered during the nucleation stage of crystal growth. Additional results from NMR spectroscopy indicate that the additives alter the fluorine-19 and phosphorous-31 levels in the phosphogypsum. It is hoped that the findings in this study will lead to increased productivity in the Florida phosphate industry.

INTRODUCTION

Improving the efficiency of phosphogypsum filtration is critical to economic utilization of the South Florida Phosphate Rock. Although physical beneficiation efforts are underway for the separation of impurities, specifications of the feed rock used in phosphoric acid plants may not be met by beneficiation alone. It appears that feed with higher impurities than presently encountered will eventually be used for phosphoric acid production. Future phosphate feed rock contains larger quantities of some impurities such as Mg, Al, Fe, and F and active silica Some of these impurities are known to decrease the cake filterability, increase the viscosity of phosphoric acid, and increase lattice and soluble P_2O_5 losses. In order to mitigate the effect of impurities and ensure high filtration efficiency, it is critical to understand their role in the phosphoric acid production process especially in changing the phosphogypsum crystal morphology.

Past studies to examine the effect of phosphogypsum morphology on filtration efficiency have been based on phosphogypsum precipitated from reagent systems.[1-4] These fmdings, therefore, have been of limited utility in the industry. Studies related to the effect of various impurities (such as Mg, Al, Fe) are more scarce. Contradictory results about the effects of impurities have been reported. No means have been found to mitigate their inhibitory effect on phosphogypsum filtration or to enhance their positive effects.

Attempts to improve the filtration rate using polymers as "filter aids" have been made on an industrial scale. The polymer in such cases is added just prior to the filtration step to flocculate the fine gypsum particles. The improvement in filtration by filter aids is usually less than 20 %. However, from a practical standpoint "overdosing", which decreases filtration efficiency, is a major limitation of filter aids.

The need to develop more efficient phosphogypsum filtration for the current and future phosphate rock with higher impuritity levels as well as the need to understand the effect of impurities and filtration enhancing additives has led to the current multidisciplinary study.

EXPERIMENTAL

Materials Characterization

This study involved three basic feed materials: current phosphate feed rock, high iron feed rock, and high dolomite feed rock. The size analysis of the feed materials used in this study is presented in Table 1. The chemical composition of the feed material is presented in Table 2.

Table 1
Comparison of Size Analyses for Various Phosphate Feed Rocks

Size (Mesh)	Current Rock Weight %	High Iron Rock Weight %	High Dolomite Rock 1 Weight %	High Dolomite Rock 2 Weight %
+ 48	-	-	8.4	12.5
- 48 to + 65	37.1	23.3	13.2	19.4
- 65 to +100	19.1	16.5	17.5	16.3
- 100 to + 150	11.1	17.7	11.6	11.7
- 150 to + 200	8.7	17.9	11.9	10.4
- 200 to + 270	-	-	-	11.1
- 270 to + 325	4.8	10.4	14.1	11.6
- 325	19.2	14.2	23.3	7.0

Note that the high dolomite rock 1 was used only in the preliminary tests, whereas the high dolomite rock 2 was used in all of the remaining digestion/filtration tests.

Phosphogypsum Batch Filtration Tests

All batch filtration tests were conducted to simulate plant conditions. This was achieved by building up the P_2O_5 content in a series of recycled batch tests to simulate the effect of recycling in plant operations. The following is an outline of the recycle gypsum and filtrate production procedure:

1) First Cycle:

The digestion solution was prepared by mixing 515 ml of tap water and 15 ml of 98 % sulfuric acid, which resulted in a 5 % sulfuric acid solution. (For the polymer or sulfonate addition tests, it was necessary to deduct the volume of the additive solution, which was going to be added into the system, from the amount of tap water). Next, the

Table 2
Chemical composition of the phosphate feed rock materials

Compound	Current Rock Weight %	High Iron Rock Weight %	High Dolomite Rock 1 Weight %	High Dolomite Rock 2 Weight %
P_2O_5	30.38	27.18	28.71	27.22
CaO	45.16	43.47	42.42	42.79
MgO	0.59	0.55	1.71	1.58
Fe_2O_3	2.31	2.11	2.56	1.56
Al_2O_3	3.76	1.53	3.46	0.95
Na_2O	0.99	0.48	0.60	0.73
K_2O	0.27	0.25	0.19	0.12
Insol.	6.03	5.84	5.50	8.05

Note that the high dolomite rock 1 was used only in the preliminary tests, whereas the high dolomite rock 2 was used in all of the remaining digestion/filtration tests.

solution was heated to **80°C** and 240 grams of feed rock sample was added simultaneously with 95 ml of 98 % sulfuric acid over a 30 minute period while the reactor slurry was agitated by an impeller with a tip speed of 1.47 m/s (600 RPM). For the modification test, polymer solution was added gradually over the entire digestion stage. Next, the slurry was agitated for an additional two and a half hours at a 1.01 m/s tip speed (450 RPM) and then filtered (0.5 atm pressure drop across the cake). Finally, the filter cake was washed twice with 400 ml of tap water at **80°C.**

2) Second Cycle:

The process outlined in the first cycle was repeated. However, in this cycle all of the filtrate plus some of the first wash solution were used to make up 530 ml of digestion solution, and 85 ml of 98 % sulfuric acid were used to digest the rock. After the digestion and crystallization processes, the cake was washed with all of the second wash solution from the first cycle and then with 400 ml of tap water, all at **80°C.** The filtrate was then analyzed for P_2O_5 and sulfate contents.

3) Third Cycle:

The second cycle was repeated with 102 ml (or slightly more depending upon the desired sulfate level) of 98 % sulfuric acid.

4) Fourth cycle:

The third cycle is repeated with 103 ml (or slightly more depending upon the desired sulfate level) of 98 % sulfuric acid. Based upon the analysis of the filtrate from the third cycle, the amount of filtrate used to make the initial digestion solution for this cycle will vary. The purpose of this cycle is to generate a filtrate of 26.5-28.5 % P_2O_5 produced under conditions which simulate a plant operation. Figure 1 illustrates the various inlet and outlet streams associated with the final cycle from which the filtration rate data is obtained.

Comparison of Industrial and Laboratory Filtration Rates

The validity of bench test filtration was evaluated with respect to the measured filtration rates by on-site filtration testing. The bench filtration assembly was transported to an industrial phosphoric acid production facility and a sample of plant slurry was filtered using the bench filtration assembly. The resulting bench filtration rate was 5.9 metric tons (m.t.) $P_2O_5/m^2/day$ in comparison to the plant filtration rate of 5.5 m.t. $P_2O_5/m^2/day$. Because the plant was not operating under normal conditions, it was decided that another analysis should be made. Under the normal operating conditions, the measured rate using the bench filtration assembly was 10.6 m.t. $P_2O_5/m^2/day$ in comparison to the plant filtration rate of 10.3 m.t. $P_2O_5/m^2/day$. These results indicate the bench filtration assembly provides a very good estimate of plant filtration rate information. In fact, it appears that no batch filtration correction factor is necessary.

In addition to comparing the rates of filtration between the bench and industrial filtration, samples were taken and analyzed by scanning electron microscopy and found to be reasonably similar as presented in Figures 2 and 3.

P_2O_5 Mass Balance

To insure that all P_2O_5 could be accounted for in each test, a mass balance was prepared as per the layout of the batch filtration test (fourth cycle) in Figure 1. All of the inlet and outlet streams for two batch experiments were weighed and analyzed for P_2O_5. The results are shown below in Tables 3 and 4 for tests A and B, respectively. A comparison of the total inlet and total outlet P_2O_5 values in Tables 3 and 4 shows that the overall P_2O_5 mass balance is excellent. The total inlet and total outlet data from tests A and B agree to within 2.1 and 1.0 %, respectively. Note that the sulfuric acid and additive solution streams were not included in the balance because they contain no measurable P_2O_5.

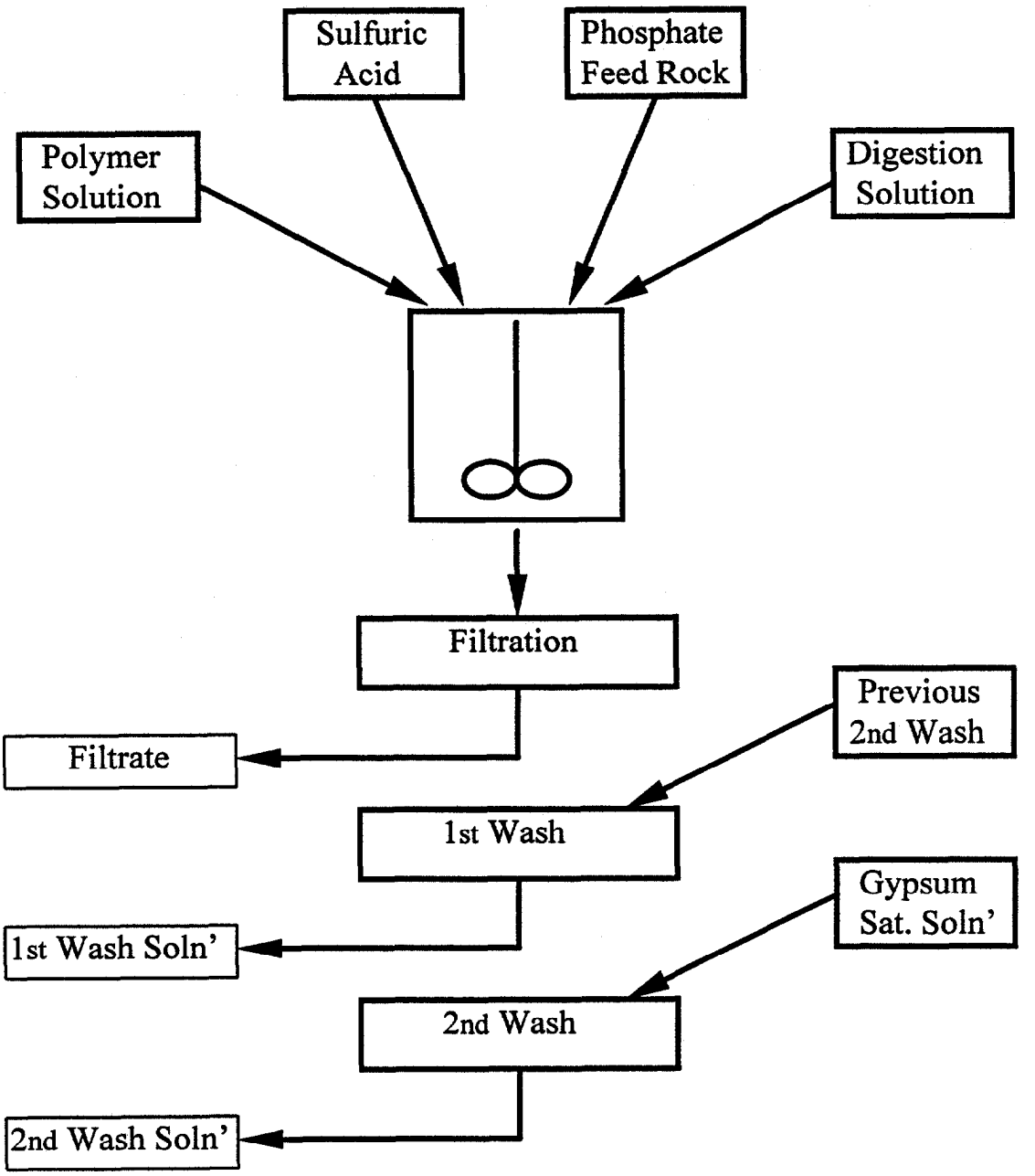

Figure 1: Schematic representation of inlet and outlet streams in the fourth cycle batch test from which the filtration rate data are obtained.

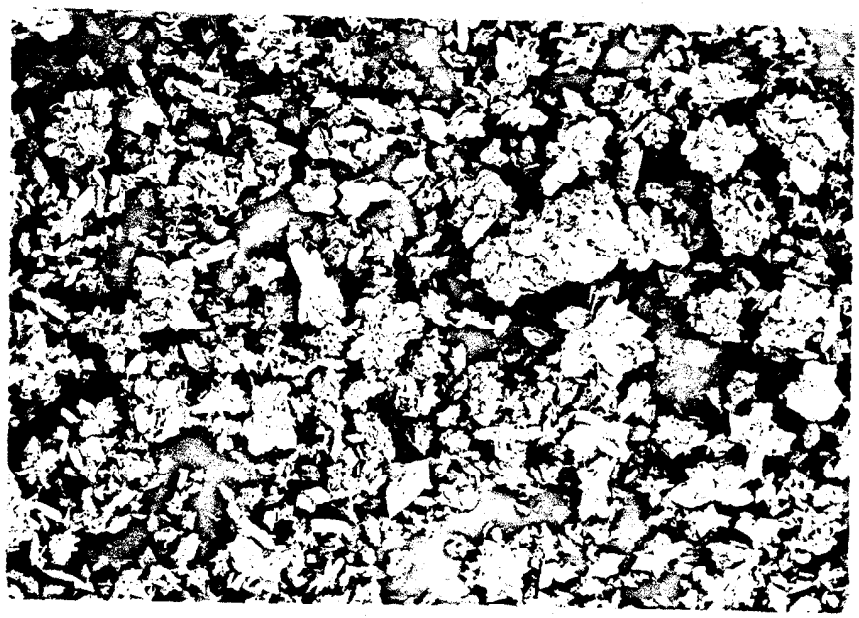

Figure 2: SEM micrograph of phosphogypsum produced in an industrial facility.

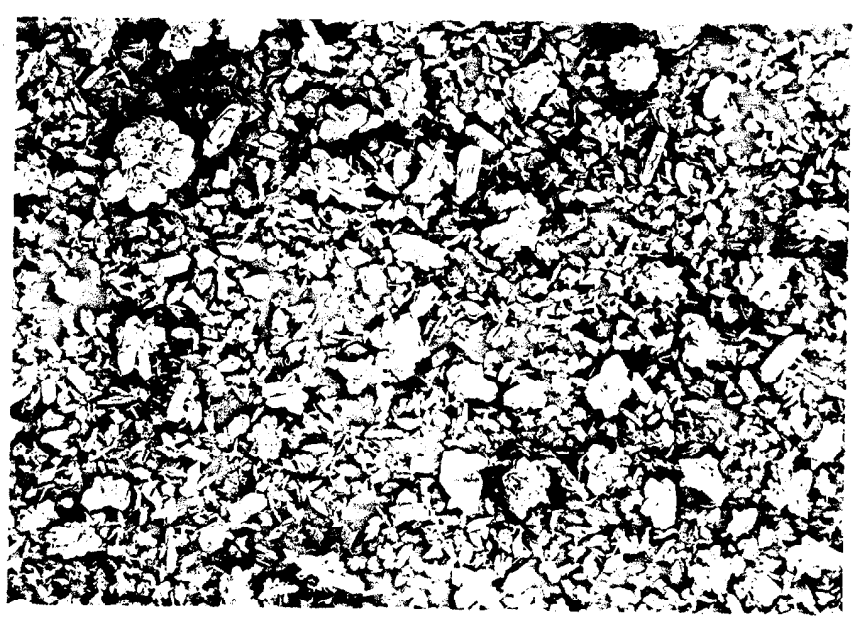

Figure 3: SEM micrograph of phosphogypsum produced in batch filtration tests.

Size Analysis

Size analysis was carried out using standard Tyler Mesh sieves and a Ro-Tap shaker. Approximately SO grams of the desired mineral substrate was split from the main sample and placed in the set of sieves for each test. Each sample was shaken for 20 minutes, following which all resulting size fractions were weighed to one one-hundredth of a gram. For the coarse material in the feed rock, the 48, 65, 100, 150, 200, 270, and 325 mesh screens were used, whereas for the gypsum product, the 100, 150, 200, 270, 325, and 400 mesh screens were used. Note that all feed material was ground to -35 mesh. All gypsum product was prescreened at 28 mesh in order to break up minor quantities of clumps of material that formed during the drying process.

Table 3

P_2O_5 mass balance for test A.

Inlet Streams	weight (g)	% P_2O_5	weight of P_2O_5 (g)
Digestion Solution	630.1	22.02	138.75
1st Wash Solution	405.8	7.73	31.37
2nd Wash Solution	435.1	0.83	3.61
Phosphate Rock	240.0	27.45	65.88
Total (Inlet Streams)			**239.61**

Outlet Streams	weight (g)	% P_2O_5	weight of P_2O_5 (g)
Filtrate	277.6	27.86	77.34
1st Wash Filtrate	588.9	19.45	114.54
2nd Wash Filtrate	435.1*	7.19	31.28
Vessel Rinse Soln'	86.4**	5.75	4.97
Gypsum Product	332.6	1.97	6.55
Total (Outlet Streams)			**234.68**

* The weight of the second wash filtrate was assumed to be the same as the 1st Wash Solution.

** The reaction vessel and impeller were rinsed and the solution collected and analyzed.

Column Settling

Initially, we proposed using an X-ray Sedigraph to determine the size distribution of phosphogypsum in the batch reactor slurries just prior to filtration, thus eliminating experimental artifacts that could arise during the processes of drying and dry screening. Unfortunately, the high dissolved solids content in the phosphoric acid precluded any analysis using the X-ray Sedigraph due to complete absorption of incident X-rays by the dissolved solution species. Other attempts using phosphogypsum in water and glycol mixtures in the X-ray Sedigraph were also unsuccessful due to inefficient bubble elimination and the unknown interactions between the ethylene glycol and the polymer. Our lack of success with the X-ray Sedigraph led us to column settling.

In order to obtain accurate size distribution information about phosphogypsum using the column settling technique, a set of procedures was established. Specifically, procedures were established with regard to the preparation of the column suspension medium, reactor slurry sampling, column sampling, and size distribution analysis.

Table 4

P_2O_5 mass balance for test B.

Inlet Streams	weight (g)	% P_2O_5	weight of P_2O_5 (g)
Digestion Solution	615.9	22.02	135.62
1st Wash Solution	398.5	5.61	22.36
2nd Wash Solution	416.8	0.83	3.46
Phosphate Rock	240.0	27.45	65.88
Total (Inlet Streams)			**227.32**

Outlet Streams	weight (g)	% P_2O_5	weight of P_2O_5 (g)
Filtrate	252.4	28.90	72.94
1st Wash Filtrate	548.0	21.51	117.87
2nd Wash Filtrate	416.8*	5.47	22.80
Vessel Rinse Soln'	93.0**	8.50	7.91
Gypsum Product	336.3	1.47	4.94
Total (Outlet Streams)			**226.46**

* The weight of the second wash filtrate was assumed to be the same as the 1st wash solution.

** The reaction vessel and impeller were rinsed and the solution collected and analyzed.

Column Suspension Medium Preparation

Before each test, a phosphoric acid solution (27.5 % P_2O_5) was prepared using o-phosphoric acid (85 %) from Fisher Scientific Company mixed with the appropriate amount of Gainesville tap water. To saturate this synthetic phosphoric acid solution with respect to phosphogypsum, 60 grams of phosphogypsum from our baseline filtration studies were added to the mixture. The resulting slurry was stirred for one hour at 40°C then allowed to settle and cool to room temperature for an additional 16 hours. After the saturation cycle was completed, the slurry was filtered using 0.2 µm pore-size filtration discs before being placed in the columns.

Batch Reactor Sampling

All samples were acquired directly from the batch test reactor at 80°C immediately prior to filtration using a 20 ml syringe 4 mm in diameter. Each slurry sample of approximately 20 ml was immediately diluted into a small graduated cylinder containing 80 ml of the column suspension medium. The diluted mixture was then added to the settling column for a total volume of approximately 1480 ml. Because each sample contained approximately 10 grams of dry solids, the solids loading in the column was approximately 0.55 % by weight, allowing the particles to settle with a minimum of hindrance by neighboring particles.

Column Sampling

After the sample was introduced into the column and the column was filled to the designated level, a stopper was placed over the open end of the column and the column was repeatedly inverted for 2 minutes to thoroughly mix the column contents. Settling time monitoring began as soon as mixing was complete and the column was placed in the upright position. At the specified time intervals (6, 18, 36, 54, and 108 minutes), an 18 ml sample of the settled column contents was extracted through a valve at the bottom of the column, making sure all of the settled solids were removed. Each sample was filtered using preweighed 0.2 µm pore-size filtration discs, then rinsed with gypsum saturated tap water. The remaining solution was also filtered after the l08-minute sample was taken. After filtration and rinsing, the samples were dried and weighed to determine the mass of solids in each sample. The size distribution was determined using the weights of phosphogypsum in each sample.

Size Distribution Calculation

The size distribution was calculated based upon Stoke's Law which assumes spherical particles, thus the resulting size distribution is in terms of Stoke's equivalent diameter rather than the actual diameter. Stoke's Law is generally accurate for Reynold's numbers below approximately 5 according to work by Lapple and Shepherd (Ind. Eng. Chem., 32, 605-617), although some small errors occur for Reynold's numbers above 0.3.

All particle sizes analyzed in this study had Reynolds numbers less than 0.6, thus ensuring reasonably accurate Stoke's equivalent size distributions.

By mixing the column immediately prior to settling, the distribution of particles in the column is uniform. In other words, all particles within a given size class are found in equal concentrations throughout the column. After settling begins, the larger particles fall faster and become more concentrated in the first samples relative to the smaller particles. Mathematically, the settling can be expressed in a discretized form according to individual samples and size classes as:

$$W_1 = (V_A \Delta t_1/H + S_{1A})W_A + (V_B \Delta t_1/H + S_{1B})W_B + ...$$
$$W_2 = (V_A \Delta t_2/H + S_{2A})W_A + (V_B \Delta t_1/H + S_{2B})W_B + ...$$
$$\vdots$$
$$W_n = (V_A \Delta t_n/H + S_{nA})W_A + (V_B \Delta t_n/H + S_{nB})W_B + ...$$

where: $W_1, W_2, ... W_n$ = Weight of sample 1, 2, ...n

$\Delta t_1, \Delta t_2, ... \Delta t_n$ = Time of sampling period for sample 1, 2, ...n

$S_{1A}, S_{2B}, ...$ = Fraction of material removed in sample 1, 2, ... that was suspended in size class A, B, ...

$W_A, W_B, ...$ = Weight of sample in size class A, B, ...

$V_A, V_B, ...$ = Terminal settling velocity of particles in size class A, B, ... (based upon Stoke's Law for spherical particles)

Please note, however, that the time intervals (6, 18, 36, 54, 108, +108 minutes) and average phosphogypsum particle sizes in each size class (141, 68, 43, 35, 25, and 13 µm) were selected to avoid singularities in the solution of the resulting matrix. The key to setting up the matrix properly is to ensure that each time and size interval allows a new class of particles to completely settle out of the column. Also, it is important to take into consideration the amount of suspended material that is removed from each size class during each sampling.

Each column was filled to a height of 85 cm. The inside diameter of each column was approximately 4.7 cm. The column solution was measured after the final filtration in two independent tests to determine the density and viscosity of the solution. The resulting values for density were 1.236 and 1.232 g/cc (average value of 1.234 g/cc). The viscosities were 2.90 and 2.94 cP at 23°C (average of 2.92 cP). These average values were used in the size distribution calculations.

Calibration and Size Analysis by Column Settling

The column settling techniqued discussed in the May 1995 quarterly progress report was calibrated this quarter using silica spheres purchased from Duke Scientific Company. The results from the calibration are presented in Figure 4. The data in Figure 4 indicate that the average size analysis obtained from two column settling experiments is close to the actual values, thus no correction factor is necessary. Actual sizes in this analysis were determined by dry screening and sedimentation/siphoning particle classification. The sedimentation/siphoning technique consisted of allowing particles to settle a known distance corresponding to a specific particle size followed by careful siphoning and resuspension. The process was repeated three times for each of two size classifications and is closely related to the Andreasen pipet size characterization method.

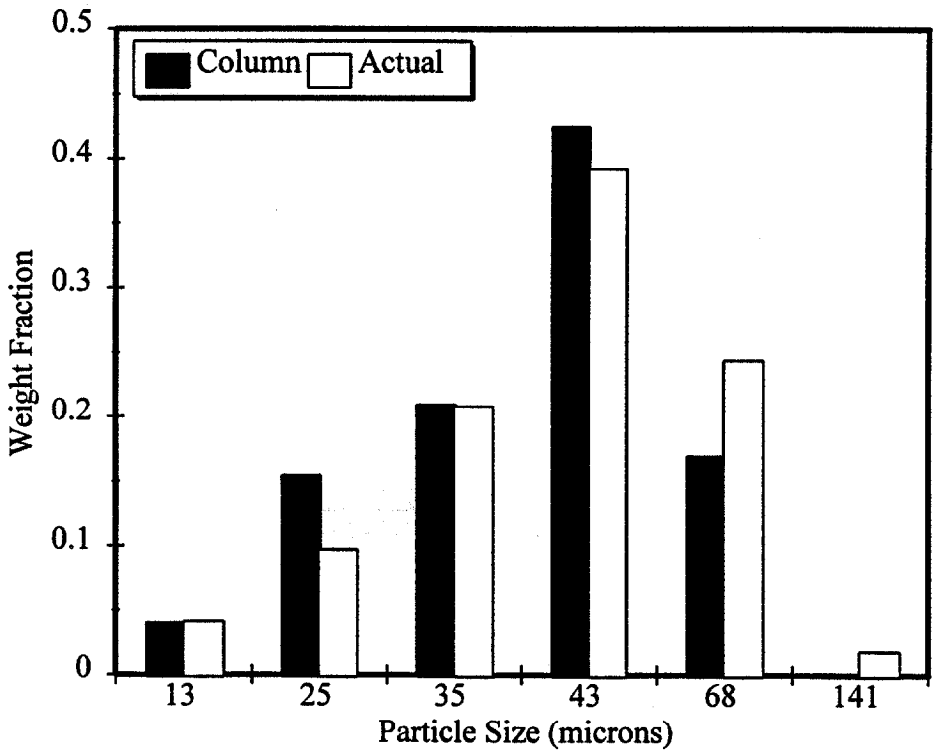

Figure 4: Comparison of measured and calculated particle sizes using the column settling technique with silica spheres in a diluted phosphoric acid medium (27.5 % P_2O_5). Note that the measured values were determined by dry screen analyses together with sucessive sedimentation/siphoning.

Effect of Drying

In general, dry sieve size analyses do not have the expected correlation with the rates of filtration as shown in Figure 5 in which the rates do not correlate with $1/area^2$. However, Figure 5 also shows that the column settling size data do correlate with the rate of filtration. The difference between the dry screen and column size data is believed to be associated with the drying and sample preparation involved in performing the dry screen size analysis. Dry screen analyses require sample preparation that involves breaking up the dried filter cake as well as prescreening to break up smaller clumps of filter cake material. In contrast, the column settling size analysis is performed using slurry directly from the reaction vessel just prior to filtration, thereby eliminating any artifacts due to sample drying and preparation. The effect of drying is clearly evident by comparing column settling results from samples before drying to those after drying as shown in Figures 6 and 7. The data in Figure 7 shows that the drying/sample preparation process leads to finer particles than were originally present in the slurry sample. These results indicate that dry screen size analyses of phosphogypsum samples are not reliable for filtration analyses. The same data also suggests that column settling, which provides the hydrodynamic or Stoke's equivalent particle diameter, leads to information that correlates well with measured filtration rate data.

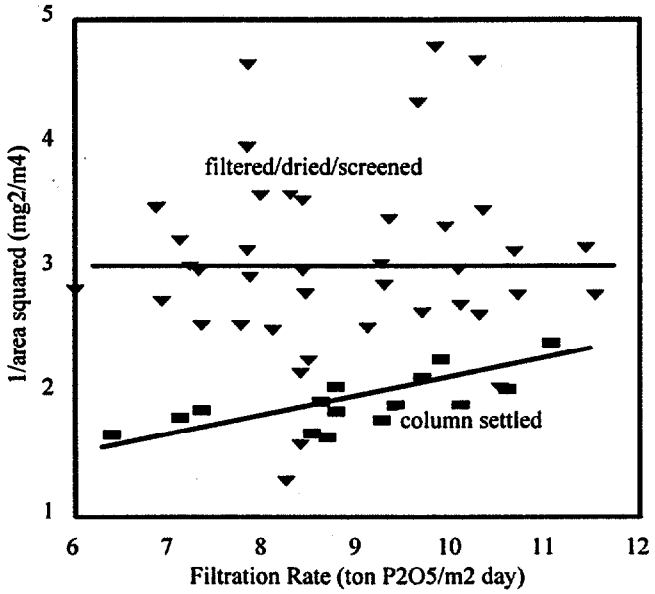

Figure 5: Comparison of the rate of filtration for various experiments with $1/area^2$ determined by both dry screen and column settling size analyses. Note that the geometric area was used in the case of the dry screen analysis and the Stoke's equivalent area was used for the column settling.

Efficiency Calculations

The efficiency calculations were made as follows:

$$\text{Digestion Efficiency} = 100 - 94\frac{(A-B)C}{DE}$$

$$\text{Filtration Efficiency} = 100 - 94\frac{BC}{DE}$$

$$\text{Overall Efficiency} = 100 - 94\frac{AC}{DE}$$

where:

A = % total P_2O_5 in gypsum cake,

B = % water soluble P_2O_5 in gypsum cake,

C = % CaO in rock used to make the acid,

D = % P_2O_5 in rock used to make the acid, and

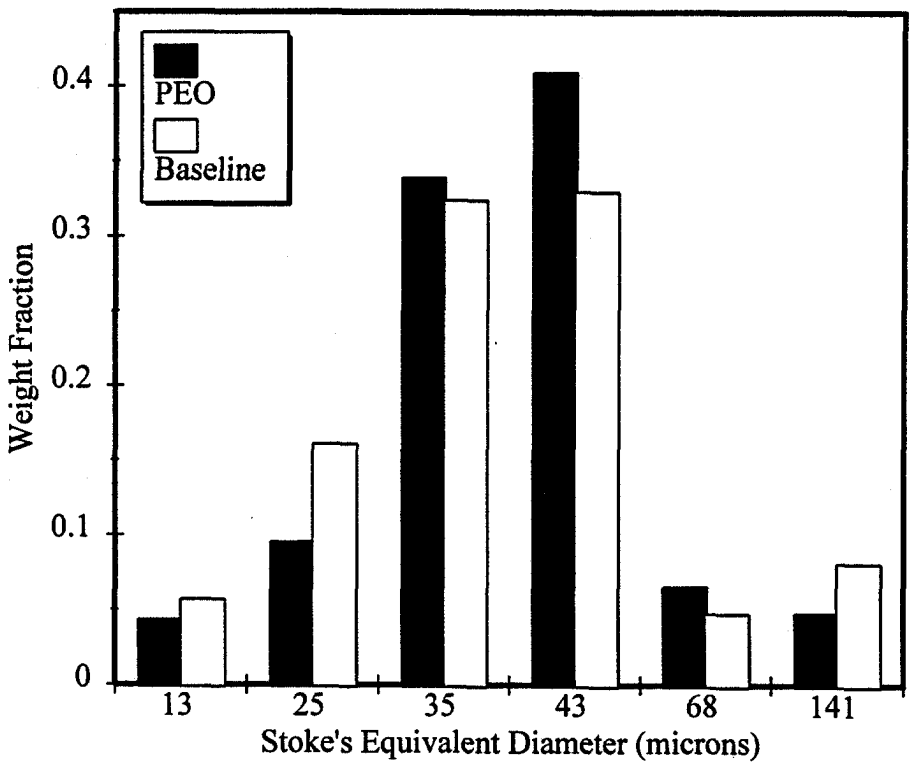

Figure 6: Comparison of column size data for PEO and baseline phosphogypsum slurry samples prior to filtration.

E = % CaO in gypsum cake.

All filtration rates were calculated using the following formula:

$$\text{Filtration Rate} = \frac{cp}{at}$$

where: c = dry gypsum cake weight,

p = weight of P_2O_5 produced per gram of gypsum, which is calculated as follows(values in %):

$$p = \frac{(Rock\%P_2O_5)}{[\frac{(Rock\%CaO)(Mol.wt.CaSO_4 \bullet 2H_2O)}{Mol.wt.CaO}] + Rock\%Insol.}$$

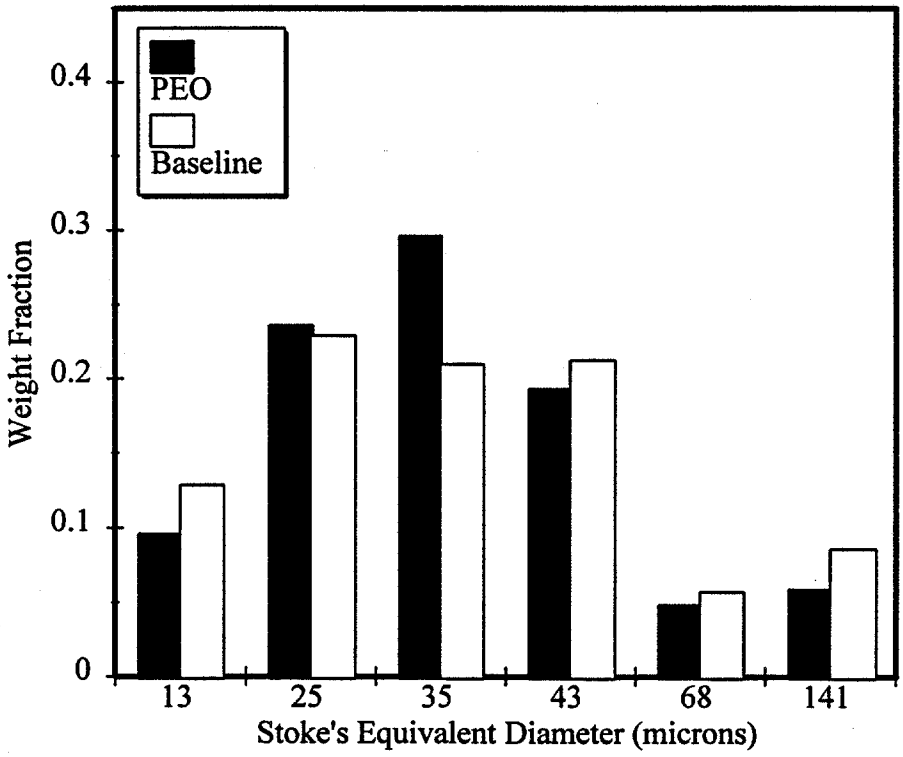

Figure 7: Comparison of column size data for dried PEO-treated and baseline phosphogypsum samples obtained from the same experiments as those used to produce Figure 6. The filter cakes were dried at 60°C for 24 hours, then broken up and prescreened using a 28 Mesh screen prior to introducing them in the columns.

t = filtration time, and
a = filtration area (0.0143 m^2).

Chemical Analysis

All chemical analyses were performed using a Perkin Elmer Plasma II ICP instrument. Solutions were diluted as necessary to reduce the concentration of species to less than 300 ppm. All solid samples were analyzed by first grinding 3 grams of material in a mortar grinder for 10 minutes. Next, 1 gram of ground sample was digested with 25 ml of aqua regia (1 HCl, 2 HNO_3, 2 H_2O) at 95°C for 30 minutes. The solution was then filtered with P5 (medium porosity) filter paper (Fisher Brand) and then diluted as needed.

Total P_2O_5 Analysis

The following sample preparation procedure was used to determine the total P_2O_5 content:

1) Weigh 1.000g of phosphogypsum sample into a small (150 ml) beaker.
2) Add 25 ml of aqua regia.
3) Heat mixture to 95°C for 30 minutes.
4) Add approximately 100 ml of deionized water and heat to 80°C for 5 minutes.
5) Filter the solution and wash the filter cake twice.
6) Dilute the filtrate/rinse solution to the appropriate volume for ICP analysis.

Water Soluble P_2O_5 Analysis

The following sample preparation procedure was used to determine the water soluble P_2O_5 content:

1) Weigh 1 .000 g of phosphogypsum into a 200 ml plastic cup.
2) Add 100 ml of phosphogypsum-saturated water and disperse the solids by sonication.
3) Let the solution settle overnight.
4) Remove a sample of the supernatant solution for ICP analysis.

Citrate Insoluble P_2O_5 Analysis

The following sample preparation procedure was used to determine the citrate insoluble P_2O_5 content:

1) Decant the liquid from the sample in step 4 of the water soluble P_2O_5 test.

2) Add 100 ml of deionized water to the solids fraction in step 1, then mix and allow to settle.
3) Decant the liquid from the sample in step 2.
4) Add 100 ml of ammonium citrate solution to the solids fraction of the sample from step 3 and heat the sample to 65°C for 1.5 hours.
5) Allow the solution to settle, then remove the liquid, add 100 ml of deionized water and allow the mixture to settle.
6) Decant the mixture from step 5.
7) Add 25 ml of aqua regia to the solids from step 6 and follow the total P_2O_5 analysis procedure to obtain the final solution sample for ICP analysis.

Flocculation Experiments

Flocculation was evaluated in this study by column settling. All samples were prepared by mixing 36.9g of baseline phosphogypsum with 85 ml of phosphogypsum-saturated phosphoric acid (27.5 % P_2O_5) then agitated at 1100 RPM for 1 minute at 80°C then a sample of the resulting slurry was removed and placed into columns and allowed to settle for 25 minutes. The settled solids were filtered, dried, and weighed as was the suspended portion of the solids.

Digestion Experiments

All digestion experiments were conducted by placing a 3-liter reaction vessel into a large water bath maintained at 80°C. The initial reaction solution consisted of phosphoric acid (27.5 % P_2O_5) and 2.7 % sulfate. Next, 15 grams of phosphate feed rock were added to the solution followed by the addition of the appropriate amount of polyethylene oxide or sodium dodecyl benzene sulfonate. Samples were taken from the reactor at selected time intervals, filtered using 1μm pore size filter discs, diluted, then analyzed for calcium using an ICP. During the digestion process, the reactor was stirred at 1100 RPM with a propeller-type impeller (2.9 m/s tip speed).

Nucleation Experiments

The nucleation experiments were performed by placing a 3-liter reaction vessel in a water bath maintained at 80°C. Two different solutions were prepared. The first solution consisted of water with 2.9 % (0.31 mol/l) sulfuric acid, 0.30 % (0.074 mol/l)

calcium, and the specified quantity of additives. The other solution was prepared by dissolving phosphate feed rock in phosphoric acid media (27.5 % P_2O_5) at 80°C after which the solution was filtered with 0.2 µm pore size filter paper. The later solution was adjusted to 2.5% sulfate by adding a phosphoric acid/sulfuric acid mixture. Each solution was stirred at 1100 RPM using a propeller-type impeller with a tip speed of 2.9 m/s. Samples were taken from the solution and analyzed for turbidity as a function of time. All turbidity measurements were made against calibrated turbidity standards using a Hach model 2100A turbidimeter.

NMR Experiments

Nuclear Magnetic Resonance (NMR) spectroscopy was utilized in this study to determine how additives affect the solution speciation, as well as how such speciation changes may be related to improvements in filtration. NMR spectroscopy is particularly useful in this study because of its sensitivity to the fluorine-19, aluminum-27, silicon-29, and phosphorus-31 nuclei, which are all found in process phosphoric acid produced from central Florida phosphate rock. The sensitivity of NMR for fluorine nuclei is high because the magnetic moment is large, the natural abundance is l00%, and the resonances are spread over a wide spectral range. Aluminum-27 is also 100% naturally abundant, but the materials used in spectrometer probes often contain high levels of this isotope. Of the remaining isotopes silicon-29 and phosphorus-31, only the phosphorus-31 is very favorable for NMR analysis. The ultimate success of the NMR analysis is a function of the magnitude of the nuclear magnetic moment, the natural abundance of the magnetic isotope, and the ability to obtain resolvable peaks in different local environments.

The liquid-phase NMR spectra were obtained using two instruments. The first instrument is a General Electric NT-300 spectrometer with a wide-bore magnet which accommodates 12-mm diameter sample tubes with samples of 3-ml volume. This instrument was especially modified by the addition of special computer and display capabilites, and operates at the appropriate frequencies for a 7.06-tesla magnetic field. The other spectrometer is a Varian Unity-500 instrument which accommodates 5-mm diameter sample tubes with 0.5-ml samples for fluorine and 10-mm diameter sample tubes with 2-ml samples for observation of other nuclei.

Several steps were taken to insure accurate solution-species NMR analyses. In some cases, solution NMR spectra were obtained at 80°C, room temperature, and -10°C to help understand the effect of temperature on speciation, as well as to obtain better resolution. Deuterium oxide was added to the solution samples to provide a lock solvent. In addition, solution samples were spun at 15 to 20 Hz to improve the resolution.

Viscosity Analysis

All viscosity values were obtained using Ubeholde viscometers that were either calibrated by the manufacturer using industry standards or at the University of Florida using high purity ethylene glycol which has a well established viscosity.[5] Using a version of the Poiseuille equation that has been modified for the Ubeholde viscometer design, the viscosity can be calculated as:[6]

$$\mu = \frac{t\rho g \Delta z \pi D^4}{128 V \Delta x}, \qquad (1)$$

in which μ is the viscosity, t is the efflux time, g is the acceleration of gravity, Δz is the change in height, D is the efflux tube diameter, V is the reservoir volume, and Δx is the length of the efflux tube. Because most of the parameters remain constant for a given viscometer, equation (1) can be rewritten as:

$$\mu = \rho K' t, \qquad (2)$$

thus a K' value can be determined for a given viscometer using a calibration standard such as ethylene glycol at the specified temperature.

Fourier Transform Infrared (FT-IR) Analyses

Samples were prepared for transmission spectroscopy by first grinding/dispersing 1.5 mg of sample with 150 mg of spectral-grade potassium bromide to < 2 µm. Next samples were desiccated to remove the interference of sorbed water. Finally the samples were compressed under a total force of 100,000 N.

Samples were prepared for diffuse reflectance analysis by first grinding/mixing 1.25 % sample in 98.75 % potassium bromide. After grinding/dispersing 200 mg of the mixture was placed in a 13 mm sample cup of a Spectra-Tech diffuse reflectance cell.

RESULTS AND DISCUSSION

Preliminary Reagent Screening

Early in the project, several polymers were tested to determine which ones would be more effective in enhancing filtration. Table 5 shows the preliminary screening results. Results from the preliminary screening indicated that for the current feed rock polyethyleneoxide was the most effective polymer, followed by the 12-million molecular weight polyacrylamide, SF 206. The resulting process efficiencies are presented in Table 6. These results show that polymers may have a slightly negative effect upon process efficiencies for current feed rock. For the high dolomite feed rock, the results were different as shown in Table 7. The results from this series of screening tests revealed that SF 206, a strongly anionic polyacrylamide, was the most effective polymer. The next most effective additive was 4 million molecular weight polyethyleneoxide. Also, results showed that the overall improvement in the rate of filtration due to the additives was generally lower for the high-dolomite feed rock.

Table 5
Comparison of Polymer-Enhanced Filtration Results Using Current Feed Rock

Additive	Polymer Type	Molecular Weight	Charge Nature	Change From Baseline
(baseline)	-	-	-	-
SF 208	acrylamide	18-20 million	strongly anionic	+35
SF 206	acrylamide	10-12 million	strongly anionic	+49
SF 127	acrylamide	10 million	nonionic	+19
PVS	vinyl sulfonate	2,000	anionic	+37
PEO	ethylene oxide	4 million	nonionic	+72
PGA	glutamic acid	50,000-100,000	anionic	-3

Note that all additives were added during the digestion stage at 0.09 kg per ton of gypsum.

Process efficiencies were also examined to determine how they might be affected by the polymer additions. The results from the efficiency experiments are presented in Table 8. The overall, digestion, and filtration efficiency values from the experiments in which polymer was added are slightly better than the baseline test efficiencies as indicated in Table 8.

Table 6
Effect of Additives on Process Efficiencies for Current Feed Rock

Additive	Digestion Efficiency (%)	Filtration Efficiency (%)	Overall Efficiency (%)
(baseline)	95.9	99.0	94.9
SF 208	94.8	96.4	91.2
SF 206	96.8	98.9	95.6
SF 127	94.8	99.0	93.7
PVS	93.0	98.7	91.7
PEO	95.7	98.9	94.6
PGA	95.6	98.5	93.7

Note that all polymers were applied in 0.09 kg per ton of gypsum dosages. The error in the efficiency determinations is approximately 0.4 %.

Table 7
Comparison of Polymer-Enhanced Filtration Results Using High-Dolomite Feed Rock 1

Additive	Polymer Type	Molecular Weight	Charge Nature	Change From Baseline
(baseline)	-	-	-	-
SF 208	acrylamide	18-20 million	strongly anionic	+17
SF 206	acrylamide	10-12 million	strongly anionic	+28
SF 127	acrylamide	10 million	nonionic	+12
PVS	vinyl sulfonate	2,000	anionic	+10
PEO	ethylene oxide	4 million	nonionic	+18

Note that all additives were added during the digestion stage at 0.10 kg per ton of gypsum. Also, note that the phosphate feed rock was different than in subsequent tests.

Table 8
Effect of Additives on Process Efficiencies for High-Dolomite Feed Rock 1

Additive	Digestion Efficiency (%)	Filtration Efficiency (%)	Overall Efficiency (%)
(baseline)	92.9	97.3	90.2
SF 208	94.1	97.4	91.5
SF 206	93.6	97.8	91.5
SF 127	93.9	97.6	91.4
PVS	93.2	97.8	91.0
PEO	93.3	97.7	91.0

Based upon the enhancements in the rate of filtration as well as the increase in process efficiencies obtained using PEO and SF 206, it was decided that both of these compounds would be studied in more detail in a series of batch filtration experiments.

Preliminary Evaluation of Addition Time

Experiments were conducted using Percol 919 and Polymer 812E added either in the digestion stage or just prior to filtration to determine the effect of additives as a function of addition time. Results from these batch filtration tests are presented in Tables 9 and 10. The improvement of filtration rate upon addition of Percol 919 ranges from 10 % when applied during the digestion stage, and 23 % when added just prior to filtration as a filter aid. The use of Polymer 812E resulted in an improvement of 14 % when added during digestion and 17 % when added as a filter aid. These tests were all performed with a free sulfate level of 1.25 %. These results compare very well with data obtained by Arr-Maz Products in plant tests (April, 1993) which show an improvement of 12 % using Polymer 812E as a filter aid.

Phosphogypsum from the Percol 919 and Polymer 812E experiments are shown in the SEM micrographs presented as Figures 7 through 11. The SEM micrographs illustrate that the application of Percol 919 results in larger phosphogypsum aggregates when added as a filter aid rather than during the digestion stage. The use of Polymer 812E did not appear to be affected by the addition time because the aggregates from the filter aid test are nearly the same size as those from the digestion test. These SEM results corroborate the filtration rate data which shows Percol 919 is most effective as a filter aid.

The efficiencies from the Percol 919 and Polymer 812E experiments are presented in Tables 11 and 12. These data show that the addition of these polymers does not significantly affect the process efficiencies. It should be noted that the feed rock

Table 9
Filtration Tests With Percol 919
(1.25 % free sulfate)

Polymer Addition Time	Dosage (kg/ton)	Change from Baseline Rate
No Polymer (Baseline)	0.00	-
Digestion Stage	0.09	+ 10 %
Just Prior to Filtration (Filter Aid)	0.05	+ 23 %

Table 10
Filtration Tests With Polymer 812E
(1.25 % free sulfate)

Polymer Addition Time	Dosage (kg/ton)	Change from Baseline Rate
No Polymer (Baseline)	0.00	-
Digestion Stage	0.06	+ 14 %
Just Prior to Filtration (Filter Aid)	0.05	+ 17 %

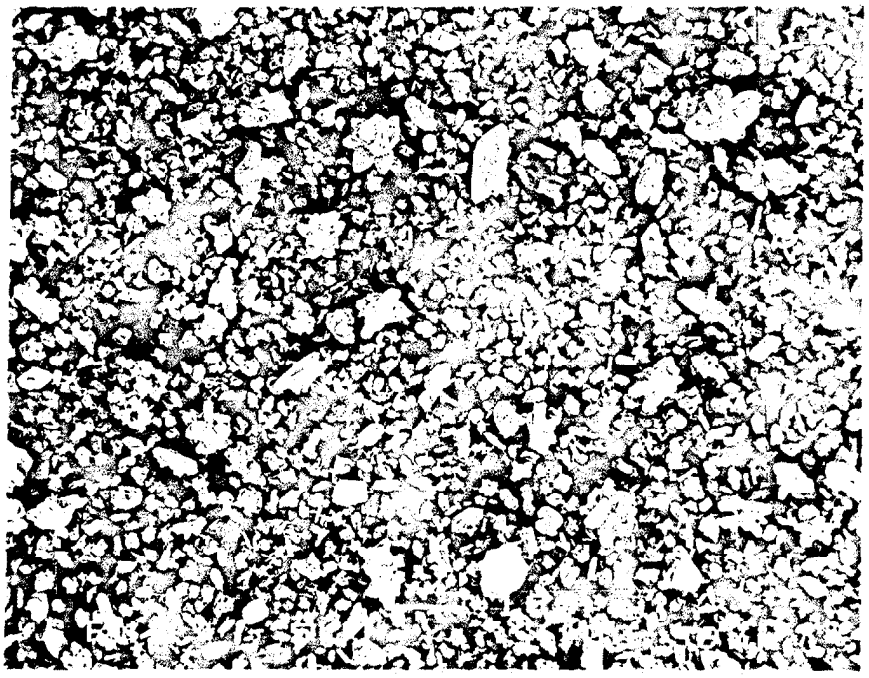

Figure 8: SEM micrograph of phosphogypsum treated with Percol 919 during the digestion stage of phosphoric acid production.

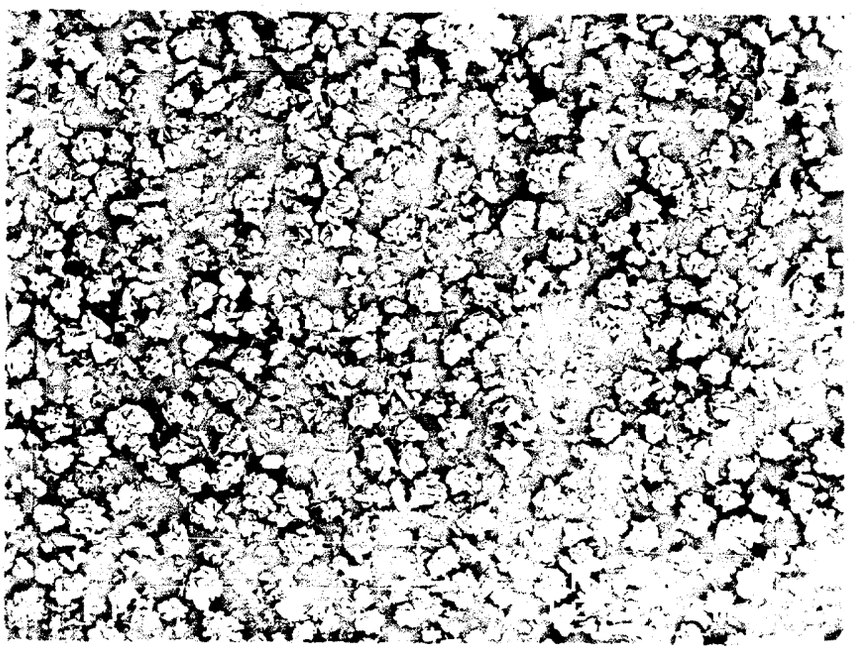

Figure 9: SEM micrograph of phosphogypsum treated with Percol 919 as a filter aid just prior to filtration.

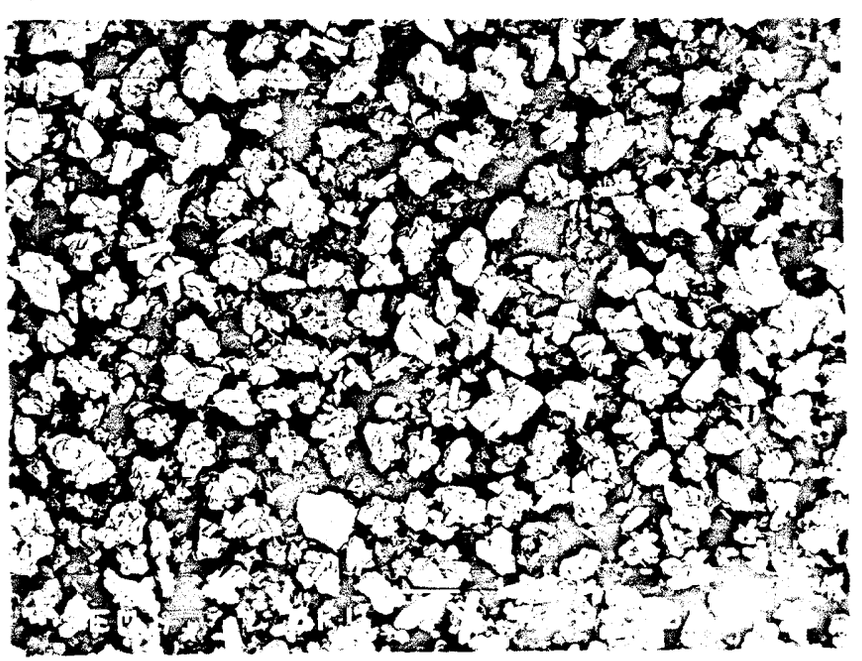

Figure 10: SEM micrograph of phosphogypsum treated with Polymer 812E during the digestion stage of phosphoric acid production.

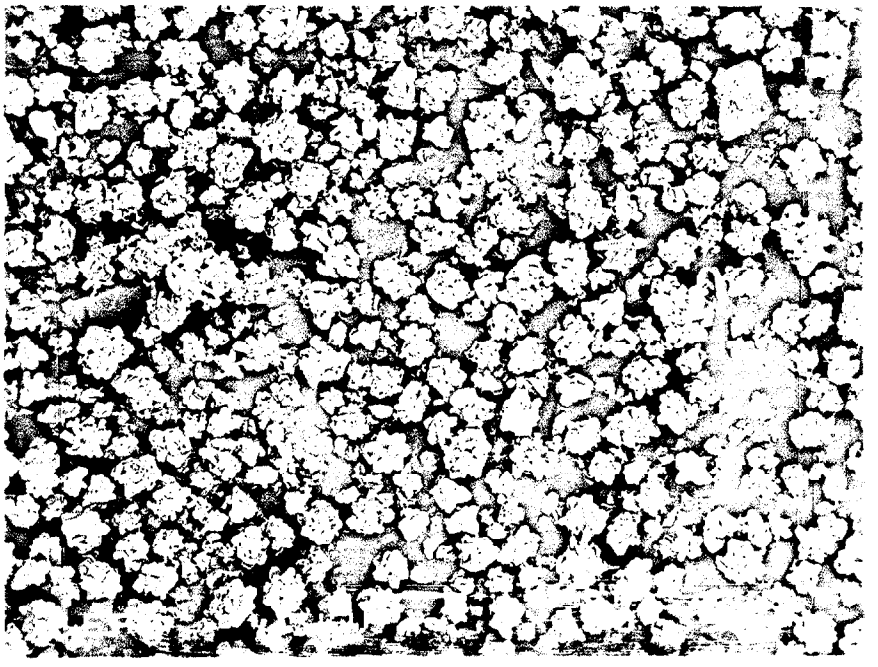

Figure 11: SEM micrograph of phosphogypsum treated with Polymer 812E as a filter aid just prior to filtration.

Table 11
Process Efficiencies Using Percol 919

Test	Digestion Efficiency (%)	Filtration Efficiency (%)	Overall Efficiency (%)
Baseline	96.0	98.9	95.0
Digestion Addition	96.0	97.6	93.6
Filter Aid Addition	95.2	98.0	93.2

Table 12
Process Efficiencies Using Polymer 812E

Test	Digestion Efficiency (%)	Filtration Efficiency (%)	Overall Efficiency (%)
Baseline	96.0	98.9	95.0
Digestion Addition	96.5	97.0	93.5
Filter Aid Addition	95.1	98.7	93.8

sample used in these tests was the same high dolomite sample used in previous preliminary testing, which is different than the sample used in most of the tests in the remainder of this study.

Effect of Kaolin

The effect of kaolin on the rate of filtration was evaluated to determine if it could enhance the rate of filtration by providing both alumina and silica to the system, which generally are believed to enhance the rate of phosphogypsum filtration.[7] The composition of the kaolin is presented in Table 13. Results from the addition of 1 % kaolin in the feed resulted in a filtration rate of 3.5 ± 0.1 m.t. P_2O_5/m^2/day, which is approximately 25 % lower than the corresponding baseline filtration rate. The digestion efficiency for the kaolin addition tests was 95.0 ± 0.1 %, the filtration efficiency was 99.3 %, and the overall efficiency was 94.2 ± 0.1 %.

It is believed that under the conditions evaluated in this study, the kaolin decreased the rate of filtration primarily by decreasing the average crystal size. Figure 12 shows what appear to be smaller phosphogypsum crystals than are generally present in baseline phosphogypsum samples (see Figure 3). Also, it is likely that the addition of kaolin increased the viscosity of the slurry and filtrate due to the added dissolved species as well as to the presence of residual particulate matter. All of these factors help to explain the observed decrease in the rate of filtration that resulted from the addition of kaolin.

Table 13
Chemical Composition of Kaolin Used in This Study

Compound	Weight Percent
SiO_2	46.5
Al_2O_3	37.6
Fe_2O_3	0.51
P_2O_5	0.19
CaO	0.25
MgO	0.16
Na_2O	0.02
K_2O	0.40
SO_3	0.21

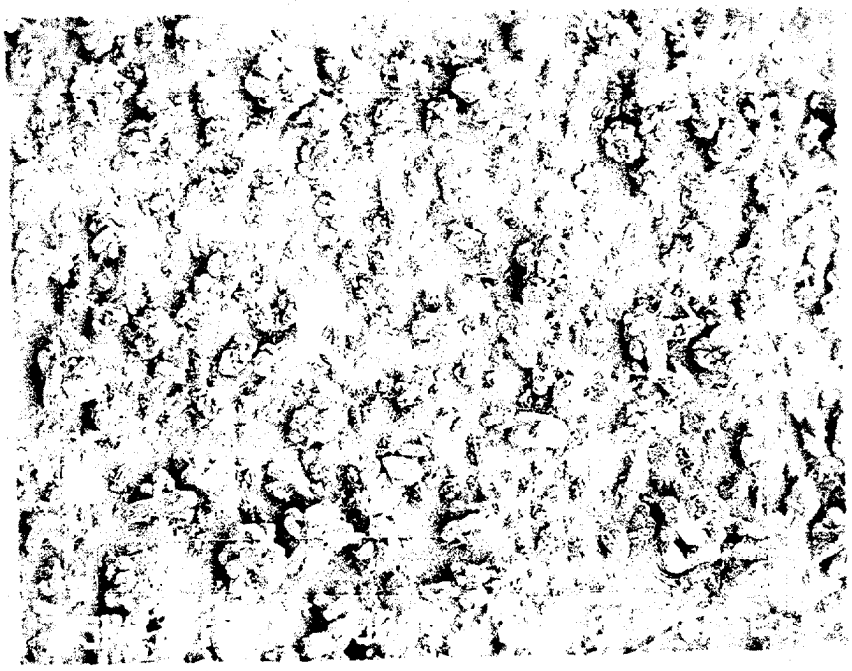

Figure 12: SEM micrograph of phosphogypsum produced in the presence of kaolin.

Effect of Polymers Using High Iron Feed Rock

Although the high dolomite phosphate rock was used for most of the tests conducted in this study, other feed rock samples such as high iron feed rock samples were examined. The effectiveness of polymeric additives on phosphate feed rock with a high iron content was evaluated using the phosphate pebble fraction from one of the Florida phosphate producers. The feed rock was ground to the distribution previously presented in Table 1 and fed into the batch reaction vessel. The sulfate level in these tests was maintained at 1.7 %. The resulting filtration rates are presented in Table 14. The filtration rate comparison in Table 14 shows that PEO is more effective than SF206 in enhancing the rate of filtration when using the high iron feed rock.

Table 14
Phosphogypsum Filtration Rate Comparison Using High Iron Phosphate Feed Rock

Polymer Added	Polymer Dosage (kg/ton)	Filtration Rate (ton P_2O_5/m^2 day)	Change from Baseline Rate
None (Baseline)	0.00	7.2	-
SF 206	0.10	7.9	+ 10
PEO	0.10	8.5	+ 18

Effect of Free Sulfate Level

The effect of sulfate on the rate of filtration was examined in this study to establish baseline filtration rate data and to evaluate the effectiveness of 4-million molecular weight PEO as a function of sulfate. The sulfate level has a pronounced effect upon the rate of filtration as shown in Figure 13 for both the current low dolomite feed rock as well as high dolomite feed rock 2. As illustrated in Figure 13, the high dolomite feed rock results in reduced filtration rates in comparison to the current low-dolomite feed rock, confirming the need for technology to enhance filtration so that future high dolomite rock deposits can be economically utilized.

The addition of 4-million molecular weight PEO enhances the rate of phosphogypsum filtration at all sulfate levels examined as shown in Figure 14. Because many plants operate at different sulfate levels and sulfate level may vary with time in the reactor, this result is of particular interest, since it indicates that PEO will enhance filtration by a substantial amount regardless of the sulfate level.

Another important factor in determining the usefulness of filtration enhancing additives is their influence on process efficiencies. The process efficiencies for the baseline and 4-million molecular weight PEO are presented in Figure 15 as a function of the sulfate level. These overall efficiency results show that the addition of PEO has a slightly beneficial influence on the process at all sulfate levels. The results in Figure 15 also show that the optimum sulfate level for process efficiency is between 2.5 and 3.0 %.

The effects of the sulfate level on the phosphogypsum crystals are seen in the SEM micrographs presented in Figures 16-21 for the baseline phosphogypsum and Figures 22-25 for the 4-million molecular weight PEO. The SEM micrographs clearly show the increase in particle size as the sulfate level is increased for both the PEO and baseline samples.

Effect of Polymer Molecular Weight

The effect of polymer molecular weight on the effectiveness of PEO and PAM on phosphogypsum filtration was evaluated by comparing the rate of filtration over a wide range of molecular weights as presented in Figure 26 and Tables 15 and 16. It is apparent from the results presented in Figure 26 that 8-million molecular weight PEO enhances the rate of filtration by 30 % over the baseline results. It is also evident from Figure 26 that PAM generally decreases the rate of phosphogypsum filtration relative to the baseline tests. In addition, from the information illustrated in Figure 26 it is clear that the effectiveness of polymers in enhancing the rate of filtration is dependent upon molecular weight. The higher the molecular weight is, the more effective the polymer is in enhancing filtration.

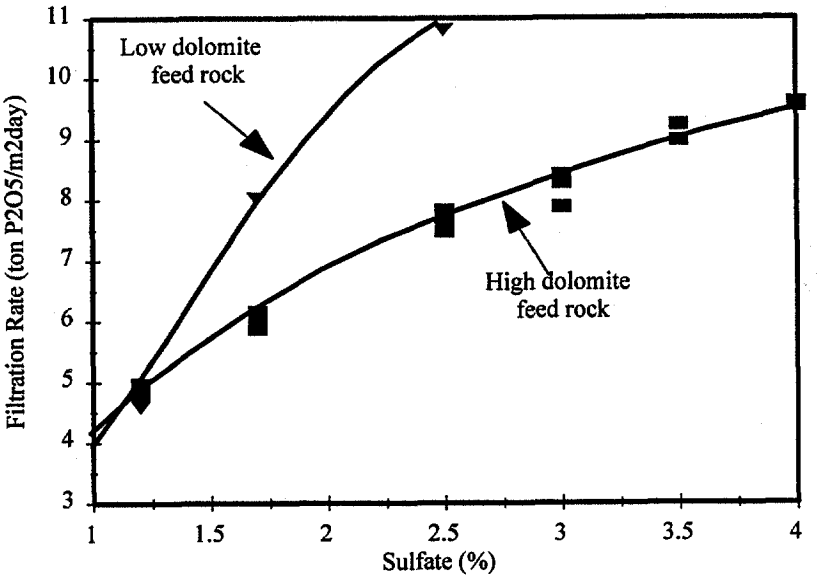

Figure 13: Baseline filtration rate data using high dolomite feed rock **2** together with data obtained using low dolomite feed rock.

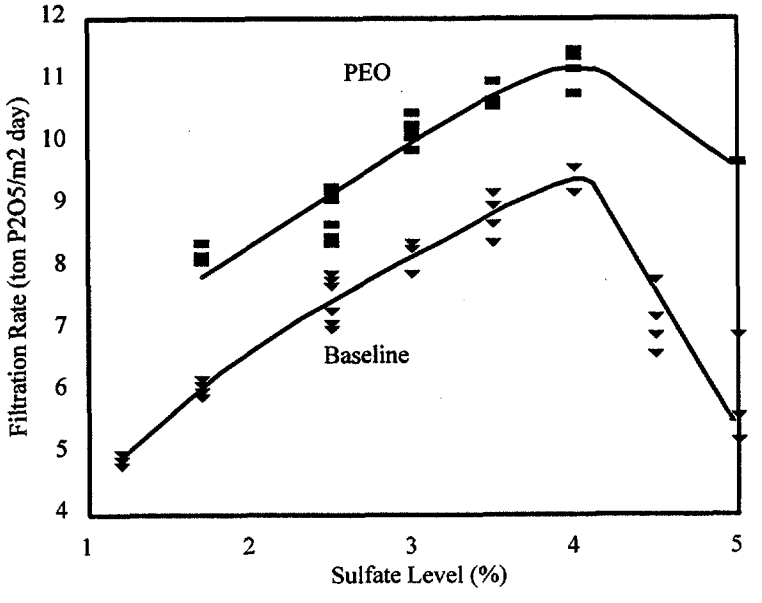

Figure 14: The effect of sulfate on the rate of filtration for baseline and 4-million molecular weight PEO samples.

Effect of Polymers Added as Filter Aids

Improvements in the phosphogypsum filtration rate upon addition of PEO during the digestion stage has been established above. In order to assess the effect of polymers as filter aids, tests were conducted by adding the polymer 5 minutes prior to filtration. Also, to determine whether adding the polymer immediately after the digestion affects filtration experiments were performed in which the polymer was added 150 minutes prior to filtration. Results presented in Table 17 indicate that the addition of PEO 5 minutes prior to filtration resulted in an average increase of 13 % in the rate of filtration relative to the baseline tests, whereas the addition of PEO 150 minutes prior to filtration resulted in a 16 % enhancement in the rate of filtration. These results indicate that although PEO is effective in increasing filtration rates by adding it just prior to filtration or immediately after the digestion stage, it is more effective when added during the digestion stage as shown previously (30 % improvement).

The effect of polymeric additives on the process efficiencies is presented in Table 18. The efficiency results show that the process efficiencies are high when the polymer is added during the digestion stage. However, the process efficiencies for the polymer addition as a filter aid were lower than the corresponding results from the digestion tests.

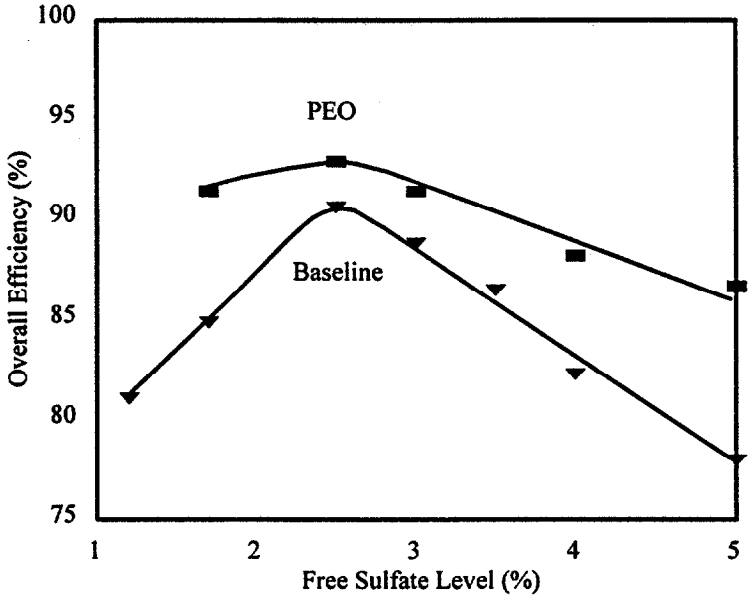

Figure 15: Efficiency comparison as a function of sulfate concentration for baseline and 4-million molecular weight PEO samples.

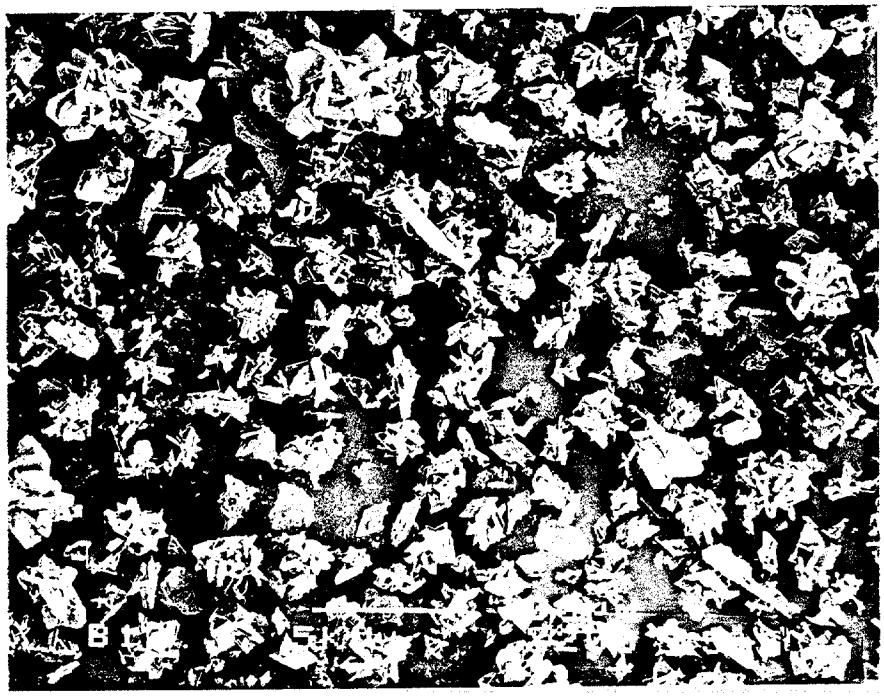

Figure 16: SEM micrograph of baseline phosphogypsum (1.2 % sulfate)

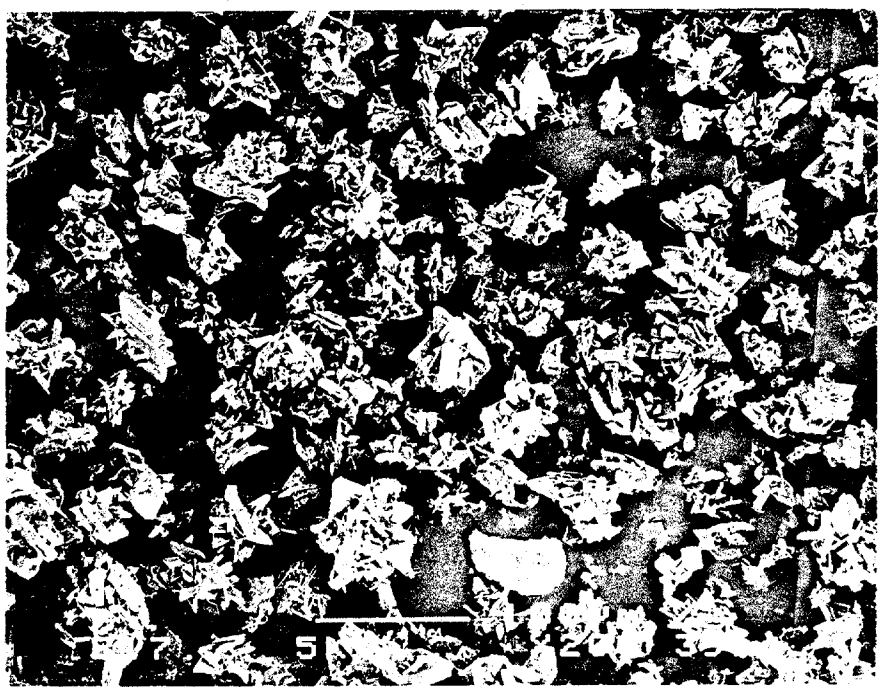

Figure 17: SEM micrograph of baseline phosphogypsum (1.7 % sulfate)

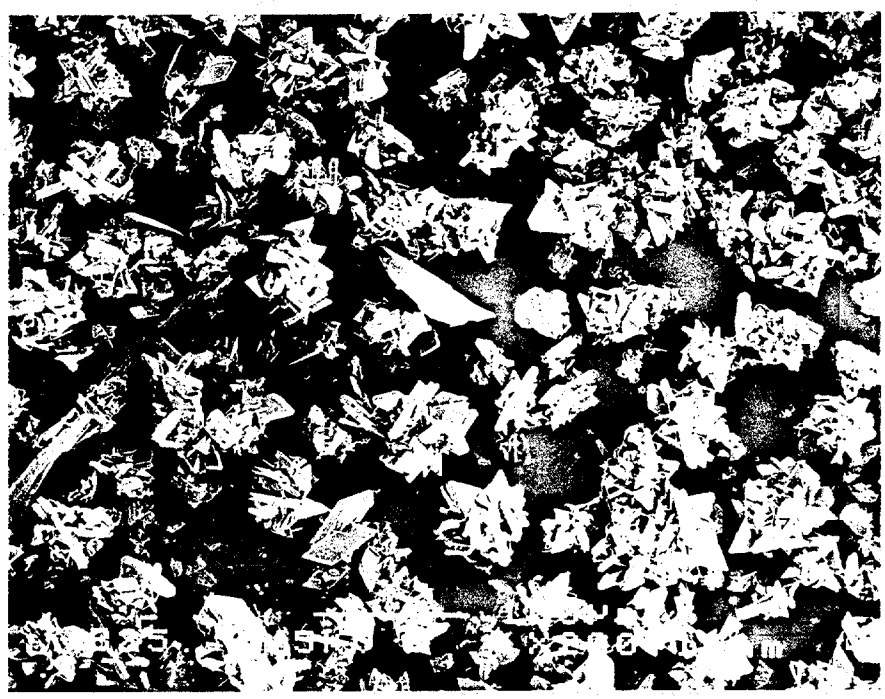

Figure 18: SEM micrograph of baseline phosphogypsum (2.5 % sulfate)

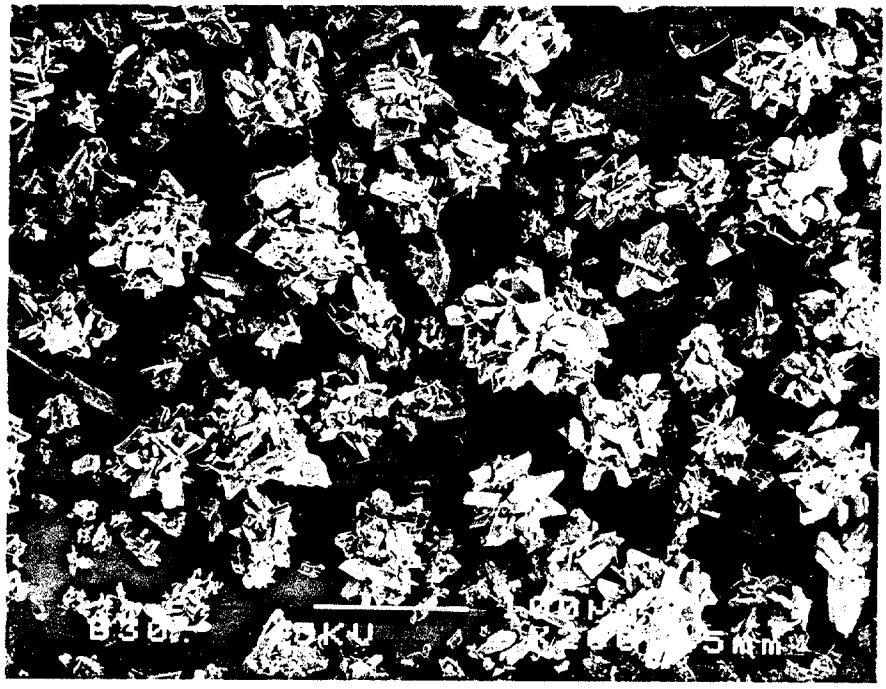

Figure 19: SEM micrograph of baseline phosphogypsum (3.0 % sulfate)

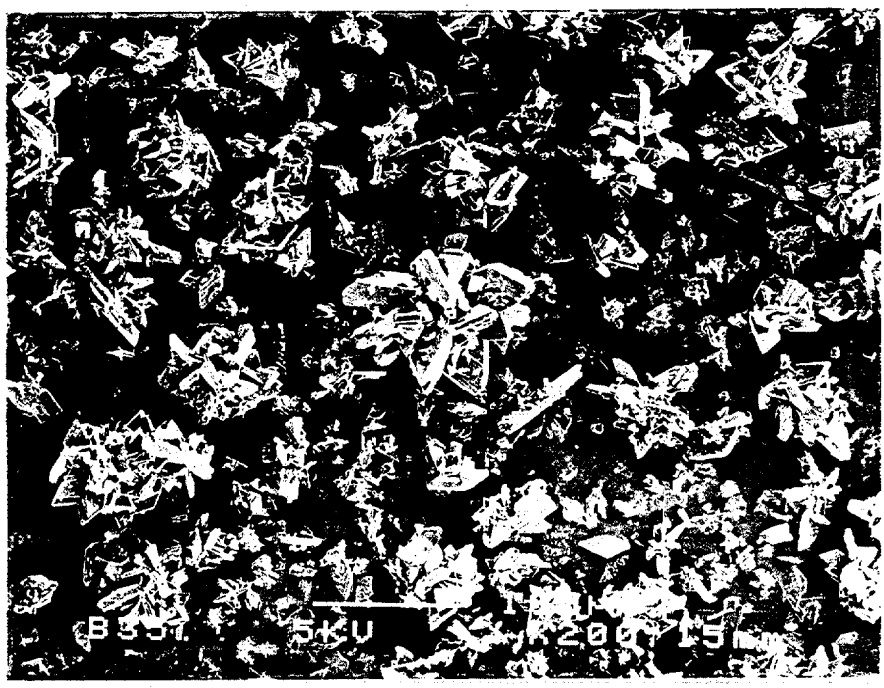

Figure 20: SEM micrograph of baseline phosphogypsum (3.5 % sulfate)

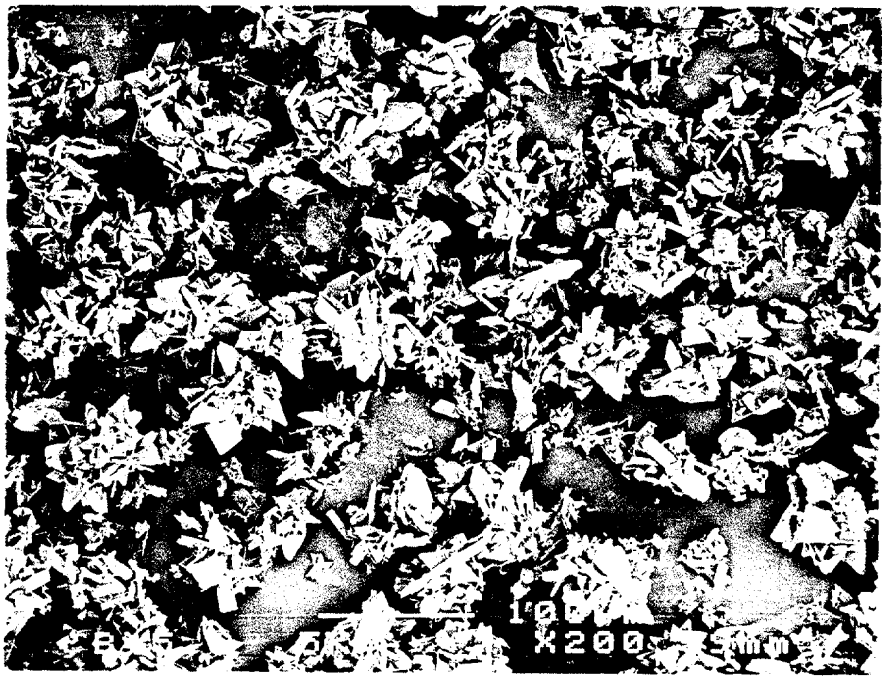

Figure 21: SEM micrograph of baseline phosphogypsum (5.0 % sulfate)

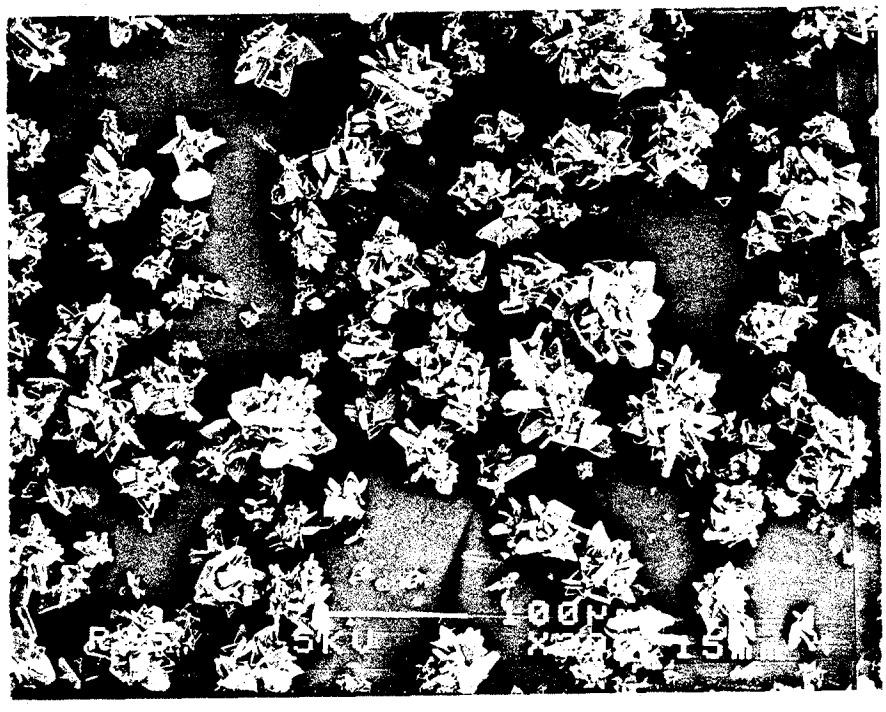

Figure 22: SEM micrograph of phosphogypsum treated with 0.1 kg of 4-million molecular weight PEO per ton of phosphogypsum during the digestion stage of phosphoric acid production. (2.5 % sulfate)

Figure 23: SEM micrograph of phosphogypsum treated with 0.1 kg of 4-million molecular weight PEO per ton of phosphogypsum during the digestion stage of phosphoric acid production. (3.0 % sulfate)

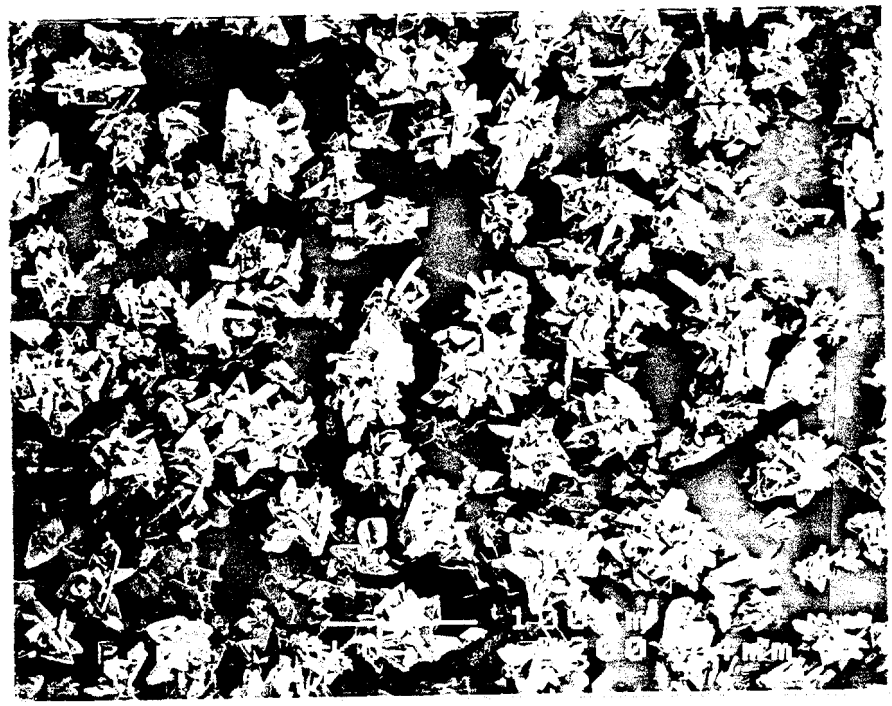

Figure 24: SEM micrograph of phosphogypsum treated with 0.1 kg of 4-million molecular weight PEO per ton of phosphogypsum during the digestion stage of phosphoric acid production. (4.0 % sulfate)

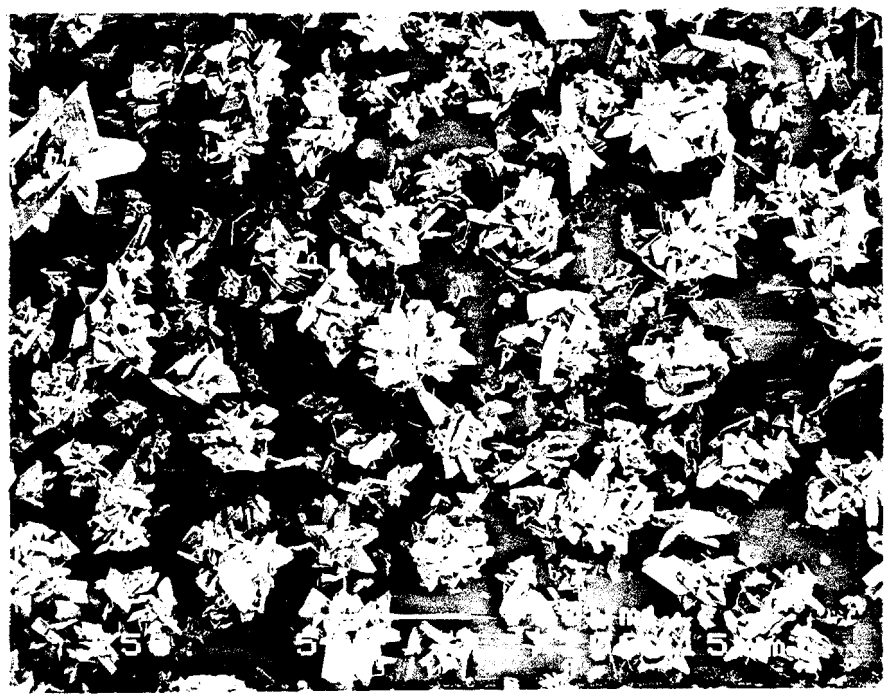

Figure 25: SEM micrograph of phosphogypsum treated with 0.1 kg of 4-million molecular weight PEO per ton of phosphogypsum during the digestion stage of phosphoric acid production. (5.0 % sulfate)

Comparison of Commercial- and Reagent-Grade PEO

The effect of PEO dosage on the rate of phosphogypsum filtration was also evaluated in this study using both commercial- and reagent-grade PEO. In each batch filtration experiment, the additive was added throughout the digestion stage of phosphoric acid production. The results of the batch filtration tests are illustrated in Figure 27 and tabulated in Table 19. These data indicate there is an optimum reagent-grade PEO dosage of approximately 0.3 kg/ton. The addition of 0.3 kg/ton gives a 46 % improvement in the rate of filtration when compared with the baseline results. By way of comparison, the commercial-grade PEO (Polyox 308) resulted in a 54 % improvement in the rate of filtration with a 0.1 kg/ton dose. The data in Figure 27 also show that there is a strong dependence upon dosage for both the commercial- and reagent-grade PEO.

The effect of dosage on process efficiency was also evaluated as shown in Table 20. These data show that all dosage levels of commercial- and reagent-grade PEO result in improvements in the process efficiencies. All but one of the filtration efficiencies for the PEO additives were in excess of 98 % in contrast to the baseline filtration efficiency of 97.6 %. All but one of the digestion efficiency values associated with PEO treatments were greater than the baseline value of 93.0 %. Finally, all of the PEO-treated samples had greater overall efficiencies than the baseline value of 90.6 %.

Comparison of Commercial- and Reagent-Grade Sulfonates

The use of both commercial-grade and reagent-grade sulfonate compounds results in substantial improvements in the rate of phosphogypsum filtration as illustrated in Figure 28 and tabulated in Table 21. The data in Figure 28 show that the commercial-grade sulfonate compounds improve the rate of filtration by 25 % for branched dodecyl benzene sulfonic acid at 0.1 kg/ton and 22 % for alkylated naphthalene sulfonate at 0.5 kg/ton. A 35 % enhancement in the rate of filtration resulted from the addition of 0.5 kg of reagent-grade branched sodium dodecyl benzene sulfonate. It is also apparent in Figure 28 that the non-branched sodium dodecyl benzene sulfonate has a negative impact upon the rate of filtration. It is believed that the branching is important to the effectiveness of the sulfonates in enhancing the rate of filtration.

As is the case with the PEO treatment, the addition of sulfonate compounds has a general positive effect upon process efficiencies as presented in Table 22. The filtration efficiencies for the sulfonate-treated samples were all above 99 %. However, only the commercial-grade Alkylated Naphthalene Sulfonate and the reagent-grade branched sodium dodecyl sulfonate showed digestion efficiencies above the baseline value of 93 %. All but one of the overall efficiencies of the sulfonate-treated samples was lower than the baseline value of 90.6 %, but the highest overall efficiency was approximately 2 % lower than the highest value from the PEO-treated sample.

Table 15
General filtration and filtrate data obtained using PEO during the digestion stage at 2.5 % free sulfate

Molecular Weight ($\times 10^6$)	Sulfate (%)	Filtration Rate m.t. P_2O_5/m^2/day	(%) over baseline	Filtrate Viscosity (cP)	Filtrate Solids (%)	Filtrate Density (g/cc)	Filtr. P_2O_5 (%)
0.3	2.5	6.8	-8.0	-	-	-	27.6
0.3	2.5	7.1	-4.0	-	-	-	26.9
4	2.5	9.2	+24	-	-	-	-
4	2.5	9.2	+24	-	-	-	-
4	2.5	8.4	+14	-	-	-	-
4	2.5	8.3	+12	-	-	-	-
4	2.5	9.0	+22	-	-	-	-
4	2.5	9.2	+24	-	-	-	-
4	2.5	8.6	+16	-	-	-	-
4	2.5	9.1	+23	-	-	-	-
8	2.5	9.4	+27	1.95	0.12	1.314	27.6
8	2.5	9.5	+28	2.02	0.41	1.328	27.0
8	2.5	9.7	+31	2.27	0.47	1.338	26.8
8	2.5	9.5	+28	1.96	0.62	1.320	27.6
8	2.5	9.9	+34	2.34	0.56	1.352	28.7
8	2.5	9.5	+28	-	0.34	1.348	27.7
8	2.5	9.5	+28	-	-	-	-
8	2.5	9.9	+34	-	-	-	-

The use of naphthalene sulfonate and sodium dodecyl benzene sulfonate to enhance filtration was originally patented by David W. Leyshon et al. in 1965. The chemical abstract for the patent (U. S. Patent 3,192,014) states "Addition of small amouts of either isopropylnaphthalene sulfonic acid, a C_{9-12} alkylbenzenesulfonic acid, or an alkali metal salt of this latter acid during the commercial production of H_3PO_4 results in substantial improvement in the filterability of the gypsum from the H_3PO_4 and the efficiency of the phosphate rock digestion in H_2SO_4." Because this patent was issued in 1965, it is no longer in effect; therefore, the use of sodium dodecyl benzene sulfonate, dodecyl benzene sulfonic acid, and isopropyl naphthalene sulfonic acid will not result in patent infringement.

It is also important to point out that some plant testing by a vendor has shown that the commercial-grade alkylated naphthalene sulfonate significantly reduces scaling in plant process acid pipes. The commercial-grade alkylated naphthalene sulfonate and

It is also important to point out that some plant testing by a vendor has shown that the commercial-grade alkylated naphthalene sulfonate significantly reduces scaling in plant process acid pipes. The commercial-grade alkylated naphthalene sulfonate and

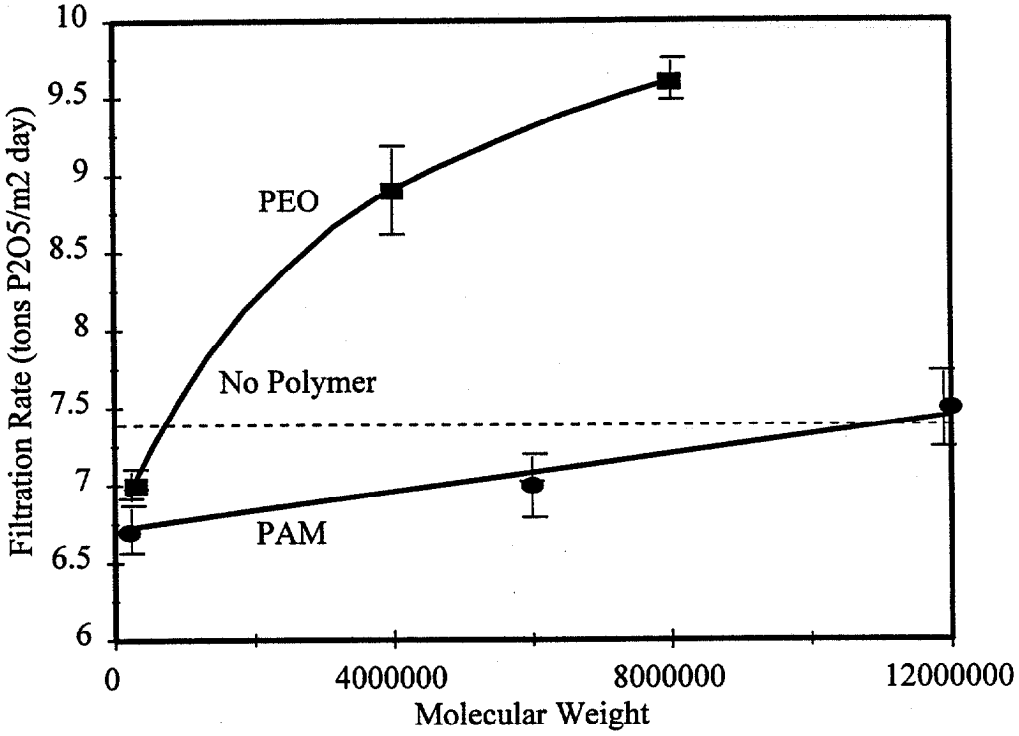

Figure 26: Comparison of filtration rate data for PEO- and PAM-enhanced batch filtration tests as a function of polymer molecular weight. The error bars represent the standard deviation of the experimental data.

dodecyl benzene sulfonic acid compounds were obtained through Rantec Corporation (406-252-5120) and Witco Corporation (614-764-6657) and sell under the trade names of Petrol-P. and Witco 1298 H, respectively. The commercial sulfonate products can be purchased for $0.60 to $1.00 per pound depending upon the product, quantity, and shipping destination.

Table 16
General filtration and filtrate data obtained using PAM during the digestion stage at 2.5 % free sulfate

Molecular Weight ($\times 10^6$)	Sulfate (%)	Filtration Rate m.t. $P_2O_5/m^2/day$	(%) over baseline	Filtrate Viscos. (cP)	Filtrate Solids (%)	Filtrate Density (g/cc)	Filtr. P_2O_5 (%)
0.2	2.5	6.7	-9.5	-	0.50	-	28.3
0.2	2.5	6.7	-9.5	-	1.36	-	27.8
0.2	2.5	6.7	-9.5	-	0.56	-	27.5
0.2	2.5	6.6	-11	-	0.96	-	27.2
6	2.5	6.9	-7.8	1.84	0.42	1.308	26.8
6	2.5	6.6	-11	1.86	1.68	1.317	26.6
6	2.5	7.1	-4.0	1.89	0.75	1.314	27.7
6	2.5	7.4	0.0	1.89	1.61	1.317	27.4
12	2.5	7.8	+5.4	-	1.16	-	29.5
12	2.5	7.2	-2.7	-	0.60	-	28.4
12	2.5	7.6	+2.7	-	0.21	-	29.2
12	2.5	7.3	-1.3	-	0.46	-	29.0

Table 17

Batch filtration data for 8-million molecular weight PEO added as a filtration aid (5-minutes before filtration) or during the crystallization stage (150 minutes before filtration)

Addition time (min.) before filtr.	Filtration Rate m.t. $P_2O_5/m^2/day$	(%) over baseline	Filtrate Viscosity (cP)	Filtrate Solids (%)	Filtrate Density (g/cc)	Filtrate P_2O_5 (%)
5	8.5	15	1.98	0.43	1.321	-
5	8.2	11	2.02	0.34	1.333	27.8
150	8.8	19	1.80	0.45	1.310	26.8
150	8.4	14	1.81	0.58	1.302	-

Table 18
Effect of Polymeric Additives on Efficiencies Using High Dolomite Feed Rock 2

Polymer	Addition Stage	Molecular Weight ($\times 10^6$)	Citr. Insol. P_2O_5 (%)	Filtration Eff. (%)	Digestion Eff. (%)	Overall Eff. (%)
PEO	Digestion	0.3	0.03	98.2	94.7	92.9
PEO	Digestion	4	0.32	98.0	95.1	93.2
PEO	Digestion	8	0.11	99.2	95.9	95.1
PAM	Digestion	2	0.08	98.2	95.9	94.1
PAM	Digestion	6	0.38	98.6	95.2	93.8
PAM	Digestion	12	0.18	98.0	95.3	93.4
PEO	5-minutes	8	1.21	99.5	91.0	90.5
PEO	150-min.	8	0.72	97.8	93.3	91.1

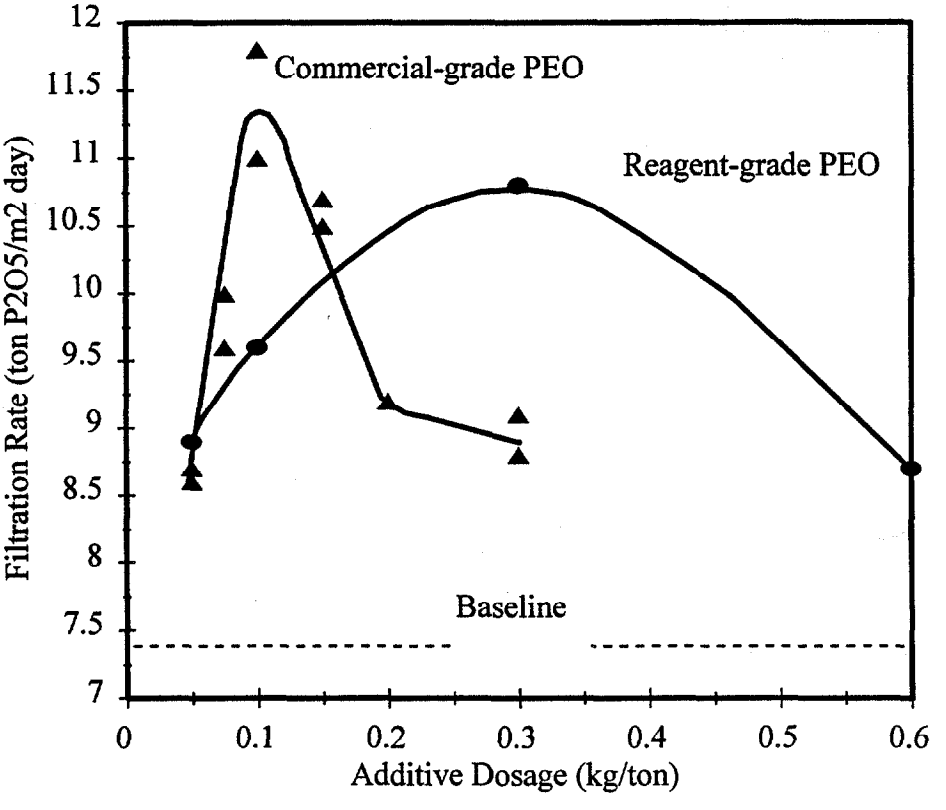

Figure 27: Comparison of filtration rates and additive dosages (in kg/ton of gypsum) for commercial- and reagent-grade polyethyleneoxide (PEO).

Table 19
Filtration Rate Data for Polyethyleneoxide Additives

Compound	Dosage (kg/ton gypsum)	Filtration Rate (ton P_2O_5/m^2 day)	Percent Change Over Baseline Rate
PEO	0.05	8.6	+16
PEO	0.05	8.5	+15
PEO	0.05	9.1	+23
PEO	0.05	8.7	+18
PEO	0.1	9.4	+27
PEO	0.1	9.5	+28
PEO	0.1	9.7	+31
PEO	0.1	9.5	+28
PEO	0.1	9.9	+34
PEO	0.1	9.5	+28
PEO	0.1	9.5	+28
PEO	0.1	9.9	+34
PEO	0.3	10.3	+39
PEO	0.3	11.4	+54
PEO	0.3	10.5	+42
PEO	0.3	11.1	+50
PEO	0.6	9.2	+24
PEO	0.6	9.2	+24
PEO	0.6	8.7	+18
PEO	0.6	8.7	+18
Com PEO	0.05	8.6	+16
Com PEO	0.05	8.7	+18
Com PEO	0.075	10.0	+35
Com PEO	0.075	9.6	+29
Com PEO	0.10	11.0	+48
Com PEO	0.10	11.8	+59
Com PEO	0.15	10.7	+45
Com PEO	0.15	10.5	+42
Com PEO	0.2	9.2	+24
Com PEO	0.2	9.2	+24
Com PEO	0.3	9.1	+23
Com PEO	0.3	9.8	+32

Table 20
Effect of PEO Additives on Efficiencies

Compound	Dosage (kg/ton)	Filtration Eff. (%)	Digestion Eff. (%)	Overall Eff. (%)
PEO 8M	0.05	99.4	93.6	93.1
PEO 8M	0.1	99.2	95.9	95.1
PEO 8M	0.3	99.9	93.3	93.2
PEO 8M	0.6	99.7	92.4	92.1
Com PEO	0.05	98.6	95.1	93.7
Com PEO	0.075	98.1	92.8	90.9
Com PEO	0.1	98.5	95.0	93.5
Com PEO	0.15	98.4	94.4	92.8
Com PEO	0.2	98.3	95.2	93.5
Com PEO	0.3	97.1	95.5	92.6
BASELINE	-	97.6	93.0	90.6

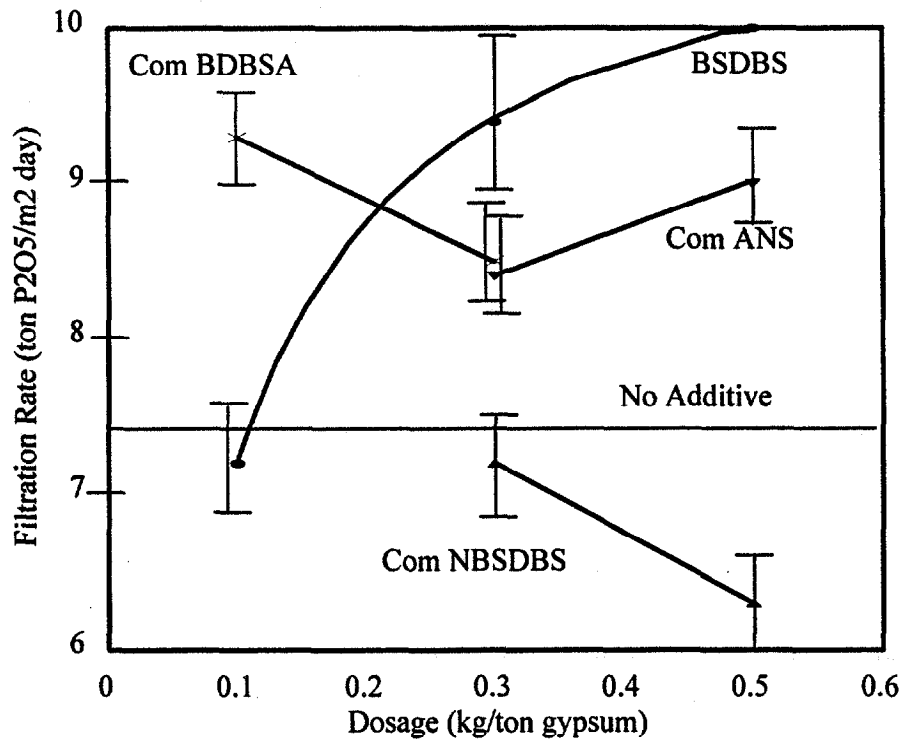

Figure 28: The effect of dosage (kg/ton of gypsum)on the rate of filtration for different additives. The additives are: BSDBS (reagent-grade branched sodium dodecyl benzene sulfonate), Com BDBSA (commercial-grade branched dodecyl benzene sulfonic acid), Com ANS (commerical-grade alkylated naphthalene sulfonate), and Com NBSDBS (commercial-grade non-branched sodium dodecyl benzene sulfonate).

Table 21

Filtration Rate Data for Comercial-Grade Alkylated Naphthalene Sulfonate (Com ANS), Commercial-Grade Non Branched Sodium Dodecyl Benzene Sulfonate (Com NBSDBS), and Commercial-Grade Branched Dodecyl Benzene Sulfonic Acid (Com BDBSA)

Compound	Dosage (kg/ton gypsum)	Filtration Rate (ton P_2O_5/m^2 day)	Percent Change Over Baseline Rate
Com ANS	0.3	8.7	+18
Com ANS	0.3	8.7	+18
Com ANS	0.3	8.0	+8
Com ANS	0.3	8.0	+8
Com ANS	0.5	9.1	+23
Com ANS	0.5	8.9	+20
Com NBSDBS	0.3	7.2	-3
Com NBSDBS	0.3	7.3	-1
Com NBSDBS	0.3	6.9	-7
Com NBSDBS	0.3	7.3	-1
Com NBSDBS	0.5	6.4	-14
Com NBSDBS	0.5	6.1	-18
Com BSDBS	0.1	9.1	+23
Com BSDBS	0.1	9.5	+28
Com BSDBS	0.3	8.8	+19
Com BSDBS	0.3	8.2	+11
Com BSDBS	0.3	8.6	+16
Com BSDBS	0.3	8.2	+11

Table 22

Effect of Sulfonate Additives on Efficiencies

Compound	Dosage (kg/ton)	Filtration Eff. (%)	Digestion Eff. (%)	Overall Eff. (%)
BSDBS	0.1	99.3	91.4	90.7
BSDBS	0.3	99.8	93.6	93.3
BSDBS	0.5	99.9	93.4	93.3
Com ANS	0.3	99.4	93.4	92.8
Com ANS	0.5	99.3	93.7	93.0
Com BDBSA	0.1	99.4	90.9	90.2
Com BDBSA	0.3	99.6	92.9	92.5
BASELINE	-	97.6	93.0	90.6

EVALUATION OF FILTRATION PARAMETERS

Filtration is dependent upon a number of factors such as viscosity, particle size, particle shape, filter cake thickness, and the size of the pores present in the filter cake. In order to understand how additives affect filtration, it is important to analyze all of the important factors and isolate the factors that are most important. Once the most important factors are isolated, the mechanism by which additives affect these important factors can be investigated.

Most industrial filtration processes involving filter media that provide little resistance compared to the filter cake can be adequately described using the Kozeny equation which is generally written as:[9]

$$\frac{dV}{Adt} = \frac{\varepsilon^3 \Delta P}{K\mu(1-\varepsilon)^2 S_p^2 L}, \qquad (3)$$

in which V is the filtrate volume, t is the filtration time, A is the filter area, ε is the porosity, ΔP is the pressure, K is a constant, μ is the viscosity, S_p is the specific surface area of the particles, and L is the thickness of the filter cake. The Kozeny equation is based upon the assumption that the filter cake is incompressible. By analyzing each of these factors, those factors that are most important in this study were isolated.

Compressibility Analysis

Filtration is directly proportional to pressure, provided that the filter cake does not compress under the applied pressure. Several experiments were performed using PEO-treated phosphogypsum to determine the effect of pressure on the rate of filtration, and the results, presented in Figure 29, clearly show that the filter cake is incompressible over the range of pressures examined in this study (I 0.6 atm). Therefore, the assumption of incompressiblity is valid in this analysis.

Analysis of Porosity, Cake Thickness, and Viscosity

The batch filtration experiments performed in conjunction with this project show that the porosity and cake thickness do not vary significantly as presented in Table 23, thus these parameters were considered to be constant in this analysis. The average viscosities for sets of experiments are 2.1 ± 0.2 cP for PEO-treated samples and 1.9 ± 0.2 cP for baseline samples and would account for a 10 % decrease in the rate of filtration rather than the observed increase of 30 %; therefore, viscosity does not explain the change in filtration and was assumed to be constant in this analysis. The only remaining variable in equation 3 is surface area. The effect of particle size, which is directly related to surface area., on the rate of filtration was analyzed using the contact probability filtration model developed in this study as well as the Kozeny equation.

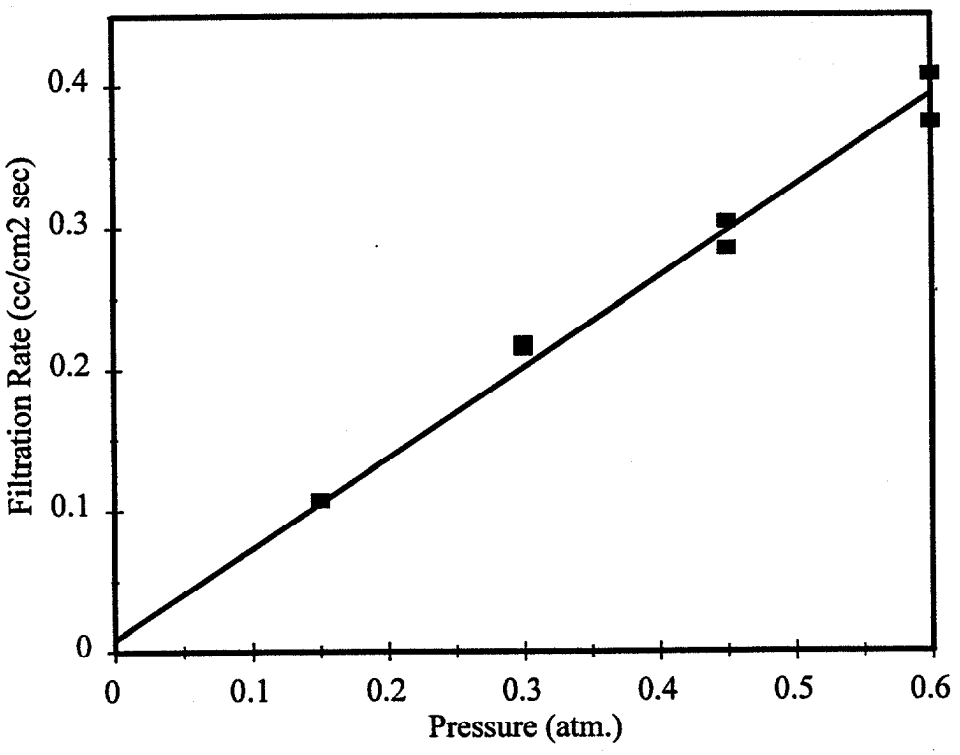

Figure 29: Comparison of the rate of filtration versus the filtration pressure.

Table 23
Comparison of PEO and Baseline Filter Cake and Filtrate Data

PEO			BASELINE		
thickness (cm)	porosity	viscosity (cP)	thickness	porosity	viscosity (cP)
36.3	0.708	1.95	35.2	0.715	1.83
36.5	0.715	2.02	35.9	0.716	1.72
36.5	0.715	2.27	36.0	0.719	1.96
36.0	0.710	1.96	36.6	0.730	1.91
36.5	0.703	2.34	36.1	0.717	1.98
36.7	0.710		34.4	0.698	2.27
36.3	0.717		36.4	0.716	1.97
36.0	0.717	2.10	35.8	0.723	1.84

Contact Probability Filtration Model

The Kozeny equation is derived from the Poiseuille equation based upon the assumption that the rate of filtration can be modeled by considering the pores between particles as small tubes. Using the tube analogy for a filter cake of unit length and unit surface area, the porosity is equal to the number of tubes times the effective cross-sectional area per tube. The Kozeny equation also assumes that the surface area of the tube is equal to the surface area of the particles times the solids volume fraction in the cake. In addition, the Kozeny equation assumes that an average tube diameter can be used to represent all of the pores present. Although the assumption of an average tube diameter does not lead to substantial errors in cases where the particle size distribution stays approximately the same, it does lead to large discrepancies in cases where the particle size distribution changes significantly. This study includes the effect of pore size distribution using geometric and probabilistic calculations in order to determine the effect of size distribution on filtration based upon the Poiseuille equation, rather than assuming an average pore size as the Kozeny equation does.

For filtration of particles that are distributed among different size classes it is useful to identify the distribution of pore sizes found in a given cross-sectional sample of filter cake normal to the direction of fluid flow. The following method was derived to analyze the effect of particle size and size distribution using spherical particles.

Consider three particles "a", "b", and "c" that are touching each other inside a filter cake as shown in Figure 30. The rate of filtration will be dependent upon the pore between the three adjoining spherical particles "a", "b", and "c". By assuming that the pore between the particles "a","b", and "c" can be represented by a tube of equivalent cross-sectional area with an equivalent diameter, the flow of fluid through the pore can be described using the Poiseuille equation:

$$\frac{d}{dt}\frac{V}{} = \frac{\Delta P \pi r^4}{8\mu L}. \qquad (4)$$

According to the Poiseuille equation the rate of filtration will depend upon the effective pore diameter. In this study the cross-sectional area of the pore, which can be determined by subtracting the individual areas A_a, A_b, and A_c from the area of the triangle (see Figure 30), is used to determine an effective pore diameter.

The number of different permutations of particles that can be placed in contact with one another is given as:

$$C = S^N \qquad (5)$$

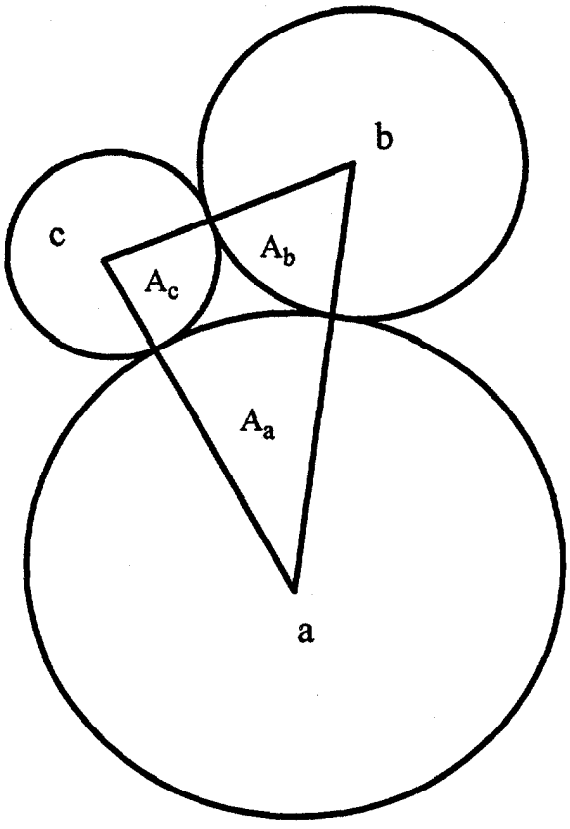

Figure 30: Schematic two-dimensional diagram of particles "a", "b", and "c" contacting each other. This two-dimensional illustration represents a cross-section of particles normal to the direction of fluid flow.

For the case of 6 particle sizes and 3 particles contacting each other, the number of permutations is 6^3 or 216. However, the probability of having particles "a", "b", and "c" together is given by invoking the multiplicative law of probability as:[11, 12]

$$P(abc) = P(a)P(b)P(c) \tag{6}$$

where:

$$P(a) = f_c(a) \tag{7}$$
$$P(b) = f_c(b) \tag{8}$$
$$P(c) = f_c(c) \tag{9}$$

In equation 6, ***P(a)*** is the probability of contacting a particle of size "a", $f_c(a)$ is the fraction of the total particle circumferences found around particles of size "a".

Silica Sphere Filtration

All silica sphere filtration was performed using silica spheres obtained from Duke Scientific that were separated into size classes using standard Tyler mesh screens. The filtration was performed using a 400 mesh screen on top of a woven polymer filter cloth that was inserted into a buchner funnel. The diameter of the filter was 3.85 cm. Other experimental set-up procedures remained the same as for the phosphogypsum filtration described previously, except that 100 ml of 38.5 % H_3PO_4 were used for the filtration and washing. The viscosity of the phosporic acid solution was 2.9 cP as determined by a calibrated Ubeholde viscometer. As was the case with the phosphogypsum filter cakes, the porosity of the silica sphere filtration cakes did not vary significantly between samples as indicated in Table 24.

A number of experiments were conducted using dried/screened phosphogypsum particles as well as glass microspheres of various size distributions to determine the effect

Table 24
Comparison of Cake Thickness and Cake Porosity for Silica Sphere Filtration Cakes

Size Distribution	Number of Observations	Cake Thickness (cm)	Cake Porosity
A	20	1.9 ± 0.1	0.44 ± 0.02
B	20	1.9 ± 0.1	0.45 ± 0.03
C	20	1.9 ± 0.1	0.45 ± 0.02
D	20	1.9 ± 0.1	0.44 ± 0.02
E	20	1.9 ± 0.1	0.45 ± 0.02

of size distribution on filtration. The size distributions of two phosphogypsum samples are illustrated in Figure 31. Using the average filtration rate for the uniform size distribution as a standard, the predicted filtration rates for the narrow size distribution were calculated using the Kozeny equation and the contact probability model as presented in Table 25. The results in Table 25 indicate that the contact probability model is considerably more accurate than the Kozeny equation in predicting the effect of the change in particle size distribution on the rate of filtration.

To evaluate the effect of adding various amounts of fine material (< 38 microns) on the rate of filtration, three different size distributions of dried phosphogypsum

particles were mixed in the proportions indicated in Figure 32. The resulting rates of filtration are presented in Table 26. The results in Table 26 show that both the contact probability filtration model and the Kozeny equation are reasonably accurate in predicting the effect of adding different amounts of fine material on the rate of filtration.

Table 25
Comparison of Measured and Predicted Filtration Rates for the Uniform and Narrow Size Distributions Presented in Figure 31

Size Distribution	Kozeny equation Rate ($cc/cm^2 sec$)	Probability Model Rate ($cc/cm^2 sec$)	Measured Rate ($cc/cm^2 sec$)
Uniform	0.22	0.22	0.22 ± 0.02
Narrow	0.29	0.48	0.42 ± 0.02

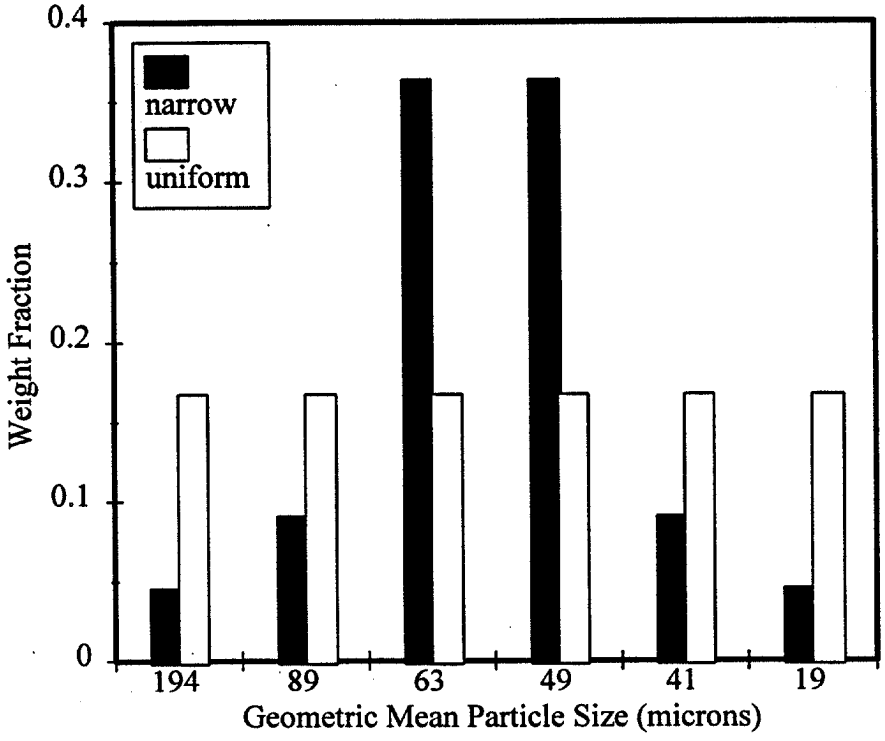

Figure 31: Comparison of uniform and narrow size distributions of phosphogypsum particles based upon the geometric mean particle sizes shown.

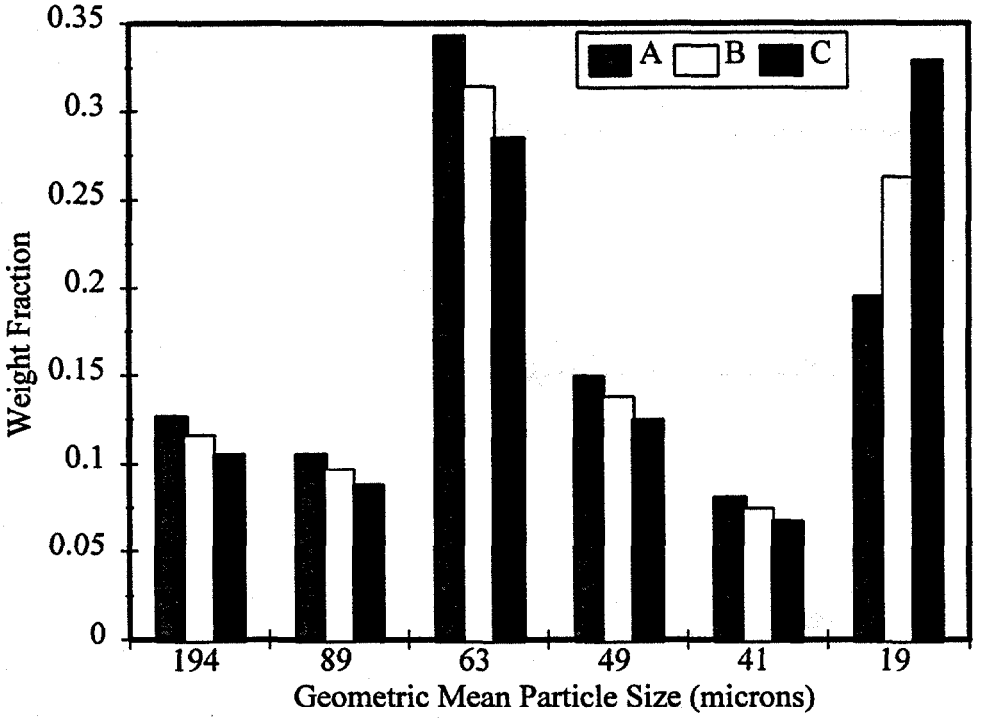

Figure 32: **Comparison of phosphosgypsum size distributions created by taking an average size distribution encountered in phosphogypsum filtration and increasing the fraction of -400 Mesh (19 micron) particles while uniformly decreasing the other size fractions to determine the effect of fines on filtration.**

Evaluation of the Effect of Crystal Growth and Nucleation in Filtration

Because the production of crystals such as phosphogypsum is the result of nucleation and crystal growth, the resulting size distribution can be characterized using an exponential distribution curve that is based upon the number density of particles as given in equation 10.[13, 14]

$$f_n(x) = \frac{1}{G\Gamma}\exp\left(\frac{-x}{G\Gamma}\right), \qquad (10)$$

where $f_n(x)$ is the fraction of particles of diameter x, G is the crystal growth rate, and Γ is the reaction time. It should be noted that equation 10 is based upon continuous flow reactor systems in which no nuclei are present in the feed. The number density function presented as equation 10 can be readily converted to a weight-based density function by simple calculus into the form shown as equation 11.

Table 26
Comparison of measured and predicted filtration rates for the phosphogypsum size distributions presented in Figure 32

Size Distribution	Predicted Rate (Kozeny Equation) ($cc/cm^2 sec$)	Predicted Rate (Probability Model) ($cc/cm^2 sec$)	Measured Rate ($cc/cm^2 sec$)
A	0.25	0.25	0.25 ± 0.04
B	0.20	0.20	0.21 ± 0.02
C	0.17	0.17	0.17 ± 0.03

$$f_w(x) = \frac{x^3[\frac{1}{G\Gamma}\exp(\frac{-x}{G\Gamma})]}{|_{x\,min}^{x\,max}[-\exp(\frac{-x}{G\Gamma})][x^3 + 3x^2G\Gamma + 6x(G\Gamma)^2 + 6(G\Gamma)^3] + C} \qquad (11)$$

This type of a modeling approach is useful because it allows the flexibility of determining the influence of crystal growth rates and reaction times on the final product particle size distribution. The information from the final size distribution can then be used in the contact probability model to predict the effect of growth rates and reaction times on the rate of filtration. In order to predict the growth rate for phosphogypsum production, size analysis data from approximately 50 batch phosphogypsum production tests were least-squares-fitted using equation 11 with the actual reaction time of 150 minutes. The resulting growth rate was 0.121 μm/min. The effect of increasing and decreasing this growth rate by 25 % on the product phosphogypsum particle size distribution is illustrated in Figure 33. The measured and predicted filtration rates that resulted from mixing dry-sieved phosphogypsum in the amounts necessary to simulate the distributions shown in Figure 33 are presented in Table 27. The data in Table 27, which are also presented in Figure 34, show that changes in the rate of crystal growth cause even larger changes in the rate of filtration. The results in Table 27 clearly indicate that the rates of filtration predicted by the contact probability filtration model are closer to the measured rates than those rates predicted by the Kozeny equation for the size distributions presented in Figure 33.

Model Evaluation Usmg Silica Spheres

Although the preceding results obtained using various size distributions of phosphogypsum particles show that the contact probability model predicts the effect of changes in particle size distributions on filtration better than the Kozeny equation, it was

Table 27
Comparison of measured and predicted filtration rates for the phosphogypsum size distributions presented in Figure 33

Growth Rate	Predicted Rate (Kozeny equation) (cc/cm^2sec)	Predicted Rate (Probability Model) (cc/cm^2sec)	Measured Rate (cc/cm^2sec)
low	0.16	0.16	0.16 ± 0.01
medium	0.32	0.28	0.32 ± 0.03
high	0.76	0.58	0.46 ± 0.02

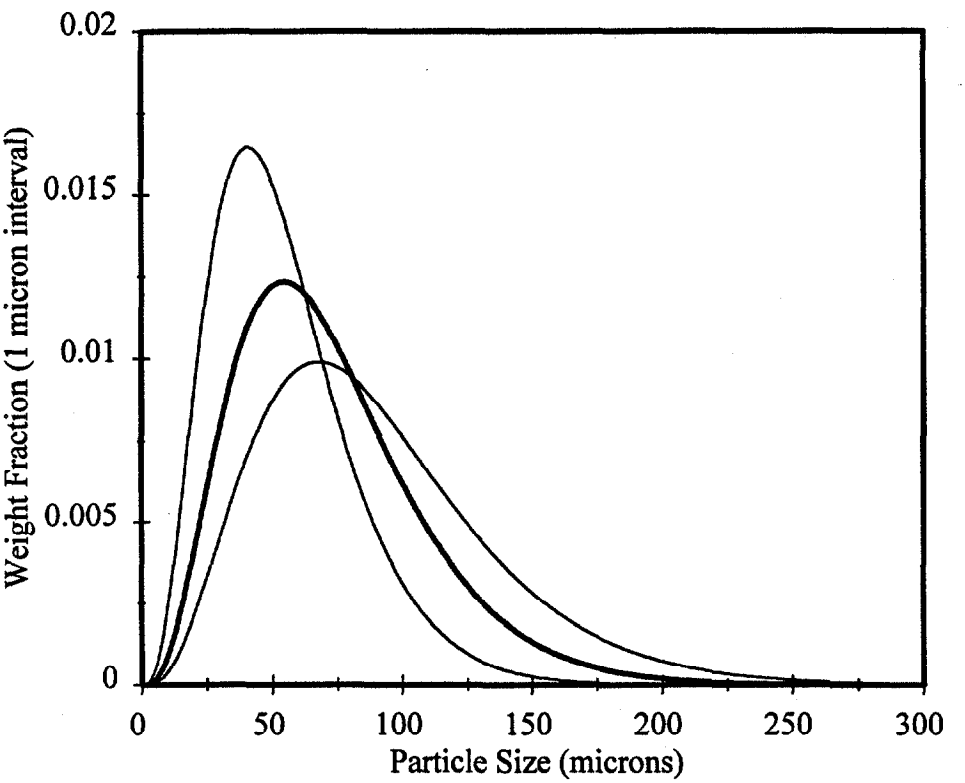

Figure 33: Comparison of model size distributions resulting from various crystal growth rates as predicted using the population balance modeling method for phosphogypsum size data (see equation 6). The medium growth rate size distribution was based upon a least-squares fit of phosphogypsum size information. The low growth rate size distribution was created by decreasing the crystal growth rate by 25 % below the medium growth rate. The high growth rate size distribution was produced by increasing the crystal growth rate by 25 % above the medium growth rate.

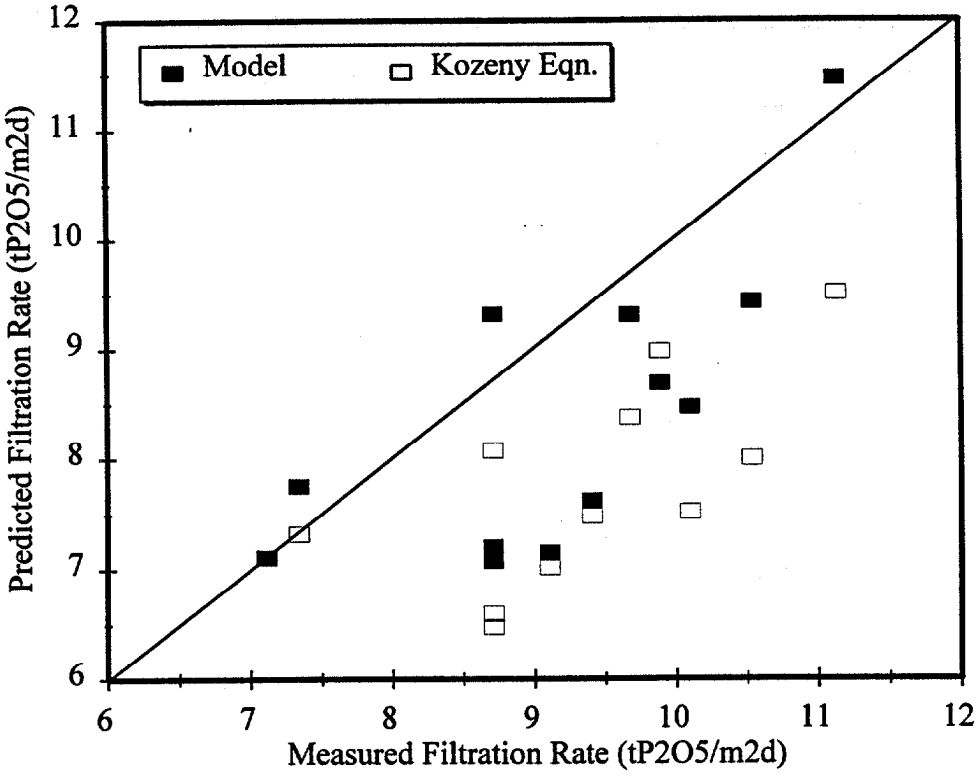

Figure 34: Comparison of measured and predicted filtration rates. The measured rates are from phosphogypsum filtration tests which include the initial filtration and two separate washes. The predicted rates were obtained using the Kozeny equation and the contact probability model based upon a calibration at the lowest measured filtration rate. The sizes used in determining the predicted values were obtained by column settling and are, therefore, Stoke's equivalent diameters.

decided that the validity of the model could more accurately be assessed using spherical particles.

Using spherical silica particles from Duke Scientific Company, several filtration tests were conducted using various particle size fractions in order to produce the size distributions presented in Table 28. The results from these tests along with the predicted results are presented in Figure 35. The data in Figure 35 show that the model gives more accurate predicted filtration rates than the Kozeny equation over an order of magnitude change in the rate of filtration.

Evaluation of Model and Kozeny Constants

The Kozeny constant was calculated for each data set using Equation 3, and the resulting values are presented in Table 29 with the necessary parameter values used in the analysis. The resulting Kozeny constants are between 47.3 and 39.5 for the three sets of data involving phosphogypsum (gypsum); however, these values are significantly different from the value of 18.6 obtained using the silica sphere data. This difference is due to the change in porosity between the phosphogypsum and silica filter cakes. In contrast to this large difference, the correction factor required to calibrate the contact probability model changed from only 5.37 in the case of silica to 7.10 for phosphogypsum because the effect of porosity is not considered. This comparison indicates that the model requires less correction than the Kozeny equation, and that one correction factor can give reasonable results for certain systems, such as those examined in this study. In theory the correction factor would be one provided that the fluid flowed through tubes, but the effect of both tortuosity and the difference between the true pore geometry and the idealistic tube geometry are believed to be responsible for the increase in the correction factor.

Table 28
Silica Sphere Size Distributions

Size Distrib.	84 μm fraction	63 μm fraction	49 μm fraction	41 μm fraction	35 μm fraction	25 μm fraction	14 μm fraction
A	0.15	0.15	0.15	0.15	0.15	0.15	0.10
B	0.00	0.05	0.25	0.40	0.25	0.05	0.00
C	0.00	0.00	0.00	1.00	0.00	0.00	0.00
D	0.00	1.00	0.00	0.00	0.00	0.00	0.00
E	1.00	0.00	0.00	0.00	0.00	0.00	0.00

Note that the sizes given in the table represent the geometric mean particle size. Also, it should be noted that in the model calculations for distribution A, the 41 and 35 μm fractions were combined into one class of 38 μm to reduce the number of classes to 6.

MECHANISMS OF FILTRATION ENHANCEMENT

The analysis of factors affecting filtration indicates that the additives enhance the rate of filtration by altering the hydrodynamic size of the phosphogypsum. This change in hydrodynamic size may be a result of altering the rock digestion, crystal nucleation, crystal morphology, or aggregation via flocculation. Additional studies were performed using FT-IR spectroscopy to verify polymer adsorption at the phosphogypsum surface.

Rock Digestion

Tests to determine the effect of additives on the rate of digestion were also carried out. These tests are important because the rate of digestion will have a significant impact upon the level of supersaturation present during the initial stages of crystal nucleation and growth. The results from the digestion tests are presented in Figure 36 and show that there is very little, if any, difference in the overall rate of digestion due to the presence of the PEO or branched-SDBS; thus, the additives do not appear to alter the crystal formation by changing the level of supersaturation during the digestion process.

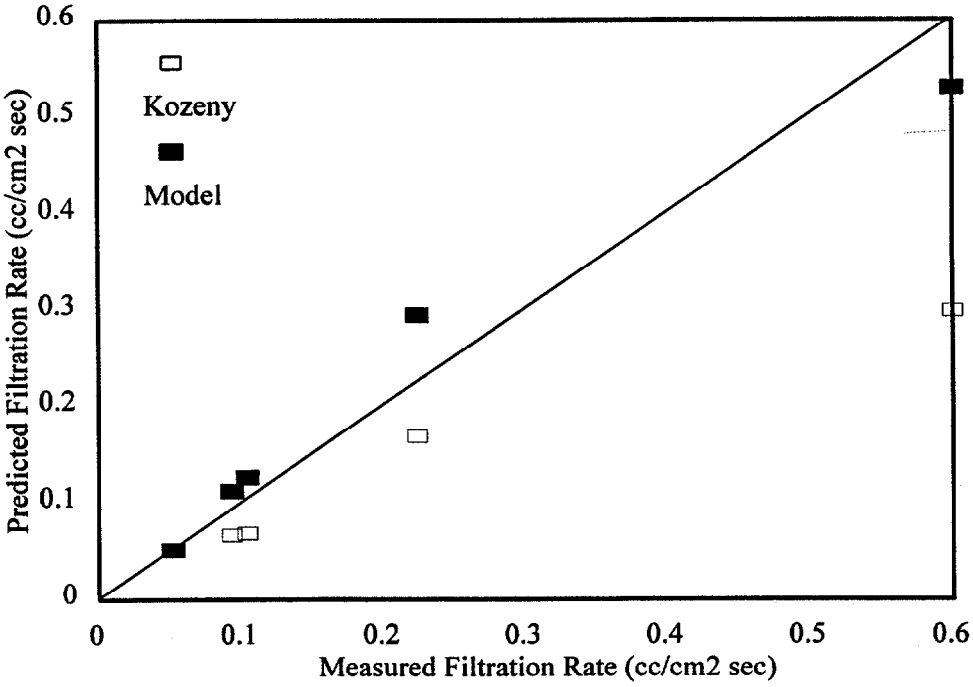

Figure 35: Comparison of predicted and measured filtration rates for silica sphere filtration. The predicted rates were calculated using the contact probability filtration model or the Kozeny equation (equation 3) as indicated.

Table 29
Comparison of Kozeny Constants and Relavent Parameters for Each Data Set

Source (Table)	Area (m^2/g)	Porosity	Thickness (cm)	Viscosity (cP)	Filtr. Rate ($cc/cm^2 sec$)	Sample	Kozeny Constant
3	0.0553	0.53	1.9	1.0	0.225	gypsum	47.3
4	0.0704	0.53*	1.9*	1.0	0.166	gypsum	39.5
5	0.0674	0.53	1.9	1.0	0.159	gypsum	45.0
6	0.0720	0.44	1.9	2.9	0.0521	silica	18.6

* Values were estimated based upon similar tests.

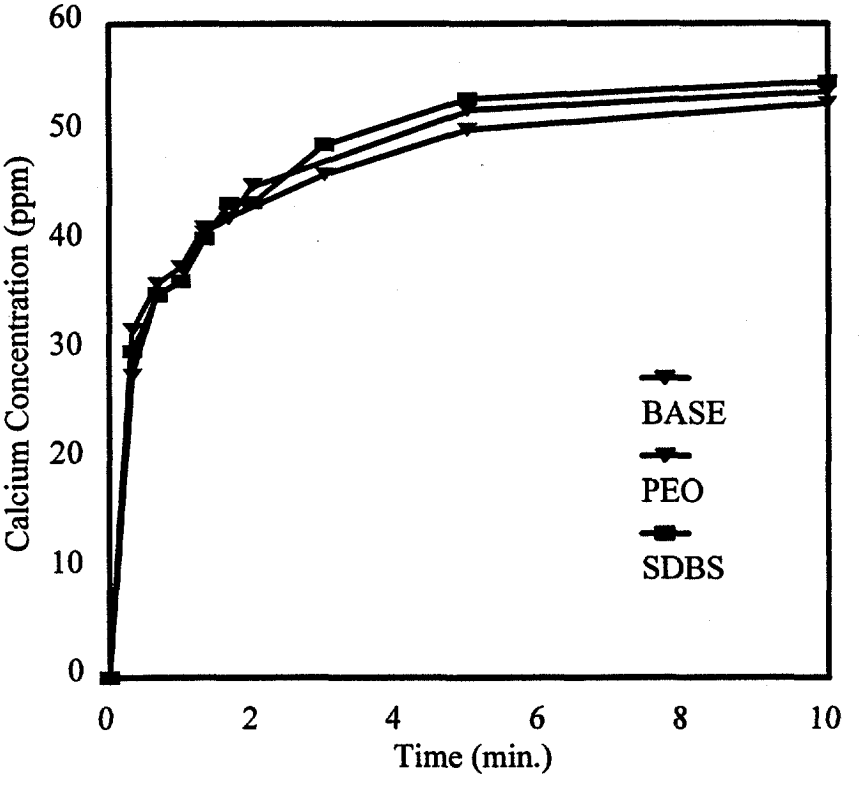

Figure 36: Comparison of calcium concentrations versus time during digestion experiments. All tests were performed at 80°C in phosphoric acid (27.5 % P_2O_5).

Nucleation

The first series of tests was performed to determine the influence of the additives on nucleation at 80°C as evidenced by changes in solution turbidity. Additional experimental details are provided in the experimental section of this report. Results from nucleation tests using 0.3 % calcium (added as calcium chloride) in a 2.9 % sulfuric acid solution are presented in Figure 37. From the data in Figure 37 it can be inferred that the

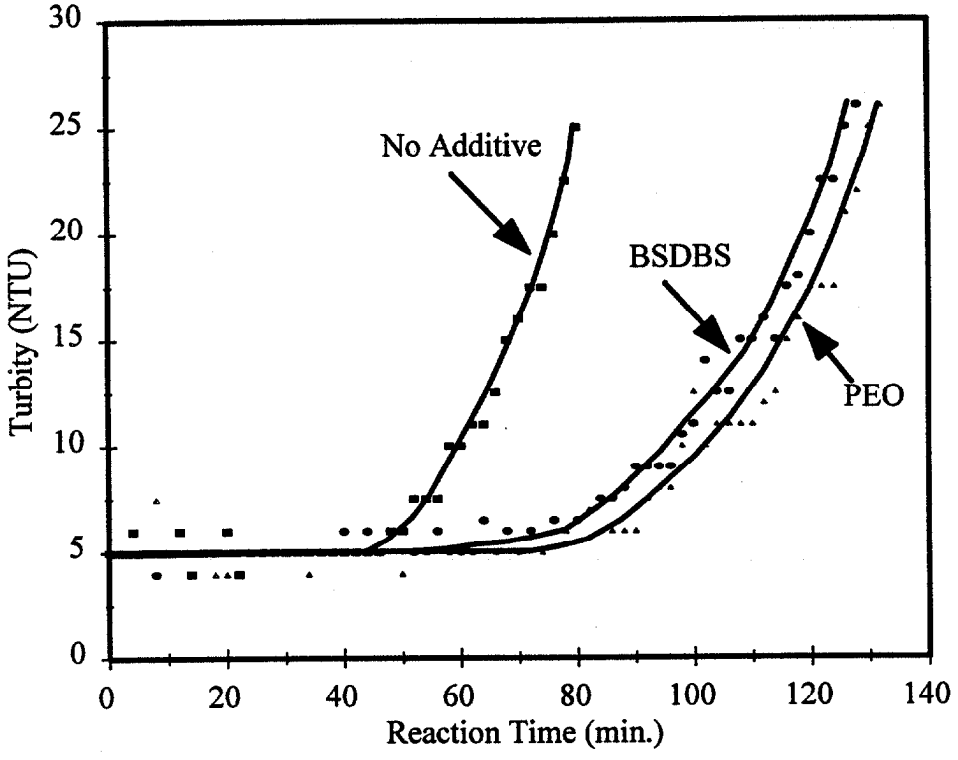

Figure 37: Comparison of turbidity values for nucleation tests with and without additives present in a solution containing 0.30 % calcium and 2.9 % sulfate at 80°C. In the additive experiments:36 ppm of 8-million molecular weight PEO was added in the PEO experiment, and 107 ppm of reagent-grade BSDBS was present in the BSDBS test.

addition of PEO and branched-SDBS delays the effective onset of nucleation. In other experiments using a solution containing digested phosphate feed rock that was filtered and mixed with a phosphoric acid and sulfuric acid solution to produce a more realistic solution, the results were similar as shown in Figure 38. The presence of additives delays

the onset of nucleation. The apparent delay in nucleation will likely lead to a significant decrease in the number of nuclei forming, thereby allowing the nuclei that form to grow larger and enhance the rate of filtration.

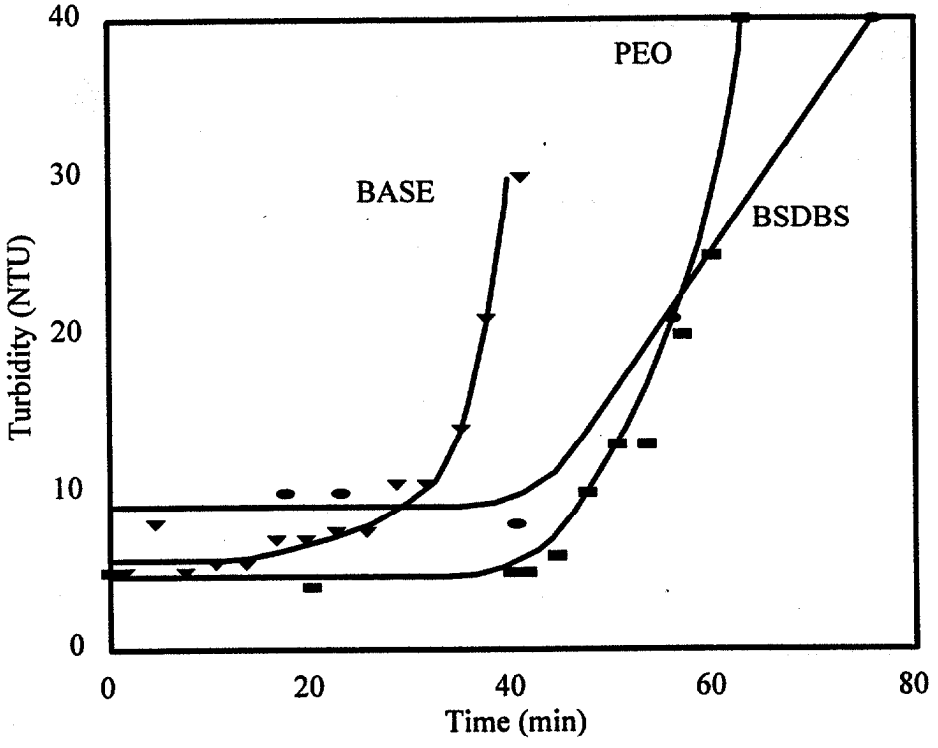

Figure 38: Comparison of turbidity and reaction time with and without additives for the crystallization of gypsum in a solution prepared by digesting 50 grams of 0.30 % dissolved phosphate feed rock, 2.7 % sulfate, and 27.5 % P2O5 at 80°C. In the PEO test, 94 ppm of reagent-grade PEO was present, whereas in the BSDBS test, 274 ppm of reagent-grade BSDBS was present.

Crystal Morphology

In order to determine whether the additives play a role in altering the way the crystals grow, phosphogypsum samples were analyzed by x-ray diffraction to see whether some of the crystallographic planes grow faster than others in the presence of additives. The results from this analysis, presented in Table 30, generally indicate that within the accuracy of the analyses, no decisive differences in crystal growth were observed due to the addition of PEO or branched-SDBS during the digestion process. Although this

analysis is not conclusive, it supports the SEM micrographs in Figures 39-41 which also do not exhibit any significant alteration in the crystal growth habit that could lead to changes in crystal shape that enhance filtration.

Flocculation

Flocculation was evaluated using column settling to determine if polyethylene oxide contributes to enhanced filtration through flocculation. The details of the flocculation tests were presented in the experimental procedures section of this report.

Table 30
Comparison of Relative X-Ray Diffraction Peak Heights of Phosphogypsum

Gypsum Plane	BASELINE	PEO 8M	BSDBS
020	1.1 ± 0.2	1.6 ± 0.6	1.1 ± 0.6
021	1.57 ± 0.03	1.7 ± 0.2	1.8 ± 0.4
040, 130	0.4 ± 0.1	0.5 ± 0.2	0.4 ± 0.1
041	2.0 ± 0.3	2.2 ± 0.5	1.9 ± 0.4
-221	1.00	1.00	1.00
-112	0.22 ± 0.05	0.19 ± 0.02	0.15 ± 0.04
150, 220	0.66 ± 0.05	0.74 ± 0.04	0.68 ± 0.06

All values in Table 30 represent the averages and standard deviations obtained from three independent analyses.

The results presented in Table 31 show that the polyethylene oxide decreases the fraction of settled phosphogypsum for the -400 Mesh size class, whereas in the 200 x 270 Mesh fraction the PEO increased the fraction of settled phosphogypsum. In the overall picture, it does not appear that the PEO enhances filtration through flocculation.

PEO Interaction with Calcium Ions

The effect of PEO in delaying the onset of nucleation was believed to be associated with its role in interacting with calcium ions. To confirm this hypothesis, calcium chloride was added in various quantities to solutions containing 50 ppm PEO (8-million molecular weight). The solutions were then filtered using 1000 molecular weight cut-off membrane filters that would allow only the calcium ions to pass through the membrane. Those calcium ions that were associated with the PEO were retained on the membrane filter. The results from these tests are presented in Table 32. The data in Table 32 reveal that PEO associates strongly with calcium ions. In fact up to 85 % of the

Figure 39: SEM micrograph of baseline phosphogypsum (2.5 % sulfate)

Figure 40: SEM micrograph of PEO-treated phosphogypsum (2.5 % sulfate)

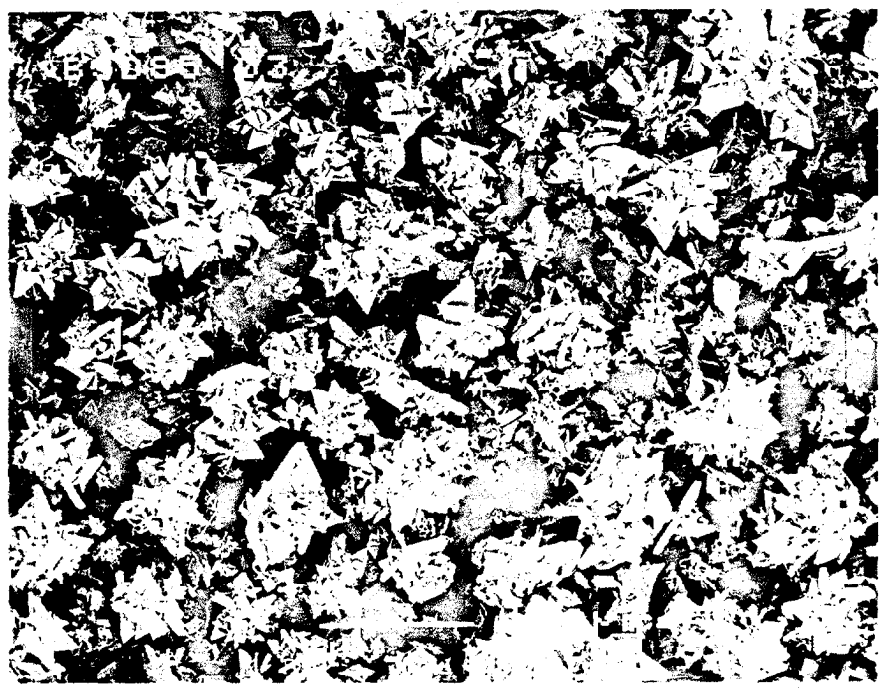

Figure 41: SEM micrograph of branched-SDBS-treated phosphogypsum (2.5 % sulfate)

Table 31
Comparison of Settled Fractions of Phosphogypsum after Agitation at 80°C with and without PEO

Size	Settled Fraction With PEO	Settled Fraction Without PEO
-28 Mesh	0.42 ± 0.02	0.48 ± 0.02
-200 + 270 Mesh	0.40 ± 0.09	0.34 ± 0.03
-400 Mesh	0.26* ± 0.02	0.26* ± 0.03

* Calculated based upon settled weight and an estimated total weight.

calcium ions were associated with the PEO when 50 ppm of calcium was added to the system. These results indicate the PEO is likely affecting phosphogypsum nucleation by effectively reducing the supersaturation level by reducing the availability of calcium ions.

FOURIER TRANSFORM INFRARED (FT-IR) STUDIES

For routine characterization of solid phases such as gypsum, the most commonly used method for IR or FT-IR analysis is the preparation of the sample as a potassium bromide pellet. One of the major advantages of this method is that only a small amount of material, 1 to 4 mg, is needed for routine analysis. Also, the spectra of potassium bromide pellets are less susceptible to anomalous light scattering due to a better match of the indices of refraction for the potassium bromide-mineral interface compared to that of the air-

Table 32
Effect of PEO on Calcium Ion Availability as Revealed by Membrane Filtration

Ca^{+2} conc. before filtration (ppm)	Ca^{+2} conc. after filtration (ppm)	Ca^{+2} associated with PEO
50	7.9	84 %
50	7.6	85 %
485	208	57 %
485	200	59 %

mineral interface. This technique is also among the most suitable sample presentation methods for quantitative analysis of mineral constituents provided that the sample has well-defined, discrete bands. The disadvantages include anomalies associated with drying and pressing at high pressures. In order to have greater confidence in spectral results, the diffuse reflectance (DR) FT-IR method was applied along with the-pellet method to analyze gypsum samples. The primary advantage of the diffuse reflectance method is the control of sample preparation conditions. The disadvantages of the DR method include light scattering anomalies and less quantitative results. Together, the DR and pellet methods provide more complete and reliable information.

The baseline phosphogypsum sample spectra analyzed by the pellet and DR FT-IR methods are presented in Figures 42 and 43, respectively. There is good agreement between the two methods regarding the positions of the bands in Figures 42 and 43. As is normally the case, there can be considerable variation in the relative intensities of the vibrational bands obtained using the two sample preparation methods.

As described previously, the interaction of polymers with phosphogypsum is of interest as it relates to the filtration process. A sample of the phosphogypsum sample was treated with 0.1 kg of poly (ethylene oxide) per ton of phosphogypsum. At present, it is not known how much of the PEO is sorbed by the phosphogypsum sample. However, if all of the PEO were sorbed, the surface loading would be 0.01 wt %.

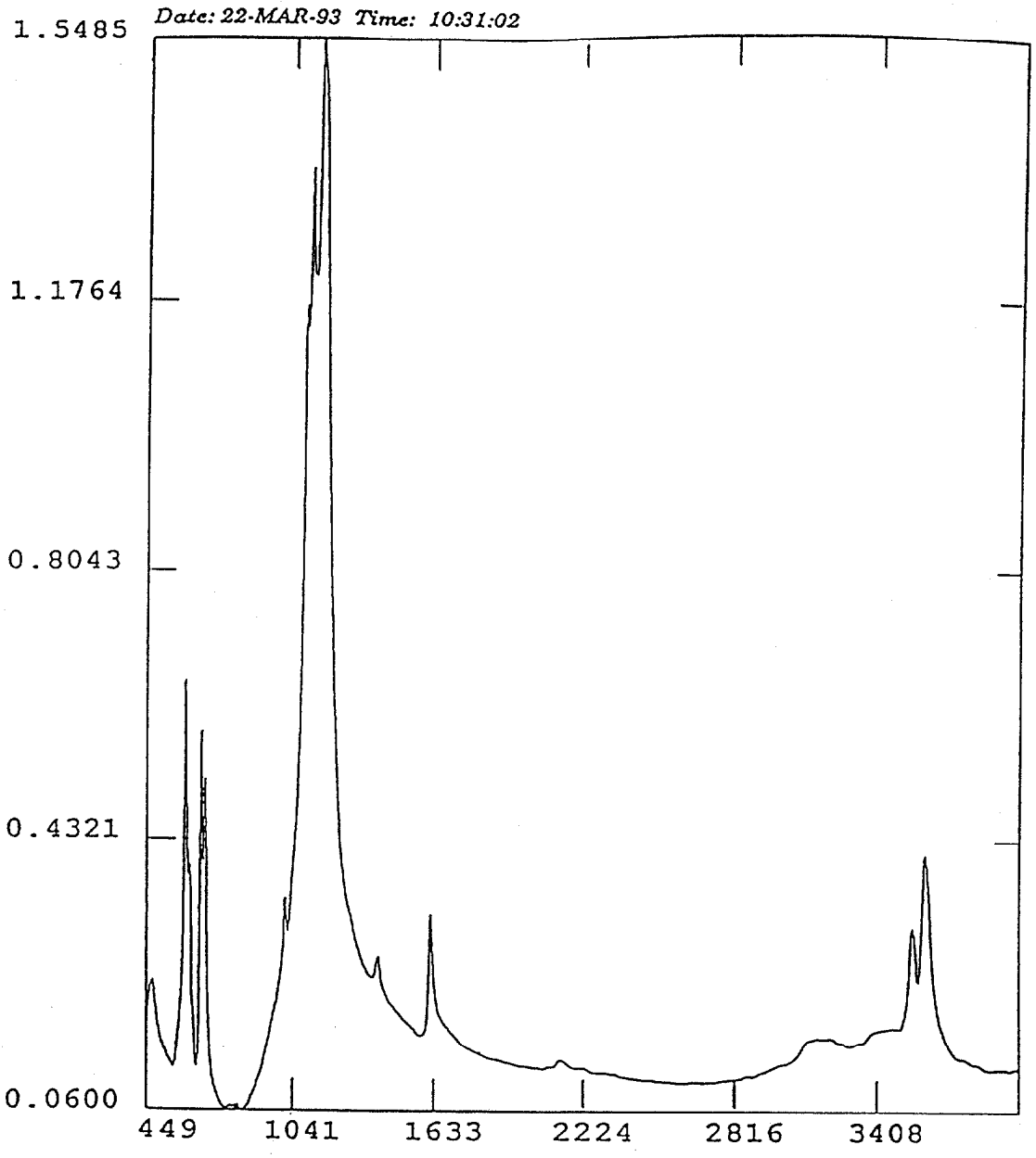

Figure 42: Baseline phosphogypsum transmission FT-IR spectrum

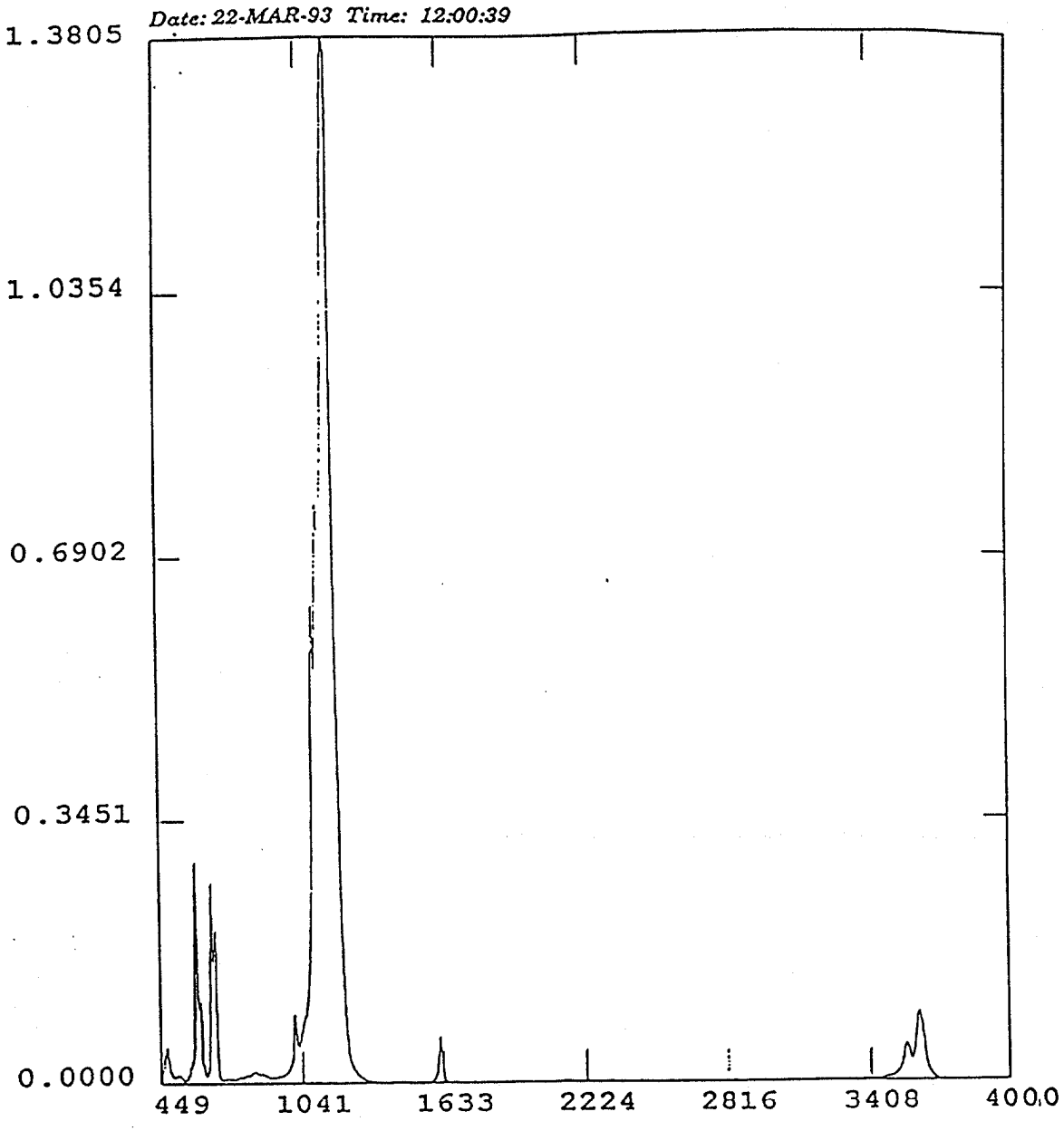

Figure 43: Baseline phosphogypsum diffuse reflectance FT-IR spectrum.

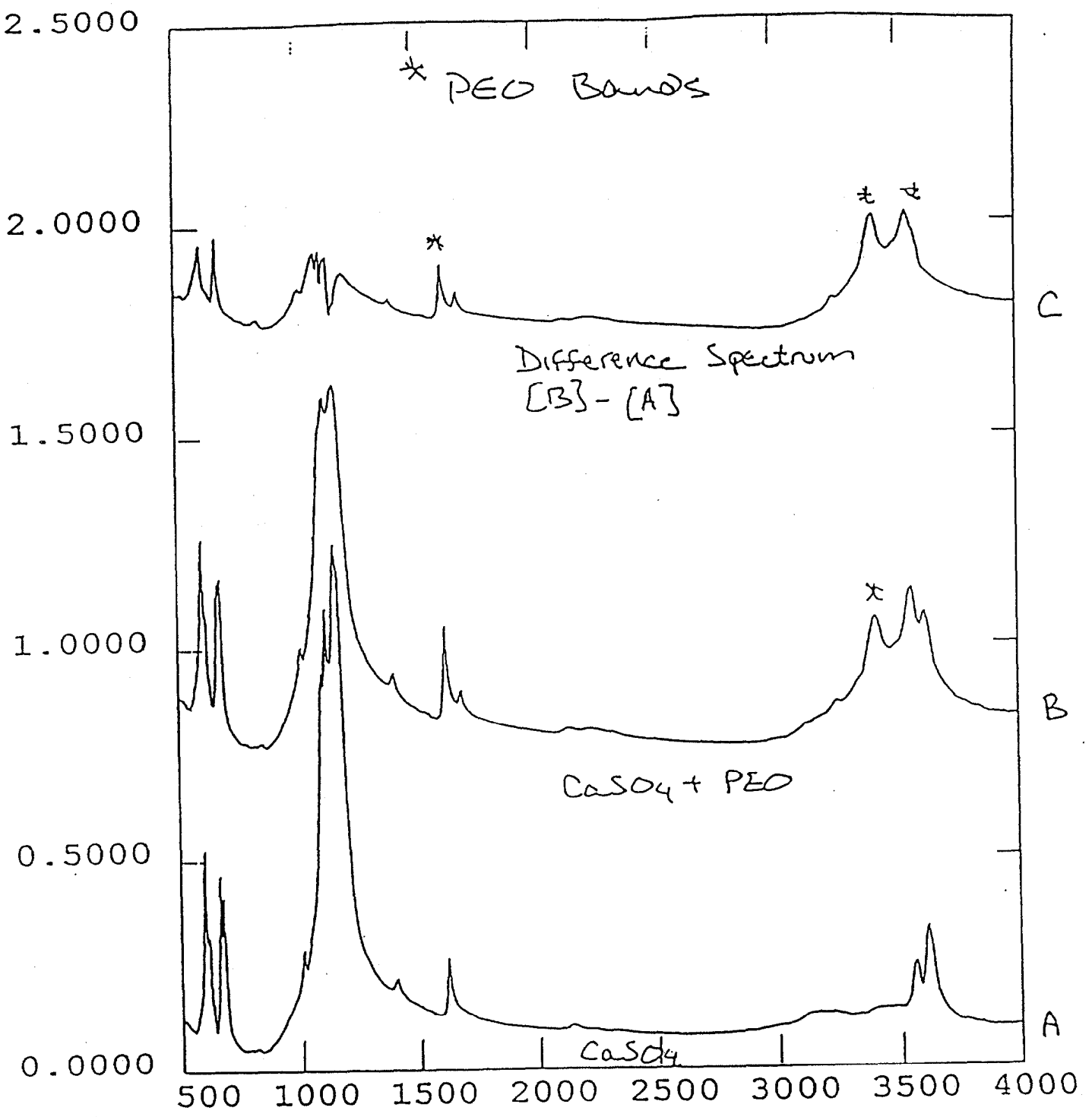

Figure 44: FT-IR transmission spectra using the pellet method. The bottom spectrum (c) corresponds to the phosphogypsum sample without PEO, the middle spectrum (b) to that of the PEO-treated phosphogypsum sample (0.01 wt %), and the top spectrum (a) corresponds to the difference spectrum of (b) - (c).

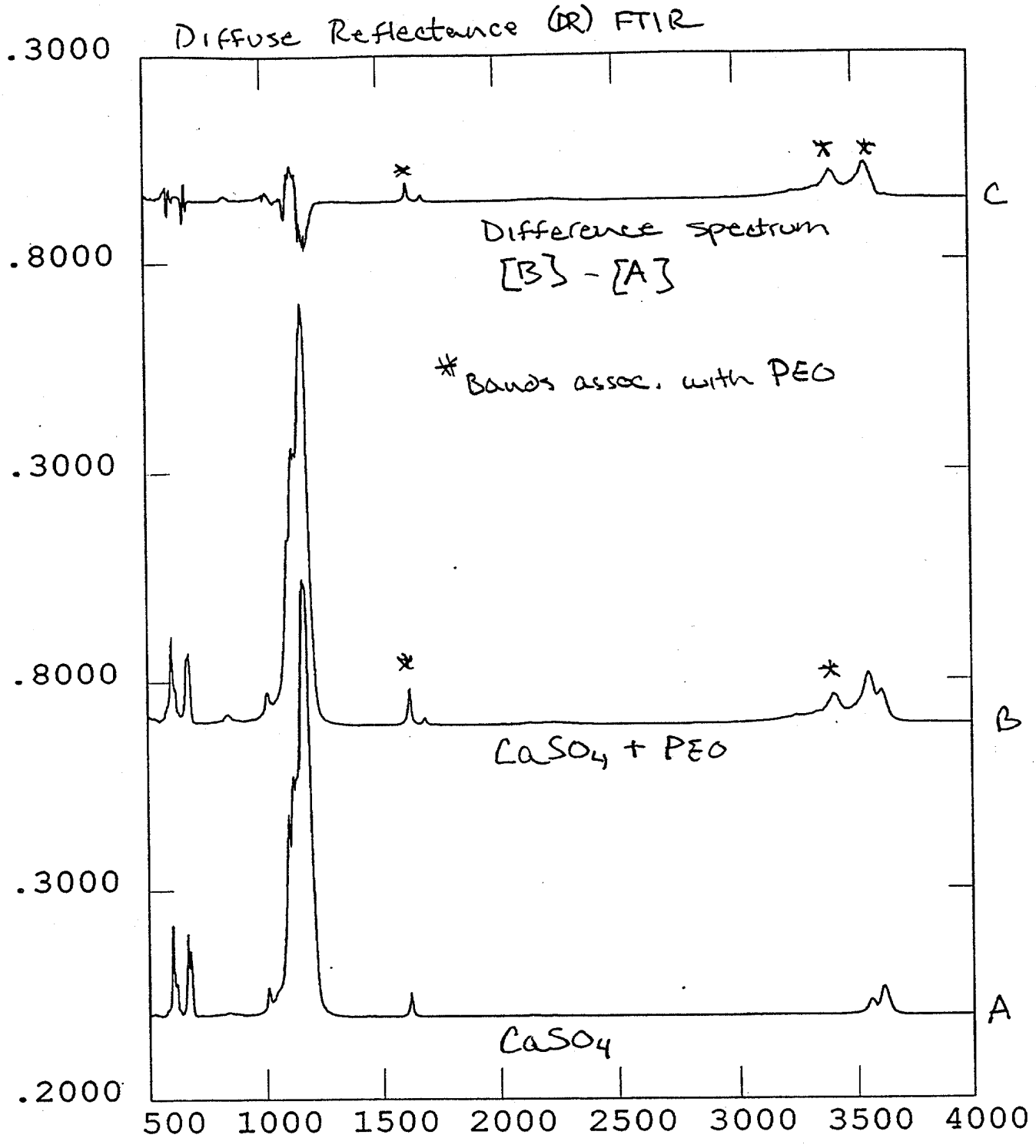

Figure 45: FT-IR diffuse reflectance (DR). The bottom spectrum (c) corresponds to the phosphogypsum sample without PEO, the middle spectrum (b) to that of the PEO-treated phosphogypsum sample (0.01 wt %), and the top spectrum (a) corresponds to the difference spectrum of (b) - (c).

The results obtained using the pellet method are shown in Figure 44. The bottom spectrum (c) corresponds to the phosphogypsum sample without PEO, the middle spectrum (b) to that of the PEO-treated phosphogypsum sample (0.01 wt %), and the top spectrum (a) corresponds to the difference spectrum of (b) - (c). The corresponding DR spectra are presented in Figure 45. As the difference in the spectra clearly show, the presence of PEO is readily detected at this concentration level.

NMR ANALYSES

Solution Species Characterization

The first objective in the analysis of the liquids was the assignment of resonances at various chemical shifts to particular species in the solution. This was based upon information in the literature, 15-20 preparation of synthetic mixtures, and the spectra of process acid to which known substances had been added.

The reference position of zero for phosphorus-31 is assigned to phosphoric acid in aqueous solution. Three other groups of peaks are observed in phosphoric acid solutions in the presence of aluminum ions. The first group, located at -8 ppm, is assigned to $Al(H_3PO_4)_3^{3+}$. The second group, located at -13 ppm is assigned to a mixture of $(AlH_2PO_4)^{2+}$ and $[Al(H_2PO_4)_2]^{+}$. The third peak, located at -16 ppm is assigned to $(AlH_3PO_4)^{+3}$. When fluoride ion is added, ternary complexes with H_3PO_4 are found to resonate at about -7 to -8 ppm and those with H_2PO_4- at about -13 ppm as shown for a synthetic mixture in Figure 46, so that it is not possible to confirm the participation of F- in a complex.

The most important silicon-29 resonance in this study, that of SiF_6^{2-}, appears in aqueous solution at -184 ppm from usual zero reference peak of tetramethylsilane or -191 ppm from the reference peak of hexamethyldisiloxane. An example is shown in Figure 47.

The zero reference position for aluminum-27 is assigned to the hydrated Al^{+3} ion in solution as shown in Figure 48. Complexes involving phosphate and fluoride also appear in this figure resonating at about -3 and -8 ppm.

The zero reference for the fluorine-19 species is assigned to the resonnance of $CFCl_3$. From our study and the data in the literature, the resonance of SiF_6^{2-} appears at 128 ppm as shown in Figure 49. The complexes with Al^{3+}, forming the series AlF^{2+}, AlF_2^{+}, AlF_3, AlF_4-, have resonances in sequence from -155 to -152 ppm as illustrated in Figure 49. Ternary complexes involving both aluminum and phosphate resonate between -143 and -150 ppm. The addition of appreciable amounts of aluminum in the synthetic mixtures removed the fluoride from the SiF_6^{2-} and eliminated the signals of this ion.

Process Acid Analysis

Generally, all the process acid samples lead to NMR spectra consisting of broad lines. There are two possible reasons for this result. The first is simply that nuclear species being observed exist in the liquid in several different chemical forms but have a lifetime in any one of them of the order of milliseconds or less, so that the nucleus exchanges between environments quite rapidly and give only a smeared-out average resonance. In this study it

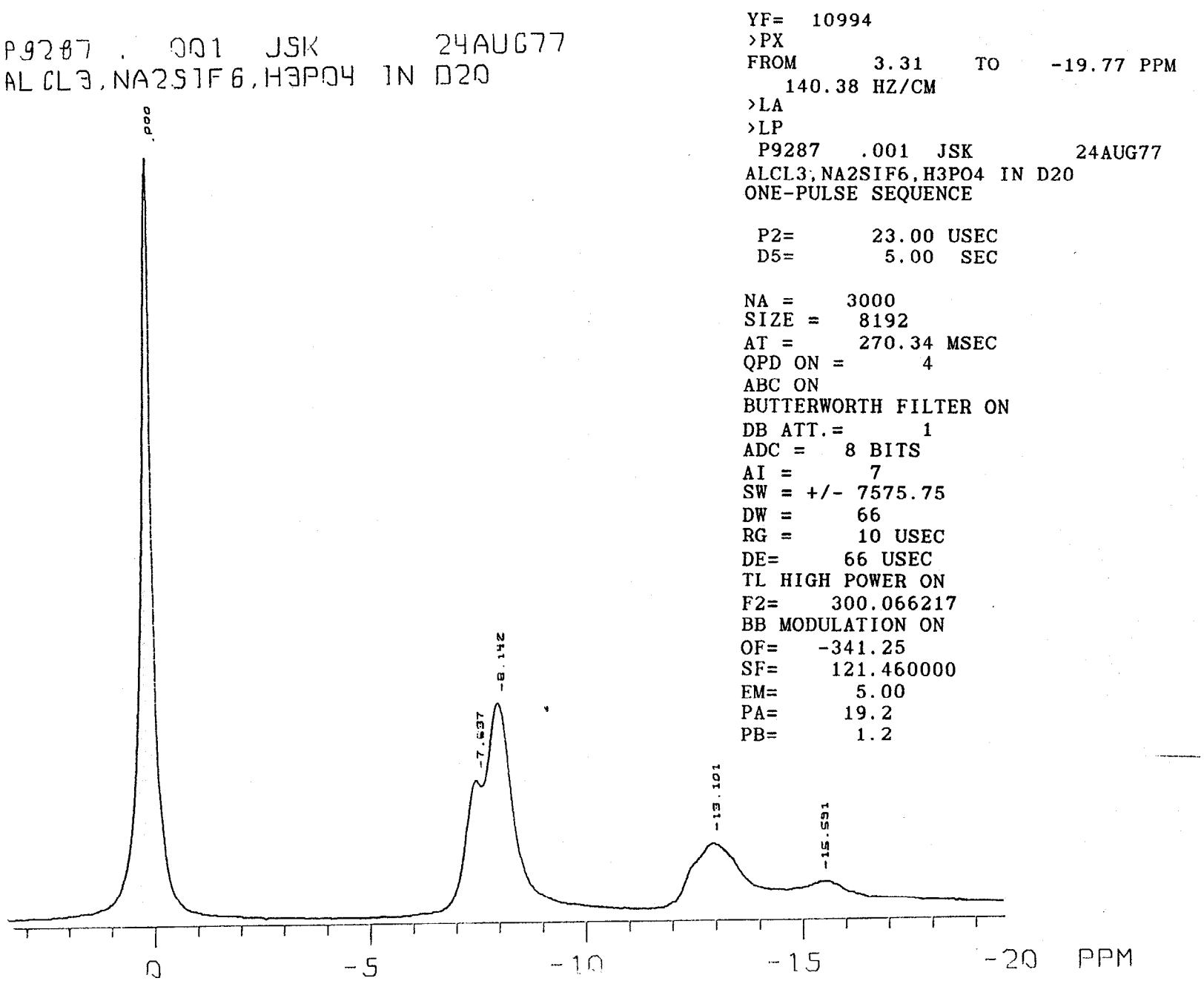

Figure 46: NMR Spectrum of Phosphorus-31 Species in the Presence of Aluminum Ions

Si spectrum of sample 9358 at 25oC June/
06/95

expl pulse sequence: s2pul

SAMPLE		DEC. & VT	
date	Jun 6 95	dfrq	499.752
solvent	D2O	dn	H1
file	/home/sam~	dpwr	30
ples/materials/935~		dof	-175.8
8/Si-9358_060695		dm	nnn
ACQUISITION		dmm	c
sfrq	99.269	dmf	200
tn	Si29	dseq	
at	1.284	dres	1.0
np	15424	homo	n
sw	6005.1	temp	25.0
fb	3400	PROCESSING	
bs	4	lb	10.00
tpwr	60	wtfile	
pw	16.0	proc	ft
d1	5.000	fn	not used
tof	-17540.4	math	f
nt	10000		
ct	1352	werr	
alock	n	wexp	wft
gain	10	wbs	wft
FLAGS		wnt	
il	n		
in	n		
dp	y		
hs	nn		
DISPLAY			
sp	-9626.5		
wp	6005.1		
vs	4.23539e+~ 06		
sc	0		
wc	250		
hzmm	6.93		
is	325520.84		
rfl	9626.5		
rfp	0		
th	11		
ins	1.000		

ai cdc ph

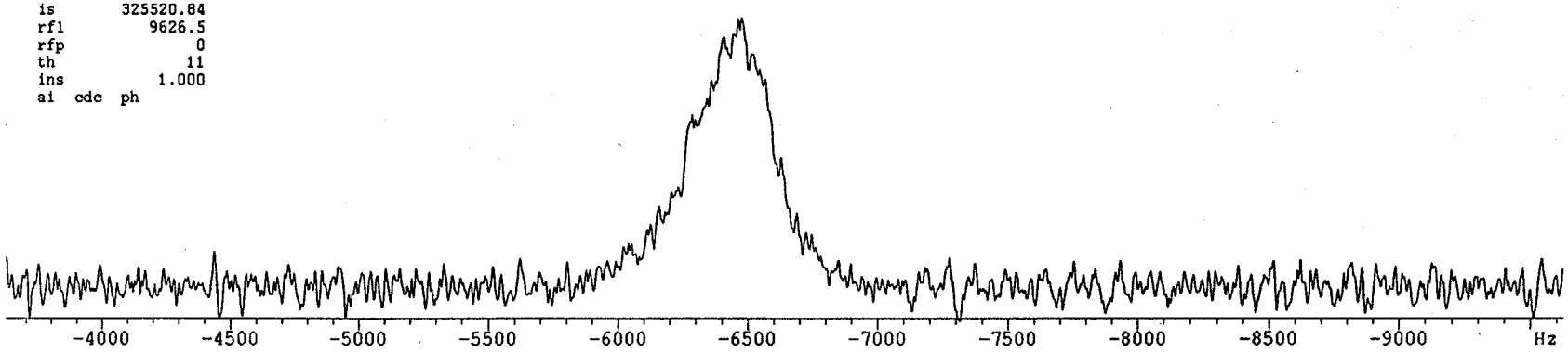

Figure 47: NMR Spectrum of Silicon-29 Species in Baseline Process Acid

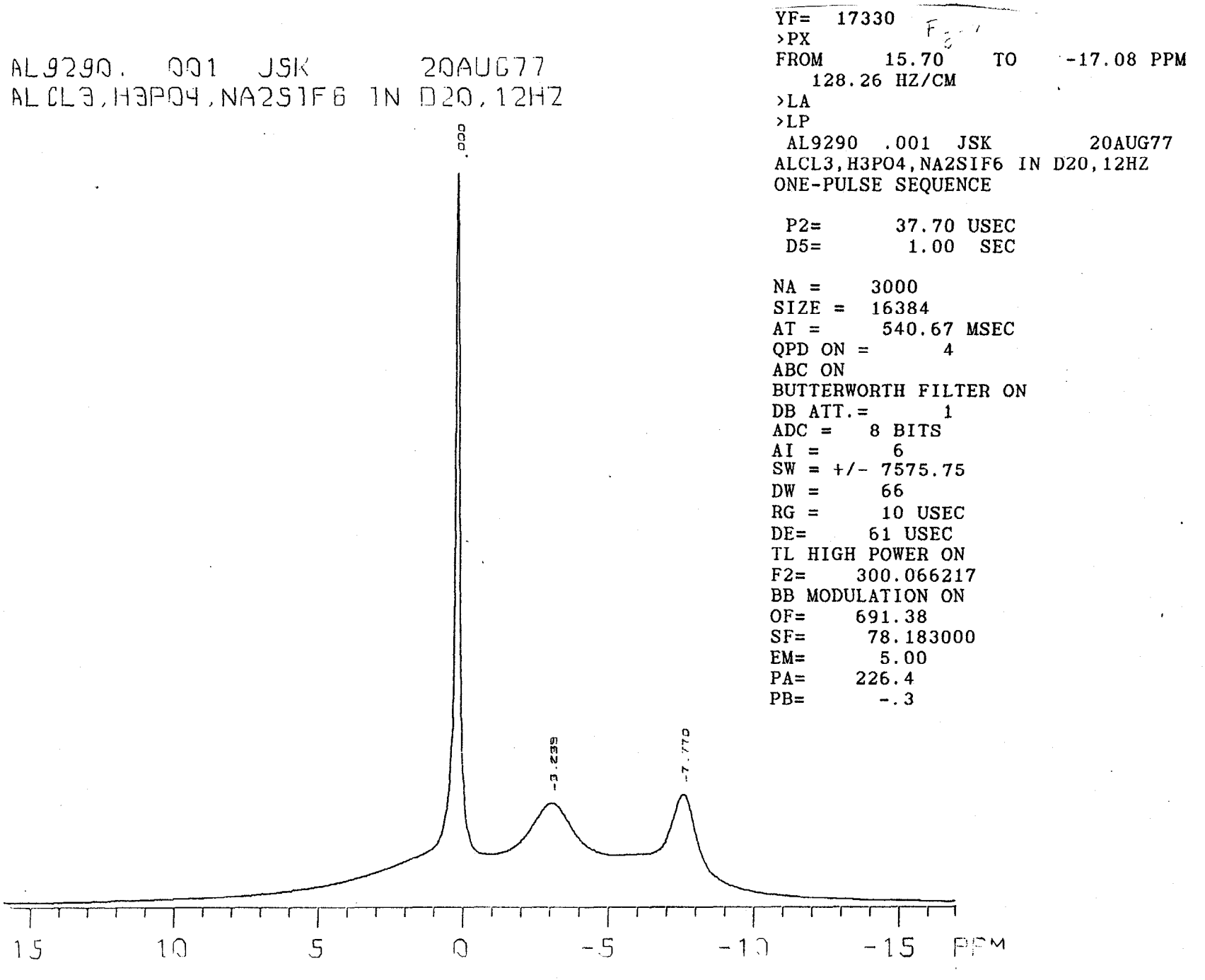

Figure 48: NMR Spectrum of Aluminum-27 Species in the Presence of Phosphoric Acid aand Sodium Fluosilicate

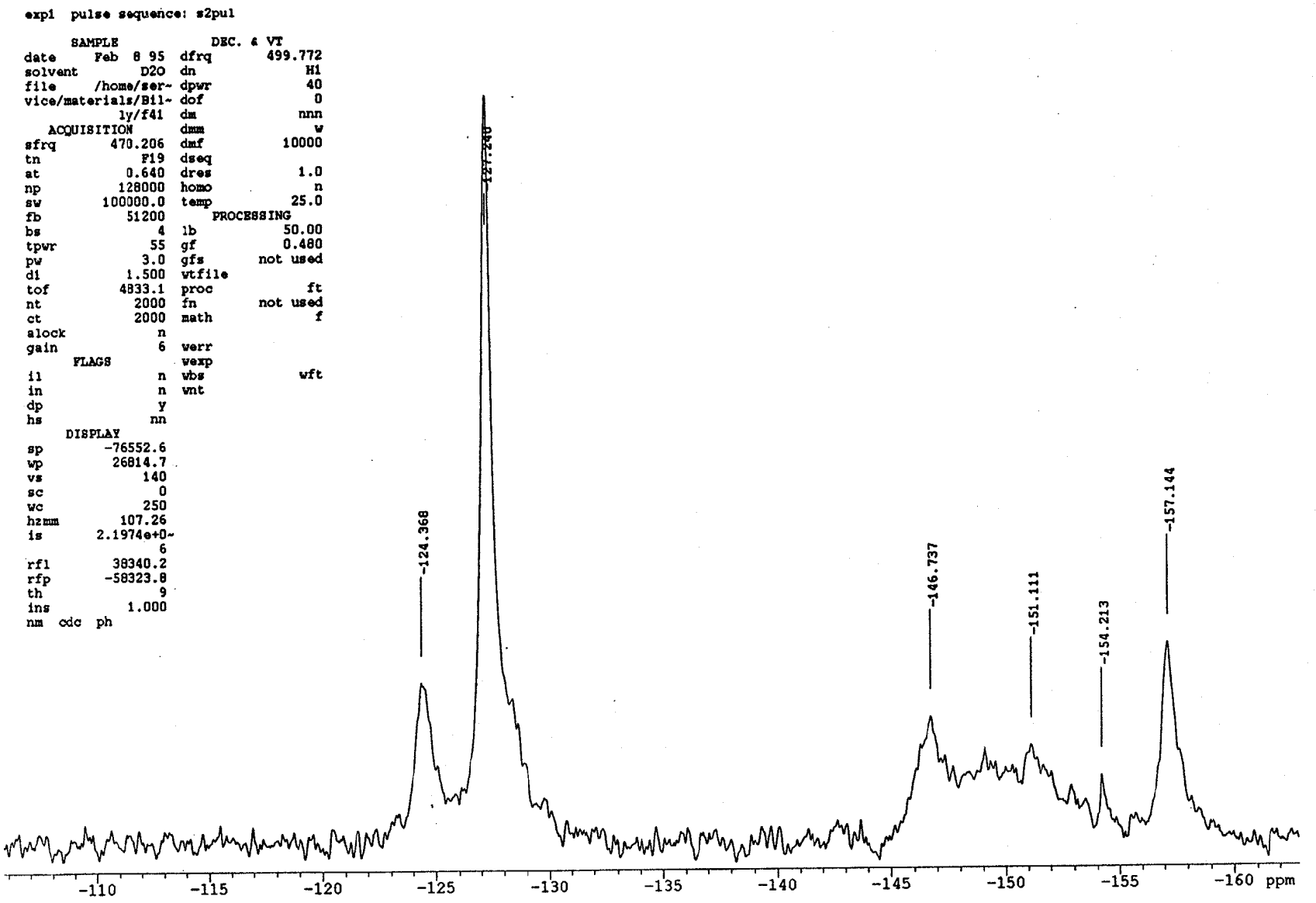

Figure 49: NMR Spectrum of Fluorine-19 Species in the Presence of Aluminum Chloride and Phosphoric Acid

has been observed that the lower temperatures tend to narrow the lines and permit better resolution, a result that is consistent with the proposal that exchange between sites produces broadening at higher temperatures. A second factor, and one which almost surely also contributes, is that the samples contain paramagnetic species such as ferric ion which cause the broadening of all signals.

In order to understand the role of additives in solution speciation, a number of NMR experiments were performed on filtrate solutions from PEO- and SDBS-treated reactor samples as well as non treated (baseline) samples. Some of the NMR studies have been centered upon fluorine resonances due to the high sensitivity of fluorine-19. The effect of doping the filtrate samples with aluminum nitrate was also evaluated to determine the corresponding changes in speciation.

Relative areas of fluorine resonances infiltrate solutions

Fluorine spectra of the samples listed in Table 33 were plotted and the areas of the various peaks measured on the plots with a planimeter. The area under an NMR peak is directly proportional to the concentration of the species responsible for the resonance, while the peak height depends upon the linewidth. Because of the large ratio of areas

Table 33
Comparison of Relative NMR Peak Areas and Phosphogypsum Filtration Rates

Compound	Sulfate (%)	-140 ppm	-145 ppm	-151 ppm	-135 to -165 ppm	Filtr. R. ton P_2O_5/ m^2day
BASELINE	2.5	1.88	5.60	6.61	1.42	7.4
BASELINE	2.5	1.81	6.17	7.62	1.58	7.4
BASELINE	3.0	2.62	4.08	6.41	1.69	8.2
BASELINE	3.5	1.21	3.96	7.00	1.84	9.0
PEO 3K	2.5	2.37	0.92	7.11	1.35	6.9
PEO 300K	2.5	1.14	6.08	6.47	1.65	7.5
PEO 4M	1.7	2.21	8.11	5.89	1.32	8.0
PEO 4M	1.7	2.30	5.25	3.61	1.76	8.0
PEO 4M	2.5	1.67	4.45	3.06	1.50	8.9
PEO 4M	3.5	1.59	8.00	10.13	1.53	10.2
PEO 8M	2.5	1.35	4.41	5.43	1.85	9.6
BSDBS	2.5	0.90	4.74	5.65	1.45	10.0

between the peaks for fluoride attached to silicon near -128 ppm and the peaks for fluoride attached to aluminum in the range of -135 to -165 ppm, it is necessary to make separate plots for the two regions and correct the measured areas for the ratio of scale factors between the two plots (see Figures 50 and 51).

In Table 33 are given the relative areas of the small peaks at -140, -145, and -151 ppm on the fluorine shift scale, and the relative area of a broad underlying resonance from -135 to -165 ppm, which is observed in the process acid solutions, all based upon the total area of the Si-F complex absorption as unity. Based on literature assignments and the earlier study of model solutions, the relatively weak peak at -140 is due to complexes of fluoride with $Al(H_2PO_4)^{2+}$ or $Al(H_2PO_4)_2^{+}$, that at -145 to complexes of the type AlF_2^{+} H_3PO_4, that at -151 to $Al\text{-}F\text{-}H_3PO_4$ or Al-F complexes, and absorption at higher field to Al-F or to HF. Figure 52 was constructed from the data in Table 33 and shows there is no distinctive peak trend that corresponds with the rate of filtration.

Close examination of the spectra of two process acid samples shows a very broad peak underlying the Al-F absorption (This is illustrated in Figure 53.), and there may be several factors contributing to the width of this resonance. One factor is the presence of paramagnetic impurities,such as Fe^{3+}. Another factor is the presence of very rapid exchange of fluoride ion among various complexes with different chemical shifts, spreading the resonance over the entire region between the points in the spectrum where resonances for the individual environments would be observed. The presence of paramagnetic impurities is indicated by the width of many of the individual resonances. The contribution of exchange is indicated by the sharpening of the resonances at lower temperatures.

The overall analysis of fluorine-19 resonances as a function of additive indicates the additives do not contribute to any significant changes in fluorine speciation in the process acid. The results also show that the fluctuations in flourine speciation, as evidenced by the changes in the relative peak ratios, are not related to the rate of phosphogypsum filtration.

Investigation of Phosphogypsum Solids

The technique of magic-angle spinning of solids permits obtaining a semi-high-resolution NMR spectrum of a magnetic species in a solid sample. The sample is contained in a rotor which is placed with its axis at an angle of 54.7° to the direction of the fixed magnetic field. Rotation at high speed eliminates the magnetic interactions between nuclei which are physically close in space, interactions which cause the normal spectra of solids to be very broad and featureless, often wider than the entire chemical shift range of a particular isotope.

Several samples of gypsum were examined by magic-angle-spinning NMR for the presence of phosphorus-31 and aluminum-27 nuclei. Using a newly obtained sample-

f9347 sample after filtering the precipi
tate at room temperature

exp2 pulse sequence: s2pul

SAMPLE		DEC. & VT	
date	Feb 20 95	dfrq	499.771
solvent	cdcl3	dn	H1
file	exp	dpwr	40
ACQUISITION		dof	0
sfrq	470.204	dm	nnn
tn	F19	dmm	w
at	0.800	dmf	10000
np	79104	dseq	
sw	49443.8	dres	1.0
fb	27200	homo	n
bs	16	temp	25.0
tpwr	55	PROCESSING	
pw	3.0	lb	10.00
d1	1.500	gf	0.480
tof	4833.1	gfs	not used
nt	1000	wtfile	
ct	1000	proc	ft
alock	n	fn	not used
gain	6	math	f
FLAGS			
il	n	werr	
in	n	wexp	wft
dp	y	wbs	wft
hs	nn	wnt	
DISPLAY			
sp	-71522.2		
wp	22769.0		
vs	140		
sc	0		
wc	250		
hzmm	91.08		
is	3000.00		
rfl	20234.2		
rfp	-60186.2		
th	28		
ins	1.000		

nm cdc ph

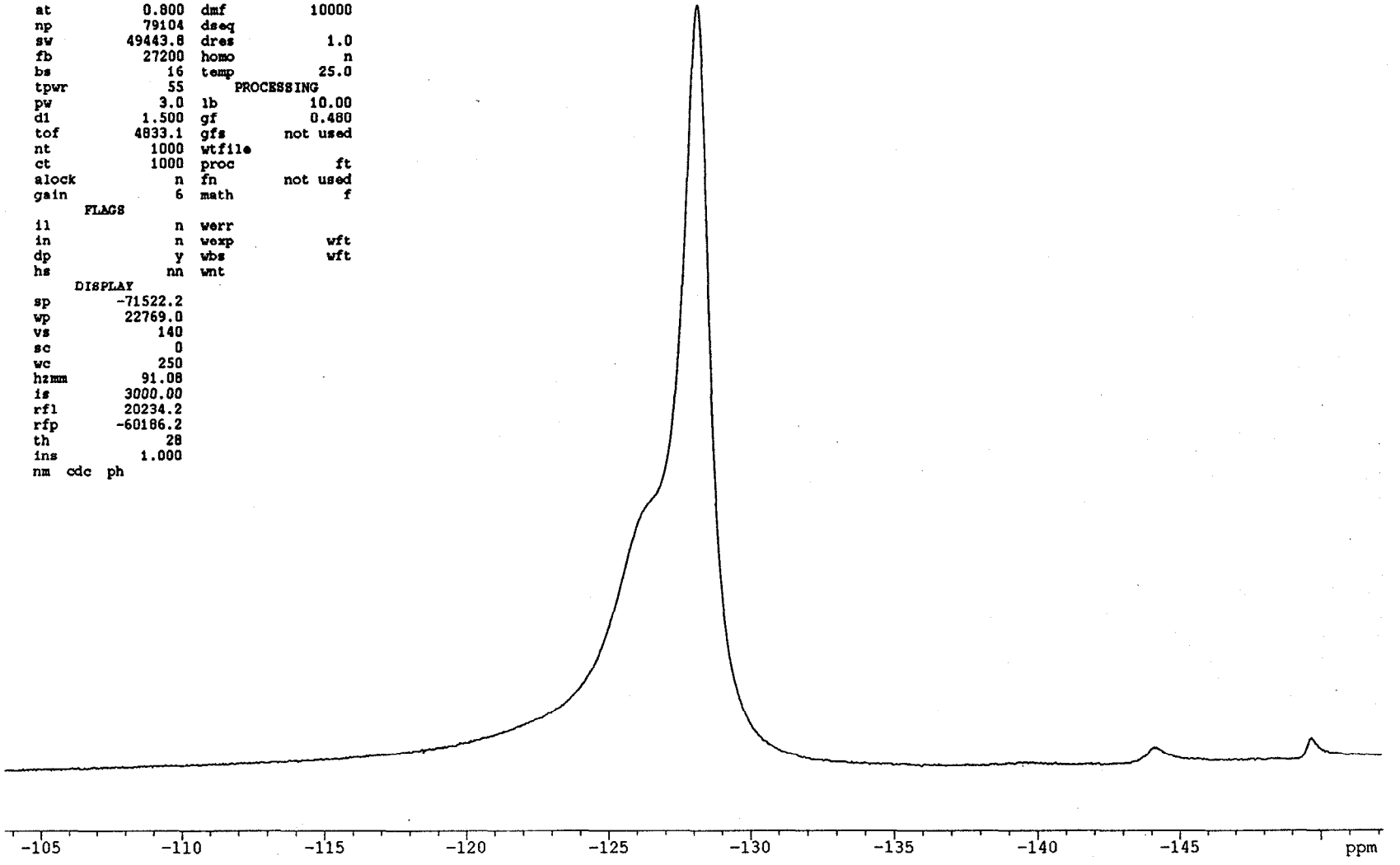

Figure 50: NMR Fluorine-19 Spectrum of Process Acid Solution

f9347 sample after filtering the precipi
tate at room temperature

exp2 pulse sequence: s2pul

SAMPLE		DEC. & VT	
date	Feb 20 95	dfrq	499.771
solvent	cdcl3	dn	H1
file	exp	dpwr	40
ACQUISITION		dof	0
sfrq	470.204	dm	nnn
tn	F19	dmm	w
at	0.800	dmf	10000
np	79104	dseq	
sw	49443.8	dres	1.0
fb	27200	homo	n
bs	16	temp	25.0
tpwr	55	PROCESSING	
pw	3.0	lb	50.00
d1	1.500	gf	0.480
tof	4833.1	gfs	not used
nt	1000	wtfile	
ct	1000	proc	ft
alock	n	fn	not used
gain	6	math	f
FLAGS			
il	n	werr	
in	n	wexp	wft
dp	y	wbs	wft
hs	nn	wnt	
DISPLAY			
sp	-73423.4		
wp	10404.1		
vs	2376		
sc	0		
wc	250		
hzmm	41.62		
is	2.09864e+06		
rf1	20234.2		
rfp	-60186.2		
th	-19		
ins	1.000		

nm cdc ph

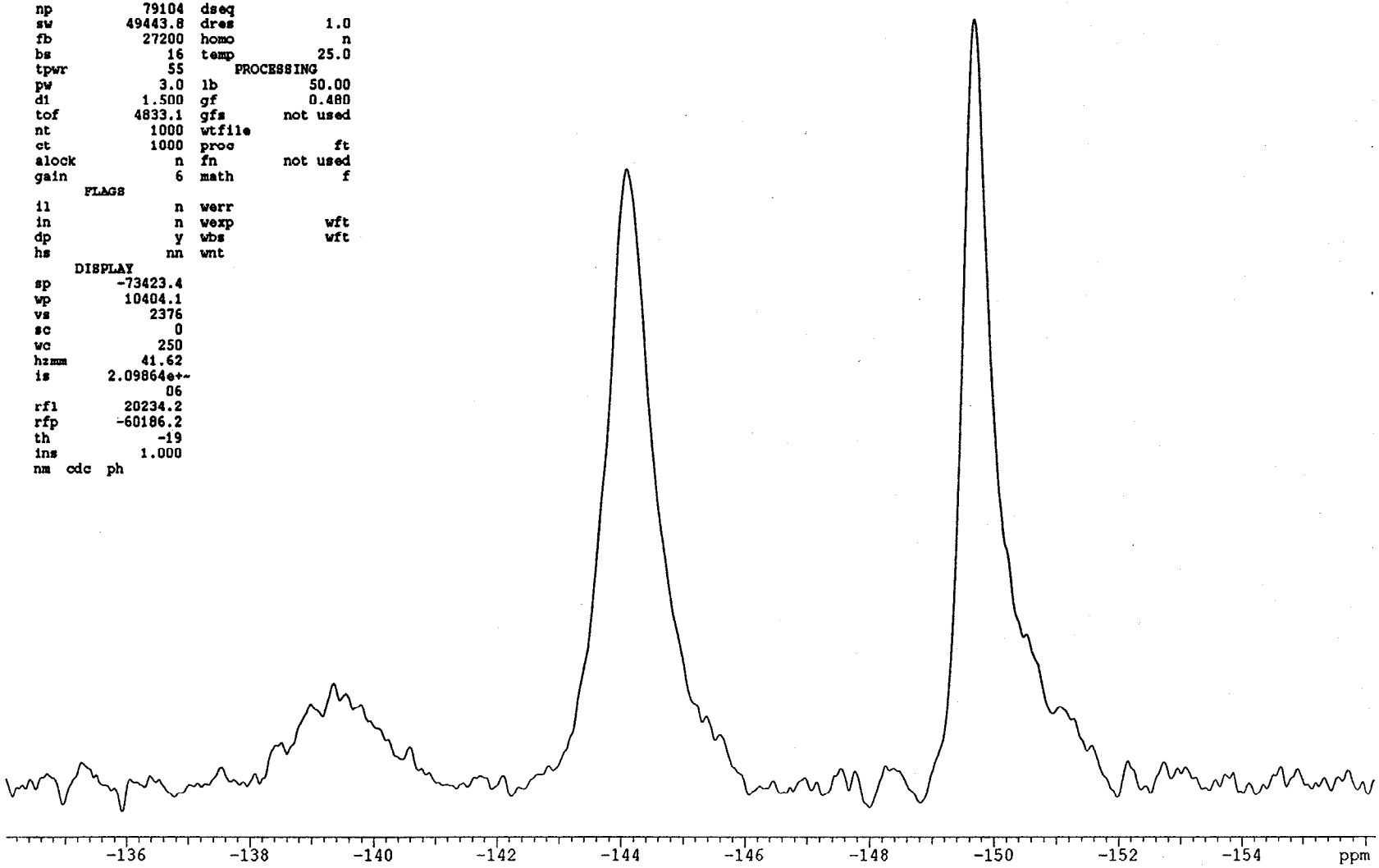

Figure 51: Expanded Region between -134 and -156 ppm of the Fluorine-19 Process Acid Spectrum Shown in Figure 50

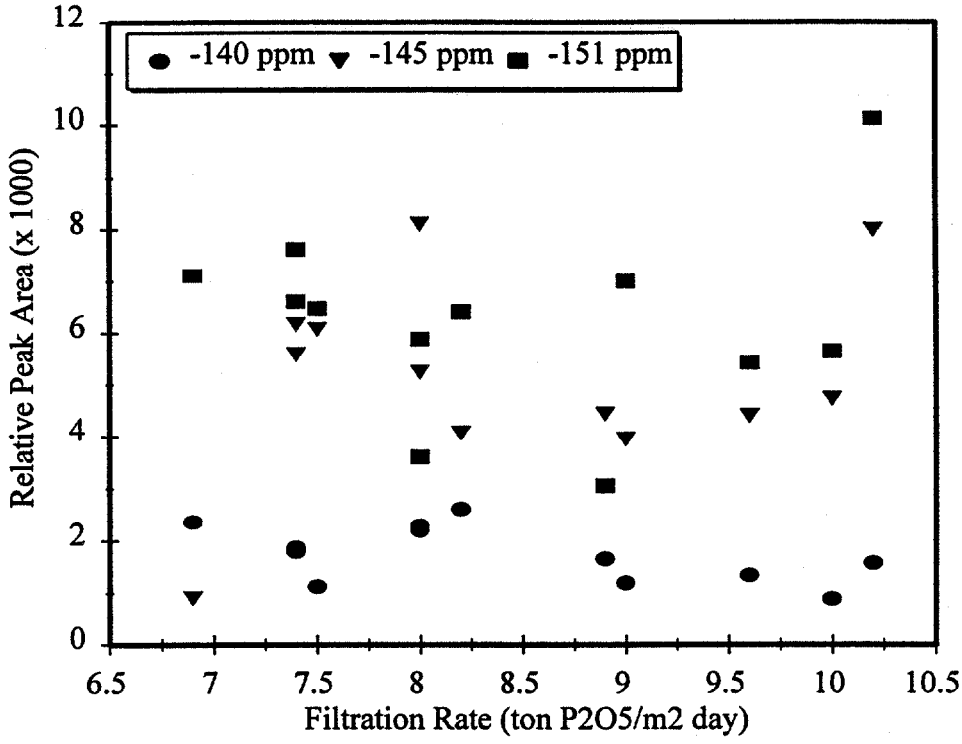

Figure 52: Comparison of relative NMR fluorine-19 peak intensities in process acid with the corresponding rate of filtration.

containg rotor with a low level of aluminum, no aluminum signals above background were found.

Phosphorus spectra, however, were quite interesting. Spinning powdered samples in 5 mm OD rotors at rates from 3000 to 6000 hertz yielded patterns consisting of center band and a number of spinning sidebands, spaced from the center band at integral multiples of the spinning frequency. Each of the samples showed two sets of resonances, indicating that there are two different environments in which the phosphate units are found in the solid, separated by about 5 ppm. In addition, the nature of the patterns - the fact that the arrays of spinning sidebands are not symmetrical about the center band - indicates that both of the environments are quite anisotropic. One or both of the signals may arise from fluorophosphate complexes.[21] The bseline and PEO-treated material show 80 to 90 % of the predominant species (Figures 54, 55). The BSDBS-treated material (Figure 56), however, shows reduction of the principal component by about three-fourths. Precise quantification is not possible because of overlap of the peaks, but approximate relative amounts of the two types of phosphate are given in Table 34.

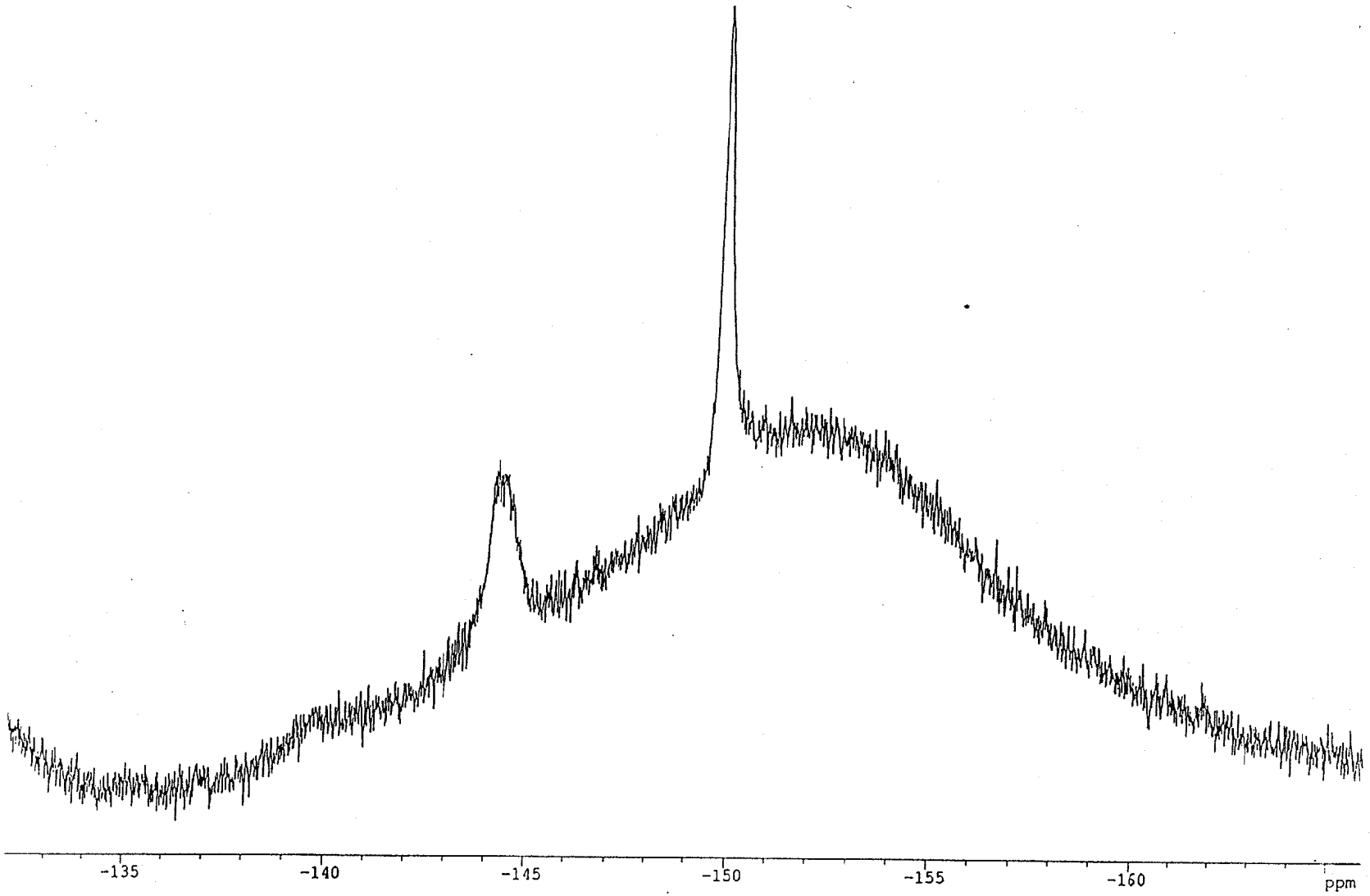

Figure 53: NMR Fluorine-19 Spectrum of BSDBS-Treated Process Acid Solution to which Aluminum was Added as Aluminum Nitrate at 25°C

Another approach that was taken to evaluate the differences in the phoshogypsum that is filtered off is by the preparation of aqueous extracts of the solid materials. These liquids were then examined by high-resolution NMR. (A weight of 0.3 grams of powdered phosphogypsum solid was slurried by vigorous stirring with 3 ml of H_2O-D_2O mixture, then allowed to stand for an hour, and then filtered off.) The NMR spectra of the filtrate were obtained for phosphorus-31 and fluorine-19 (see Figures 57, 58 and 59 for the phosphorus-31 spectra). Relative intensities, within samples for fluorine-19, and between samples for both phosphorus-31 and fluorine-19, are tabulated in Table 35 for two samples of each of the baseline material, the PEO-treated material, and the BSDBS-treated material.

From these results, it is clear that the addition of the treating agent has a substantial effect on the composition of the gypsum. It is of course possible that these results are influenced by the strength with which the solid gypsum retains the impurities, and that this is what is modified by the agent. However, the results of the magic-angle-spinning experiments on the solids indicate that there is an actual decrease in the amount of phosphate in the gypsum precipitate brought about by the SDBS treatment. It also seems very significant that the treatment, by either agent completely eliminates the SiF_6^{2-} component from the extracts.

Table 34
Relative Amounts of Phosphate Retained in Phosphogypsum

Sample Type	Relative Major Peak Height	Relative Minor Peak Height
Baseline	750	75
PEO	910	50
BSDBS	145	50

Table 35
Relative Amounts of Components in Aqueous Extracts of Phosphogypsum Solids

Sample Type	phosphorus-31	fluorine-19 -128 ppm	fluorine-19 -153 ppm	fluorine-19 -155 ppm	fluorine-19 -157 ppm
Baseline A	140	90	3	40	11
PEO A	30	0	1	30	20
BSDBS A	30	0	4	33	5
Baseline B	80	75	3	40	11
PEO B	20	0	0	25	18
BSDBS B	0	0	3	22	4

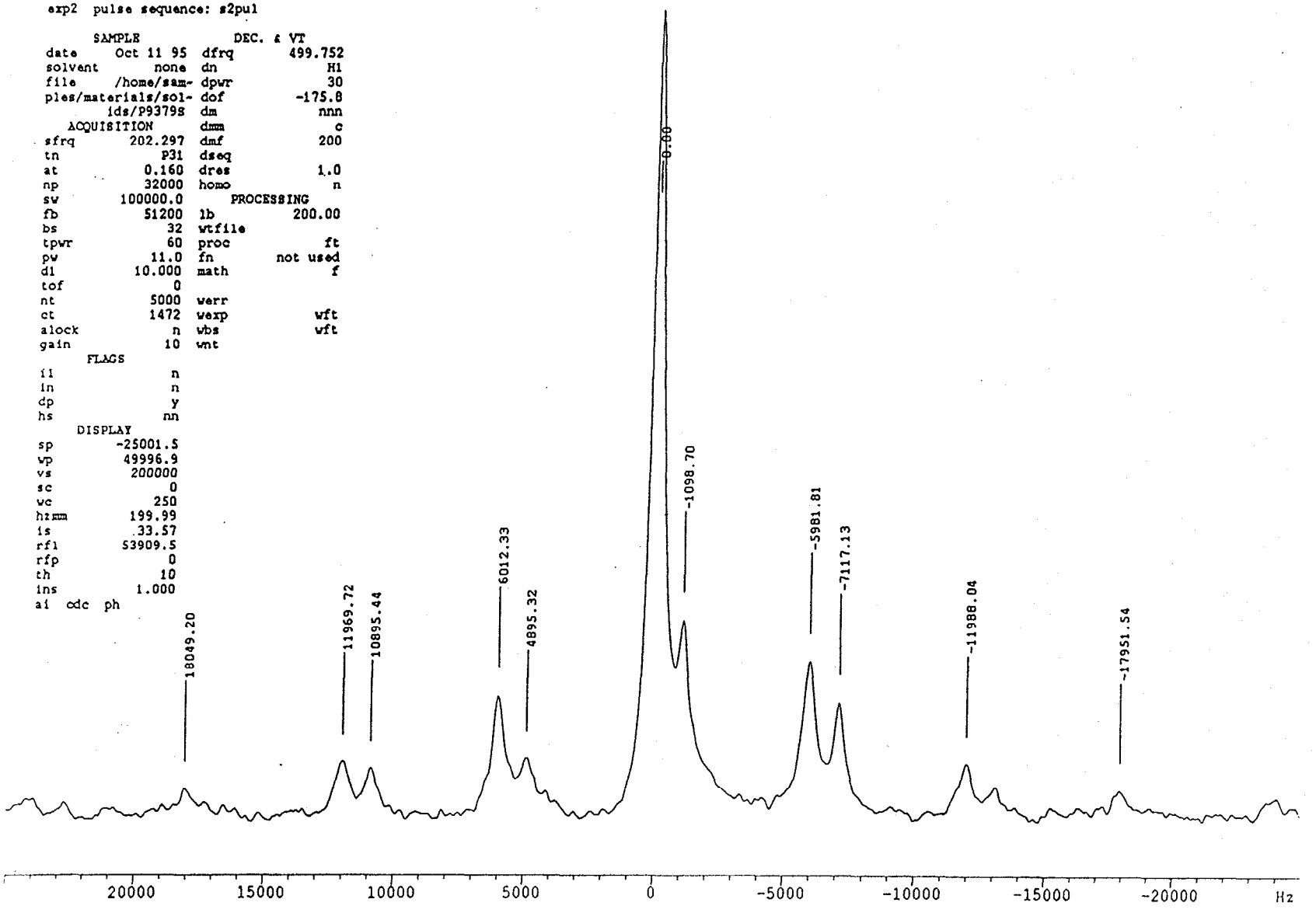

Figure 54: NMR Phosphorus-31 Spectrum of Baseline Phosphogypsum Obtained Using Magic Angle Spinning

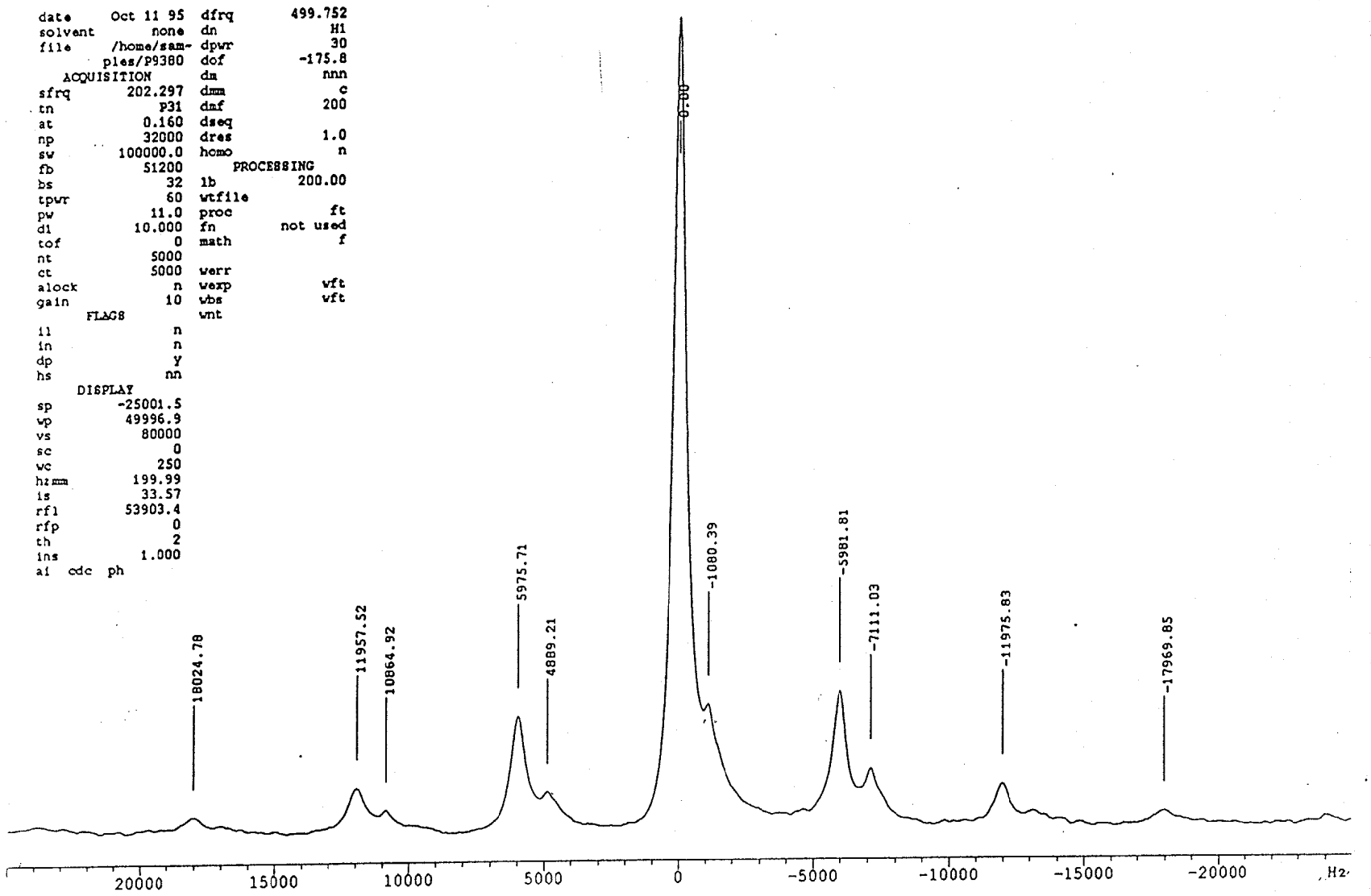

Figure 55: NMR Phosphorus-31 Spectrum of PEO-Treated Phospohgypsum Obtained Using Magic-Angle Spinning

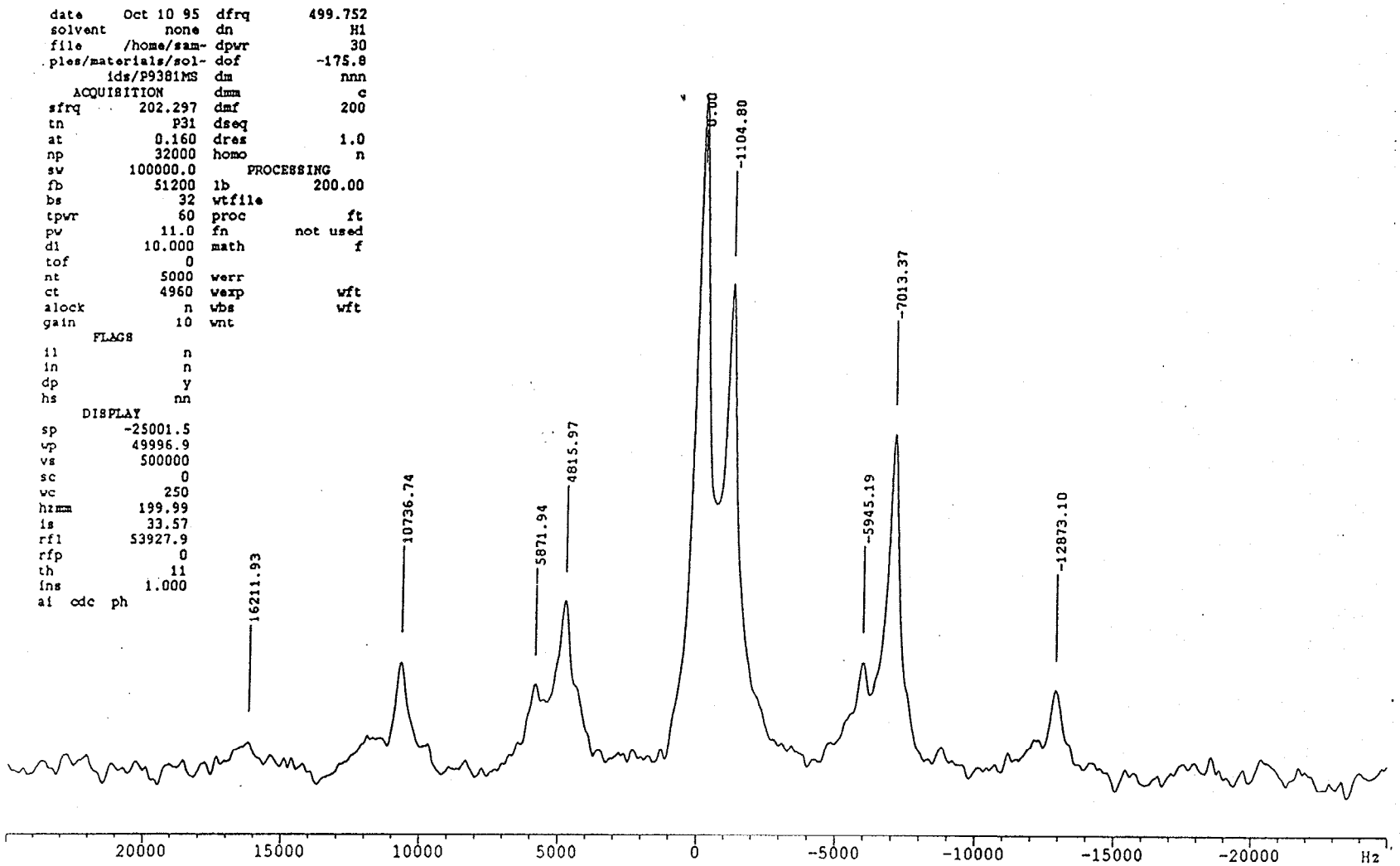

Figure 56: NMR Phosphorus-31 Spectrum of BSDBS-Treated Phosphogypsum Obtained Using Magic-Angle Spinning

P31 9386

exp1 pulse sequence: s2pul

SAMPLE		DEC. & VT	
date	Sep 27 95	dfrq	499.752
solvent	d2o	dn	H1
file	/home/wsb~	dpwr	40
rey/additions/Au28~		dof	0
95/P31_9386_092795~		dm	nnn
	-short	dmm	w
ACQUISITION		dmf	10000
sfrq	202.302	dseq	
tn	P31	dres	1.0
at	0.800	homo	n
np	79104	temp	25.0
sw	49443.8	PROCESSING	
fb	27200	lb	100.00
bs	16	gf	0.480
tpwr	59	gfs	not used
pw	12.0	wtfile	
d1	2.000	proc	ft
tof	4833.1	fn	not used
nt	2000	math	f
ct	2000		
alock	n	werr	
gain	6	wexp	
FLAGS		wbs	wft
il	n	wnt	
in	n		
dp	y		
hs	nn		
DISPLAY			
sp	-24173.8		
wp	49443.8		
vs	2e+06		
sc	0		
wc	250		
hzmm	197.78		
is	864000.00		
rf1	24173.8		
rfp	0		
th	28		
ins	1000.000		
ai cdc ph			

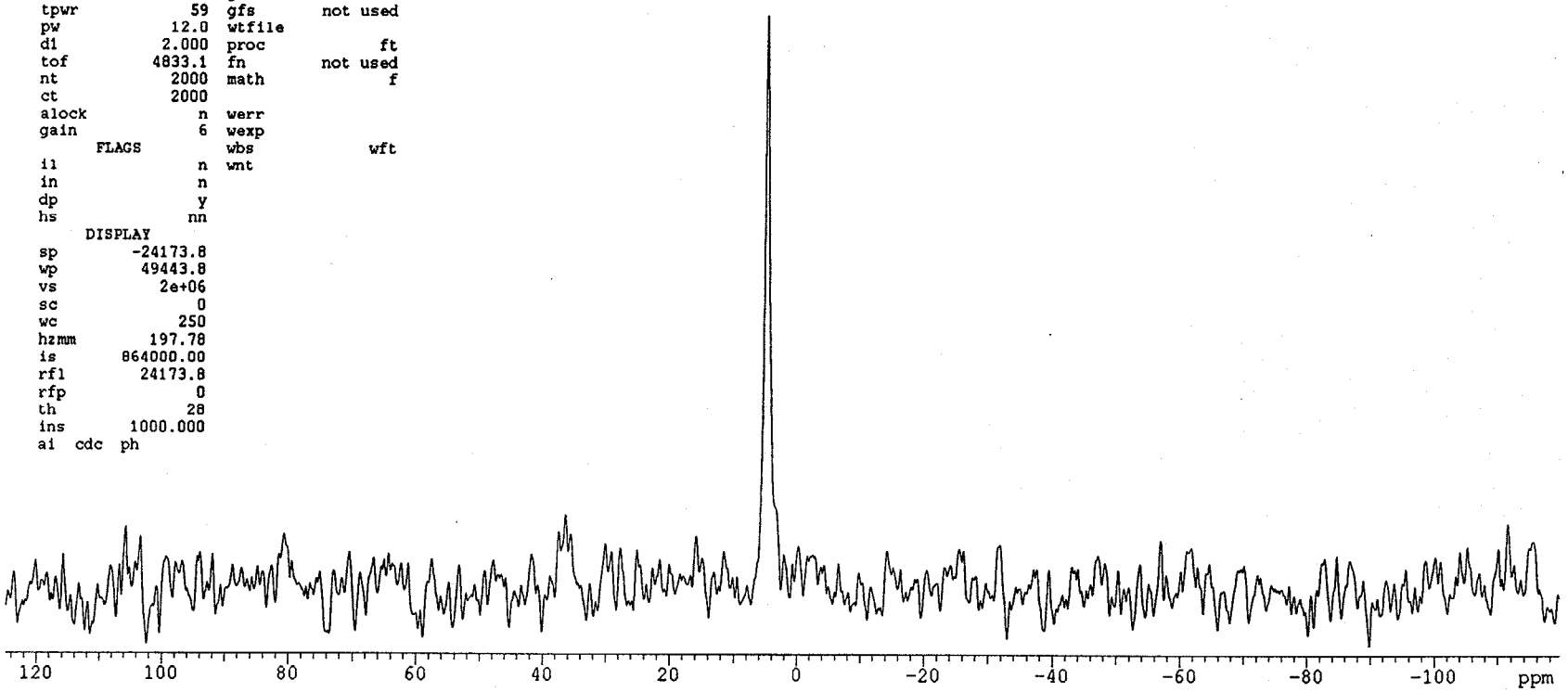

Figure 57: NMR Phosphorus-31 Spectrum Obtained from Water Saturated with Baseline Phosphogypsum

P31_9387

exp1 pulse sequence: s2pul

SAMPLE		DEC. & VT	
date	Sep 27 95	dfrq	499.752
solvent	d2o	dn	H1
file	/home/wsb~	dpwr	40
rey/additions/Au28~		dof	0
95/P31_9387_092795		dm	nnn
ACQUISITION		dmm	w
sfrq	202.302	dmf	10000
tn	P31	dseq	
at	0.800	dres	1.0
np	79104	homo	n
sw	49443.8	temp	25.0
fb	27200	PROCESSING	
bs	16	lb	100.00
tpwr	59	gf	0.480
pw	12.0	gfs	not used
d1	2.000	wtfile	
tof	4833.1	proc	ft
nt	2000	fn	not used
ct	2000	math	f
alock	n		
gain	6	werr	
FLAGS		wexp	
il	n	wbs	wft
in	n	wnt	
dp	y		
hs	nn		
DISPLAY			
sp	-24173.8		
wp	49443.8		
vs	2e+06		
sc	0		
wc	250		
hzmm	197.78		
is	864000.00		
rfl	24173.8		
rfp	0		
th	28		
ins	1000.000		

ai cdc ph

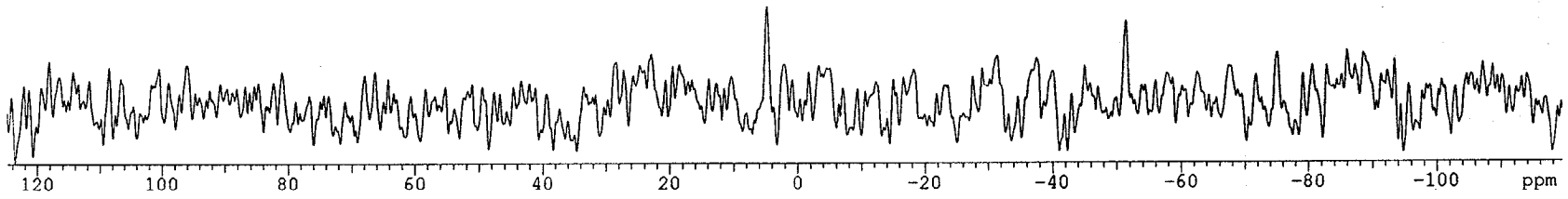

Figure 58: NMR Phosphorus-31 Spectrum Obtained from Water Saturated with PEO-Treated Phosphogypsum

P31 9388

expl pulse sequence: s2pul

SAMPLE		DEC. & VT	
date	Sep 26 95	dfrq	499.752
solvent	d2o	dn	H1
file	/home/wsb~	dpwr	40
rey/additions/Au28~		dof	0
95/P31_9388_092695		dm	nnn
ACQUISITION		dmm	w
sfrq	202.302	dmf	10000
tn	P31	dseq	
at	0.800	dres	1.0
np	79104	homo	n
sw	49443.8	temp	25.0
fb	27200	PROCESSING	
bs	16	lb	100.00
tpwr	59	gf	0.480
pw	12.0	gfs	not used
d1	2.000	wtfile	
tof	4833.1	proc	ft
nt	2000	fn	not used
ct	2000	math	f
alock	n		
gain	6	werr	
FLAGS		wexp	
il	n	wbs	wft
in	n	wnt	
dp	y		
hs	nn		
DISPLAY			
sp	-24173.8		
wp	49443.8		
vs	2e+06		
sc	0		
wc	250		
hzmm	197.78		
is	864000.00		
rfl	24173.8		
rfp	0		
th	28		
ins	1000.000		
ai cdc ph			

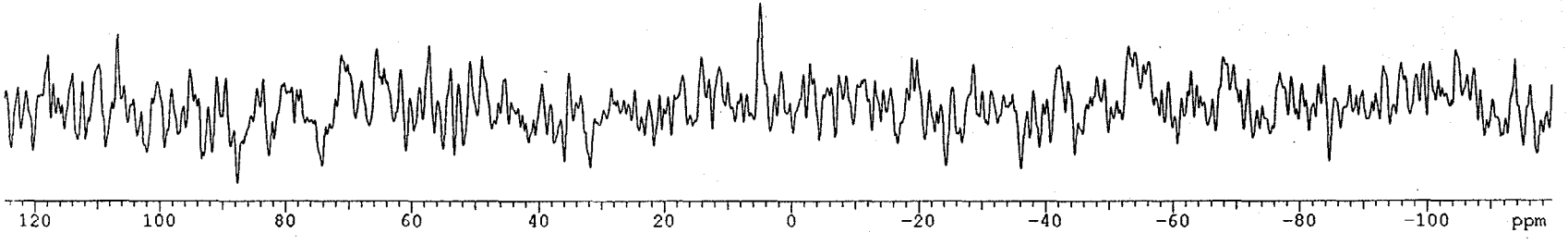

Figure 59: NMR Phosphorus-31 Spectrum Obtained from Water Saturated with BSDBS-Treated Phosphogypsum

Addition of Al^{3+}

An aqueous solution of 16 % aluminum was added as $Al(NO_3)_3$ in varying amounts to several of the filtrate samples. The percentages added as indicated in Table 36 represent the fraction of the total volume of the mixture represented by the $Al(NO_3)$ solution. A comparison of the ratio of peak areas as presented in Figure 60 reveals that,

Table 36
Comparison of NMR fluorine peak ratios (relative to the -128 ppm resonance)

Added Aluminum Concentration (%)	-145 ppm peak ratio x 100	-150 ppm peak ratio x 100	-135 to -165 ppm peak ratio
0.0	0.411	0.605	0.13
1.6	0.475	0.305	0.16
2.3	0.448	0.224	0.32
2.9	0.428	0.377	0.22
4.2	0.762	0.586	0.27
4.7	0.910	0.520	0.67
6.3	1.29	0.993	0.59

as expected, the fluorine compounds are strongly affected with large additions of aluminum. However, it is uncertain why small additions of aluminum do not change the fluorine speciation significantly. Representative spectra of the resulting mixtures are shown in Figures 53 and 61. As expected, the relative areas for the aluminum complexes involving fluoride as compared to fluoride attached to silicon increase (primarily in the broad underlying resonance rather than in the sharper peaks). The broad region shifts to higher field, indicating an increase in complexes of the type AlF^{2+} or AlF_2^{+} compared to those involving phosphoric acid. These experiments with aluminum additions have helped to identify aluminum/fluoride complexes that are important in phosphoric acid production.

Effect of Lowering Temperature

Spectra of a number of the process acid samples, both as produced and with added aluminum nitrate, were obtained at -10° for comparison with the results at room temperature as shown in Figures 62-64. The lower temperature provides much better resolution of resonances for the various species present.

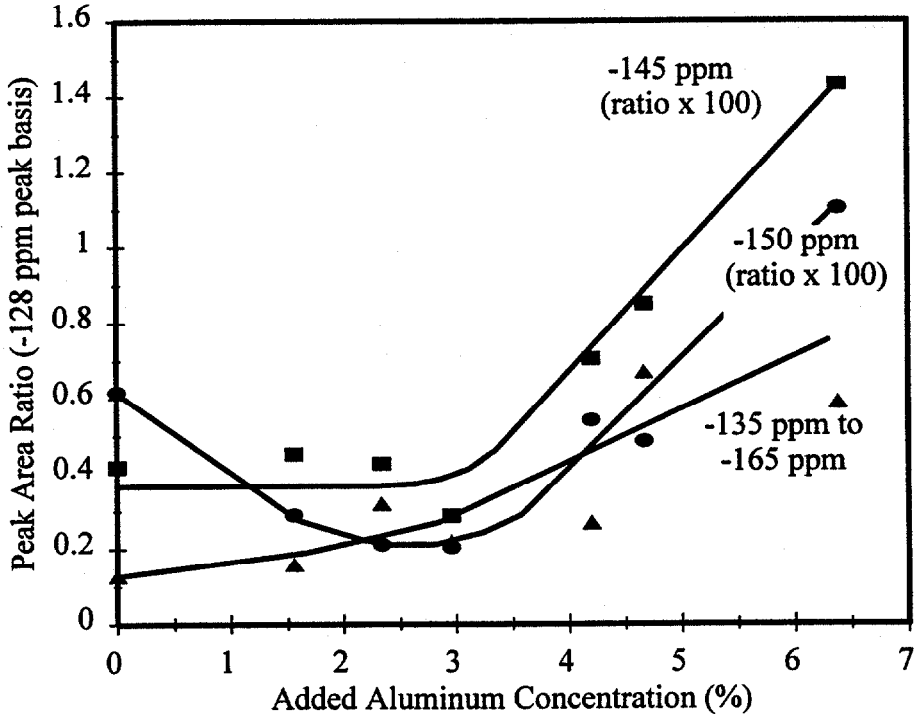

Figure 60: Comparison of NMR peak ratios relative to the -128 ppm resonance at 25°C for filtrate solutions to which aluminum was added as aluminum nitrate.

Most striking is the change observed for the higher concentrations of added $Al(NO_3)_3$, illustrated for sample 9358 in Figure 62. The resonance corresponding to silicon complexes of fluoride is now clearly resolved into two peaks, The low-field portion, to the left in the spectrum, is only a shoulder at room temperature, and this is probably from $SiF_5(H_2O)^-$. This assignment is consistent with literature reports, and is reasonable in light of the greatly increased concentation of Al-F complexes. The region from -138 to -146, with six resolved resonances, probably corresponds to complexes of fluoride and aluminum with $H_2PO_4^-$, although these have not been clearly identified in model solutions or in the literature. The two tallest peaks, at the right of the spectrum, are at the positions for AlF^{2+} and AlF_2^+ in H_3PO_4. In the middle region are the resonances for Al–F–H_3PO_4 complexes in various ratios of the components. The low temperature test data provide insight into solution speciation that is not possible at room temperature or at 80°C.

Silicon Spectra

Silicon-29 spectra have been obtained on the Unity-500 spectrometer for three typical WPA samples. All show peaks corresponding to the SiF_6^{2-} complexes, at about the same concentration. Additional silica may be present as silicate, but the resonance corresponding to this species is obliterated by the resonance of the silicate in the glass sample container which must be employed. Because of the low natural abundance of silicon-29, 4.6%, and the lower rf frequency at which it absorbs, the sensitivity of this nucleus is about 10^{-3} times that of fluorine, meaning that an acquisition time 10^6 as long is required for silicon as for fluorine to obtain spectra with, the same signal/noise.

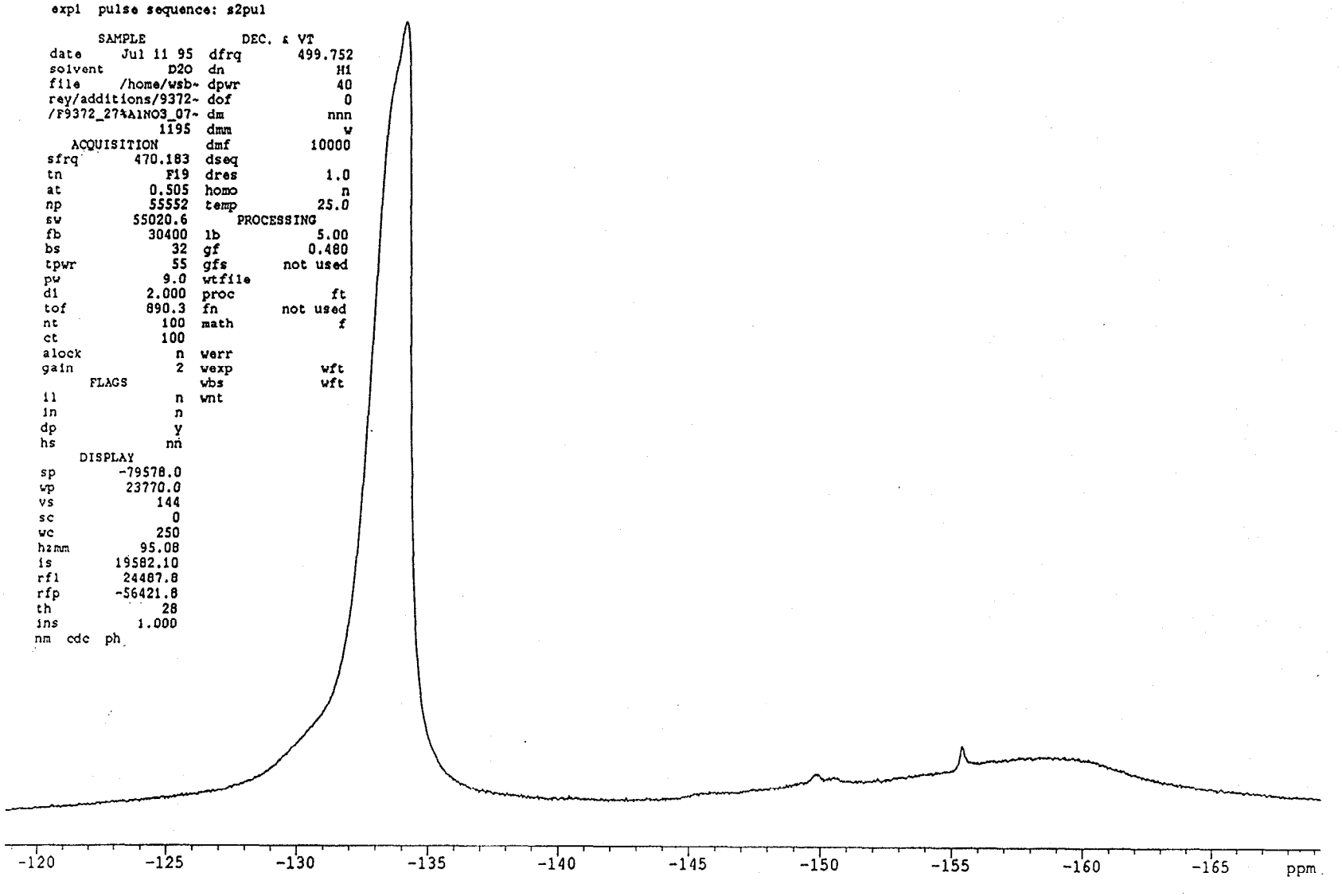

Figure 61: NMR Fluorine-19 Spectrum of Baseline Process Acid Solution to which Aluminum was Added as Aluminum Nitrate at 25°C

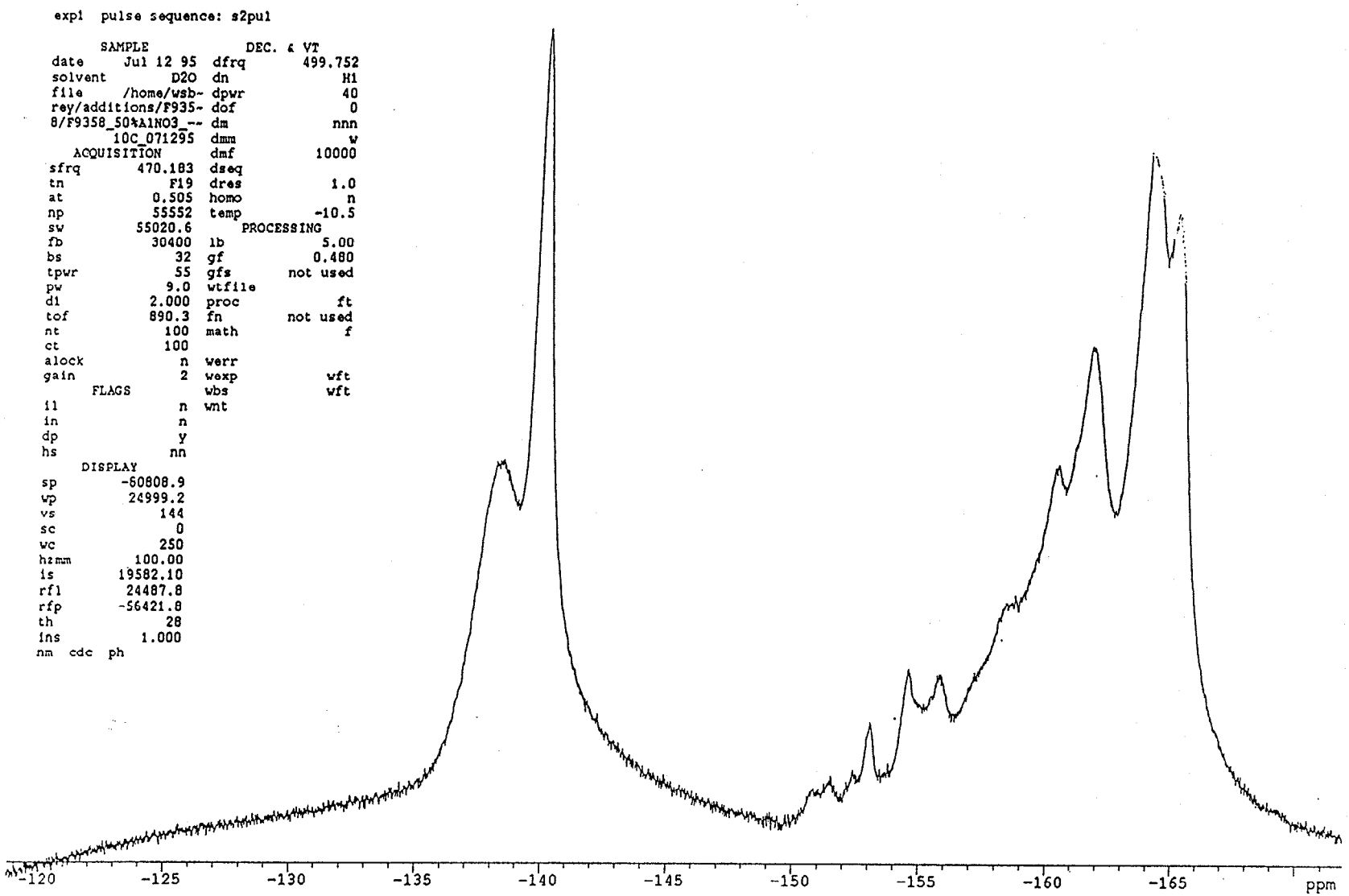

Figure 62: NMR Fluorine-19 Spectrum of Baseline Process Acid at -10°C to which 7.5% Aluminum was Added

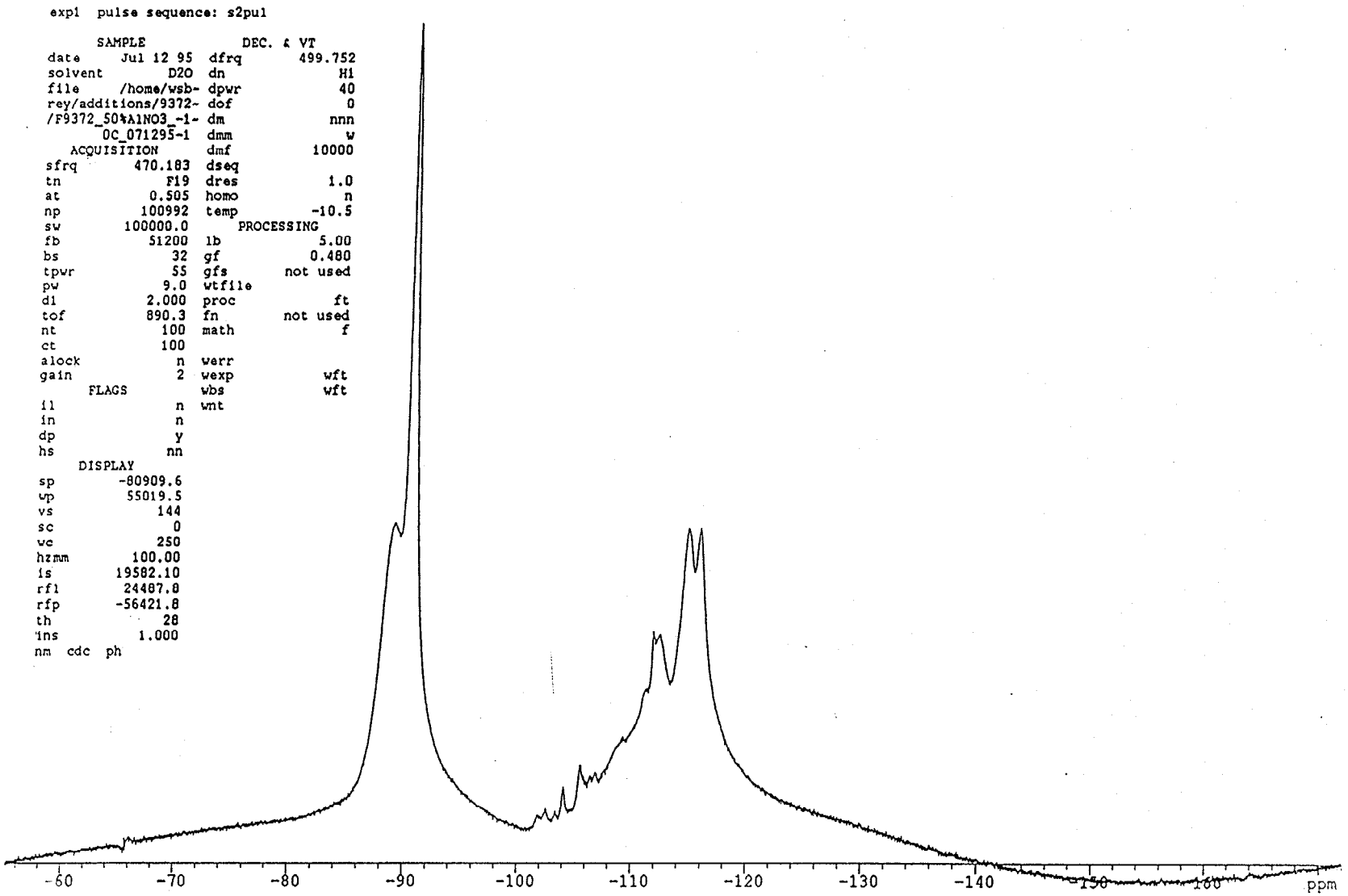

Figure 64: NMR Fluorine Spectrum of PEO-Treated Process Acid (3.5% Sulfate) at -10°C to which 4.6% Aluminum was Added

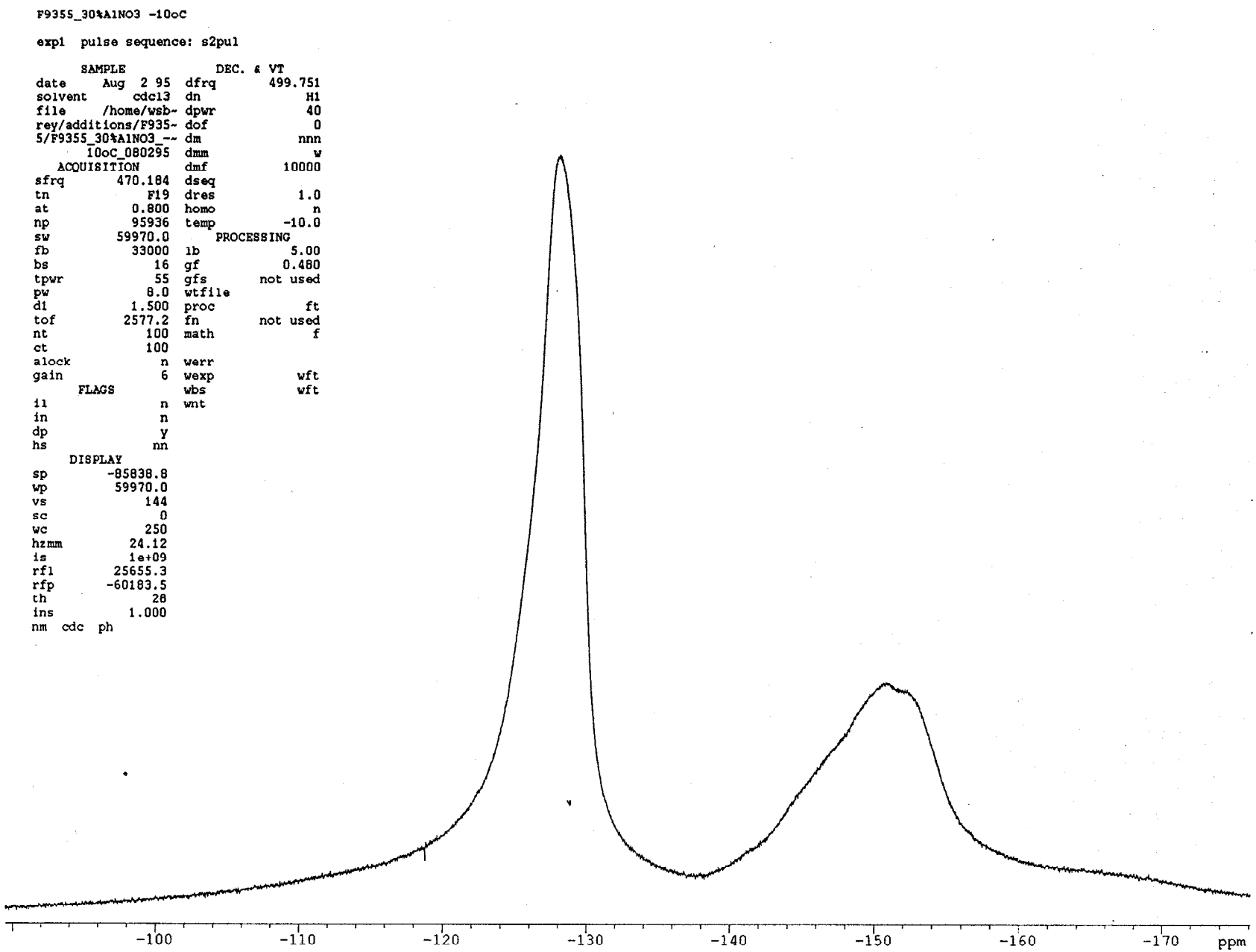

Figure 63: NMR Fluorine-19 Spectrum of BSDBS-Treated Process Acid at -10°C to which 7.5% Aluminum was Added

CONCLUSIONS

This study has led to a number of conclusions that can be summarized as follows:

- Reagent-grade PEO enhances the rate of phosphogypsum filtration by 46 % over the baseline rate with a 0.3 kg/ton polymer dosage
- Commercial-grade PEO enhances the rate of phosphogypsum filtration by 54 % over the baseline rate with a 0.1 kg/ton polymer dosage.
- Reagent-grade BSDBS enhances the rate of phosphogypsum filtration by 35 % over the baseline rate with a 0.5 kg/ton additive dosage.
- Commercial-grade BSDBS enhances the rate of phosphogypsum filtration by 26 % over the baseline rate with a 0.1 kg/ton additive dosage.
- Commercial-grade ANS enhances the rate of phosphogypsum filtration by 22 % over the baseline rate with a 0.5 kg/ton additive dosage.
- Nonbranched commercial-grade SDBS decreases the rate of filtration relative to the baseline rate.
- The presence of additives generally increases process efficiencies
- PEO and PAM are more effective in filtration enhancement when added during the digestion stage of phosphoric acid production.
- Process acid additives enhance filtration for low dolomite feed rock, high dolomite feed rock, and high iron feed rock processing.
- The addition of kaolin decreases filterability.
- Sample drying/preparation leads to incorrect particle size information.
- The hydrodynamic particle size is increased by the presence of additives as evidenced by column settling size data.
- The contact probability model is more accurate that the Kozeny equation in predicting the effect of large particle size distribution changes on the rate of filtration.
- The presence of additives delays the onset of nucleation as evidenced by sample turbidity.

- PEO interacts strongly with calcium ions, thereby reducing their availability for phosphogypsum formation.

- NMR Filtrate analysis of fluorine-19 species suggests that the fluorine speciation is not related to the rate of filtration or to the presence of additives.

- NMR magic-angle spinning analysis of phosphogypsum indicates that the presence of additives does affect the phosphorous-31 speciation.

- NMR analysis of fluorine-19 in phosphogypsum-saturated solution suggests that the additive treatment decreases the level of soluble fluorine in the phosphogypsum.

SUGGESTIONS FOR FUTURE WORK

- Gain a better understanding of the mechanism of additive-enhanced filtration.
- Select reagents that more effectively complex with calcium ions.
- Test selected additives at plant facilities.
- Perform a production cost analysis of the most effective additives.

REFERENCES

1. B. M. Moudgil, J. F. Taylor, and T. V. Vasuvedam, "Effect of Crystal Habit on Filtration Characteristis of Gypsum," *Production and Processing of Fine Particles*, ed. A. J. Plumpton, Canadian Institute of Mining and Metallurgy, (1988), pp. 703.

2. S. D. F. Rocha and V. S. T. Ciminelli, "Effect of Surfactants on Calcium Sulfate Crystallization in Phosphoric Acid," *Minerals and Metallurgical Processing*, (1995), pp. 166-171.

3. G. J. Witkamp and G. M. van Rosmalen, "Recrystallization of Calcium Sulfate Modifications in Phosphoric Acid," *Proceedings of the Second International Symposium on Phosphogypsum*, (1988), vol. 1, pp. 377-405.

4. J. F. Taylor, M. S. Thesis, University of Florida, (1988).

5. R. J. Lee, A. S. Teja, "Viscosities of Poly (ethylene glycols)," *Journal of Chemical and Engineering Data*, (1990), 35, pp. 385-387.

6. Noel de Nevers, *Fluid Mechanics*, Addison-Wesley, (1970), p.167.

7. Pierre Becker, Phosphates and Phosphoric Acid: Raw Materials, *Technology, and Economics of the Wet Process*, Marcel Dekker, Inc., New York, (1983), pp. 107-110.

8. David W. Leyshon et al., U. S. Patent 3,192,014, (1965).

9. Richard J. Akers, and Anthony S. Ward, "Liquid Filtration Theory and Filtration Pretreatment," Ch. 2 in *Filtration: Principles and Practice*, ed. Clyde Orr, Marcel Dekker, Inc. New York, (1977), pp. 169-250.

10. T. C. Fry, *Probability and Its Engineering Uses*, 2nd edition, D. Van Nostrand Co. Princeton, NJ, (1965), pp. 23-39.

11. William Mendenhall, *Introduction to Statistics*, Wadsworth Publishing Company, Inc., Belmont, CA, (1964), pp. 62-64.

12. T. C. Fry, *Probability and Its Engineering Uses*, 2nd edition, D. Van Nostrand Co. Princeton, NJ, (1965), pp. 73-75.

13. R. K. Rajamani, "Mathematical Modeling of Extractive Metallurgical Processes," class notes for Met. E. 655, University of Utah, 2nd edition, (1991), pp. 18-21.

14. A. D. Randolf, M. A. Larson, *Theory of Particulate Processes: Analysis and Techniques of Continuous Crystallization*, 2nd ed., Academic Press, (), pp. 135-173.

15. V. M. Norwood and J. J. Kohler, "Characterization of fluorine-, aluminum-, silicon-, and phosphorus-containing complexes in wet-process phosphoric acid using nuclear magnetic resonance spectroscopy," *Fertilizer Research* (1991) 28, pp. 221-228.

16. J. W. Akitt, N. N. Greenwood, and G. D. Lester, "Nuclear Magnetic Resonance and Raman Studies of the Aluminum Complexes Formed in Aqueous Solutions of Aluminum Salts Containing Phosphoric Acid and Fluoride Ions," *Journal of the Chemical Society A*, (1971) 2450.

17. M. A. Wilson, P. J. Collin, and J. W. Akitt, "Composition of Aluminum Phosphate Solutions - Evidence from Aluminum-27 and Phosphorus-31 Nuclear Magnetic Resonance Spectra," *Analytical Chemistry*, (1989) 61, 1253.

18. S. J. Karlik, G. A. Elgavish, R. P. Pillai, and G. L. Eichorn, "Aluminum-27 NMR Studies of Al(III)-Phosphate Complexes in Aqueous Solution, *Journal of Magnetic Resonance*, (1982) 49, 164.

19. R. E. Connick and R. E. Poulson, "Nuclear Magnetic Resonance Studies of the Aluminum Fluoride Complexes," *Journal of the American Chemical Society*, (1957) 79, 5153.

20. R. E. Connick and R. E. Poulson, "F^{19} Nuclear Magnetic Resonances of Various Metal-Fluoride Complexes in Aqueous Solutions," *Journal of Physical Chemistry*, (1959) 63, 568.

21. A. W. Frazier, J. R. Lehr, and E. F. Dillard, "Chemical Behavior of Fluorine in Production of Wet-Process Phosphoric Acid," *Environmental Science Technology*, (1977) 11, 1007.